Summer 2014

Manufacturing of vegetable oils-based epoxy and composites for structural applications

Rongpeng Wang

Department: Chemistry

MANUFACTURING OF VEGETABLE OILS-BASED EPOXY AND COMPOSITES FOR STRUCTURAL APPLICATIONS

by

RONGPENG WANG

A DISSERTATION

Presented to the Faculty of the Graduate School of the

MISSOURI UNIVERSITY OF SCIENCE AND TECHNOLOGY

In Partial Fulfillment of the Requirements for the Degree

DOCTOR OF PHILOSOPHY

In

CHEMISTRY

2014

Approved by

Thomas P. Schuman, Advisor
K. Chandrashekhara
Harvest Collier
Paul Nam
Michael Van De Mark

PUBLICATION DISSERTATION OPTION

This dissertation has been prepared in the form of four manuscripts for publication. A general introduction is added from pages 1-10. Paper I, pages 11-71 has been accepted for publication as a book chapter in RSC Green Chemistry Series book entitled: Green Materials from Plant Oils. Paper II, pages 72-118, was published in *eXPRESS Polymer Letters*, 2013, 7(3), 272-292. Paper III, pages 119-154, was published in *Green Chemistry*, 2014, 16(4), 1871-1882. Paper IV, pages 155-179, will be submitted to *Composites Part A: Applied Science and Manufacturing*.

ABSTRACT

Epoxidized vegetable oil (EVO) is one of the largest industrial applications of vegetable oils (VOs) and is widely used as a plasticizer and as a synthetic intermediate for polyol or unsaturated polyester. However, the utility of EVO as monomer for high performance epoxy thermoset polymer is limited by its reactivity and by the resulting physical properties. Herein, VO-based epoxy monomers, *i.e.*, glycidyl esters of epoxidized fatty acids derived from soybean oil (EGS) or linseed oil (EGL), have been synthesized and were benchmarked against commercial available diglycidyl ether of bisphenol A (DGEBA) and also epoxidized soybean oil (ESO) controls. EGS and EGL possessed higher oxirane content, more reactivity and lower viscosity than ESO or epoxidized linseed oil (ELO), provided better compatibility with DGEBA as a reactive diluent, and yielded thermally and mechanically stronger polymers than polymers obtained using ESO. Glass transition temperatures (T_g) of the VO-based epoxy thermoset polymers were mostly a function of monomer oxirane content with some added structural influences of epoxy reactivity, and presence of a pendant chain. Organo-modified montmorillonite clay (OMMT) and long glass fiber reinforced composites (FRC) were efficiently manufactured using anhydride cured EGS as matrices. The OMMT nanocomposites showed higher mechanical and thermal strength than the neat polymers but were also dependent on the dispersion techniques and the clay concentration. Surprisingly, the neat EGS-anhydride matrix FRC showed comparable properties, such as flexural and impact strengths and slightly lower T_g, versus DGEBA based counterparts. These high performance monomers, polymers, and composites have potential to replace petroleum-based epoxy as value-added products from VOs compared to EVOs.

ACKNOWLEDGMENTS

I would like to express my deep sense of gratitude to my advisor Dr. Thomas Schuman for his guidance, support, and encouragement through the course of pursuing my PhD. His creative thinking and critical attitude improved my research skills and prepared me for future challenges. I extend my gratitude to my committee members, Dr. Michael Van De Mark, Dr. Paul Nam, Dr. Harvest Collier and Dr. K. Chandrashekhara for their time and assistance with my graduate study and research work.

I would like to thank my former and current lab members, Dr. Subramani, Dr. Siddabattuni, Dr. Ranaweera, Dr. Vuppalapati, Nayak, Chen, and all undergraduates for their help with the completion of my research work. I thank the Department of Chemistry, Materials Research Center and Missouri S&T for financial support and other resources.

Sincere gratitude and respect to my parents, Yuanhai Wang and Lanying Li, my grandfathers, Wenzhen Wang, Wencai Wang, and Pengchao Li, my aunt Dr. Caihong Wang and my other family members for their unconditional love, inspiration, and financial support.

My deepest gratitude must be given to my wife, Hongfang Zhao and our children, Ella and Aiden for their constant love, understanding and encouragement.

TABLE OF CONTENTS

Page

LIST OF ILLUSTRATIONS

PAPER IV

LIST OF TABLES

LIST OF ABBREVIATIONS

AESO	acrylated epoxidized soybean oil
BPA	bisphenol A
DGEBA	diglycidyl ether of bisphenol A
EAS	epoxidized allyl soyate
ECO	epoxidized castor oil
EGL	glycidyl esters of epoxidized fatty acids derived from linseed oil
EGL-P	EGL with partially epoxidized fatty acids
EGL-S	EGL included saturated fatty acids
EGS	glycidyl esters of epoxidized fatty acids derived from soybean oil
EGS-P	EGS with partially epoxidized fatty acids
EGS-S	EGS with saturated fatty acids
ELO	epoxidized linseed oil
EMO	epoxidized methyl soyate (epoxidized biodiesel)
EMI	2-ethyl-4-methylimidazole
EMS	epoxidized methyl ester of soybean oil
ENLO	epoxynorbornane linseed oils
EPCH	epichlorohydrin
EPO	epoxidized palm oil
ESO	epoxidized soybean oil
EVO	epoxidized vegetable oil
FFA	free fatty acid
MCPBA	meta-chloroperoxybenzoic acid
MHHPA	4-methyl-1,2-cyclohexanedicarboxylic anhydride
PACM	bis (4-aminocyclohexyl) methane
TETA	triethylenetetramine
VO	vegetable oil

SECTION

1. PREFACE

The use of naturally occurring polymeric materials such as cotton, wool, silk, starch, and leather has existed throughout the history of human civilization. In fact, early synthetic polymers such as nitrocellulose or vulcanized natural rubber were also derived from natural polymeric materials. Since the invention of Bakelite, a completely synthetic polymer, the 20th century witnessed exponential growth of synthetic polymers that was accompanied with a booming petrochemical industry. In the last two decades, the development of bio-based polymers, *i.e.*, polymers derived from renewable feedstocks such as starch, cellulose, lignin, lipids, and proteins, has found renewed interest in the polymer industry.[1-3] This trend has been driven by the growing societal concerns about sustainability, depletion of fossil raw materials, and a perceived negative environmental impact of petroleum-based polymers.

Vegetable oils (VOs) are an attractive natural resource for the synthesis of bio-based polymers because of their low and stable cost, ready availability in large quantity, and potential biodegradability.[4-6] The world total production of VOs was more than 150 million tons in 2012 (Figure 1.1). Palm oil is the single largest oil production volume followed by soybean, rapeseed and sunflower oil, respectfully. Soybean is the second largest crop plant in U.S. behind corn and U.S. was second in production to Brazil in soybean production. The U.S. production of soybean oilseed and soybean oil in 2012 were 82 million tons and 8.6 million tons, respectively.[7] VOs are primarily used in food

and feed applications, whereas only about 20% are used as industrial feedstocks for biofuels, coatings, paints, lubricants, plasticizers, surfactants, *etc*.[8]

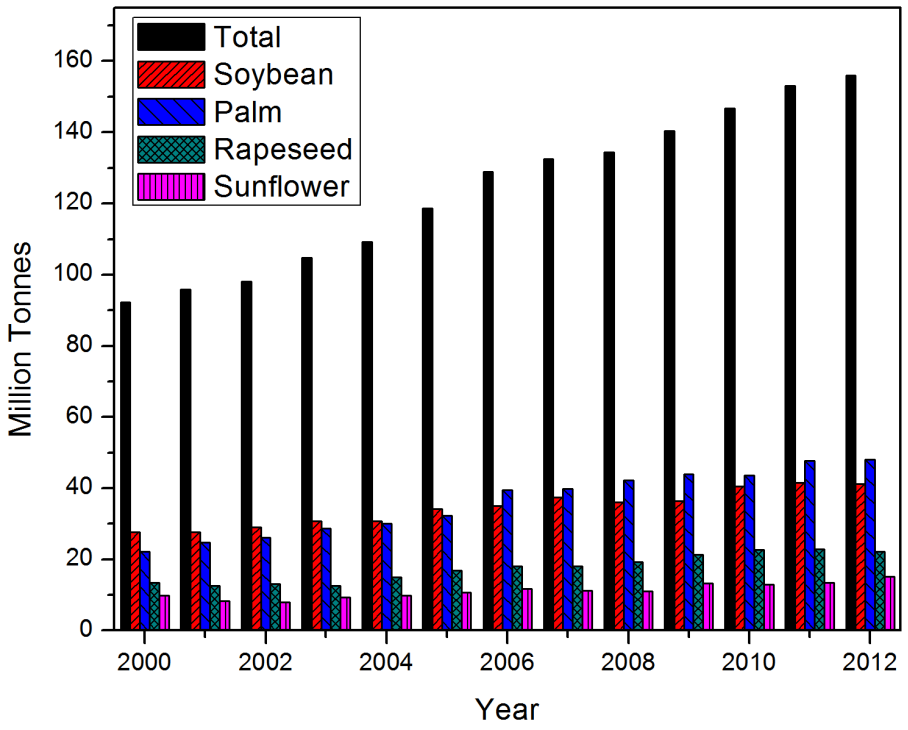

Figure 1.1. The global total vegetable oil production and that of four major oilseed crops since the year 2000 [9]

Vegetable oils predominantly consist of triglyceride, the glycerol esters of fatty acids. Fatty acids are achieved as one of the hydrolysis products of triglycerides with five major types of fatty acids of chain lengths ranging from 16 to 18 carbons with 0 to 3 double bonds: palmitic, stearic, oleic, linoleic and linolenic acids. The structures of these triglyceride and fatty acids are shown in Figure 1.2. The amounts of the different fatty acids varies within different VOs and even within the same plant oil that is dependent on

the plant species and, seasonally, on the growing conditions. The fatty acid composition and degree of unsaturation for some common VOs are summarized in Table 1.1.

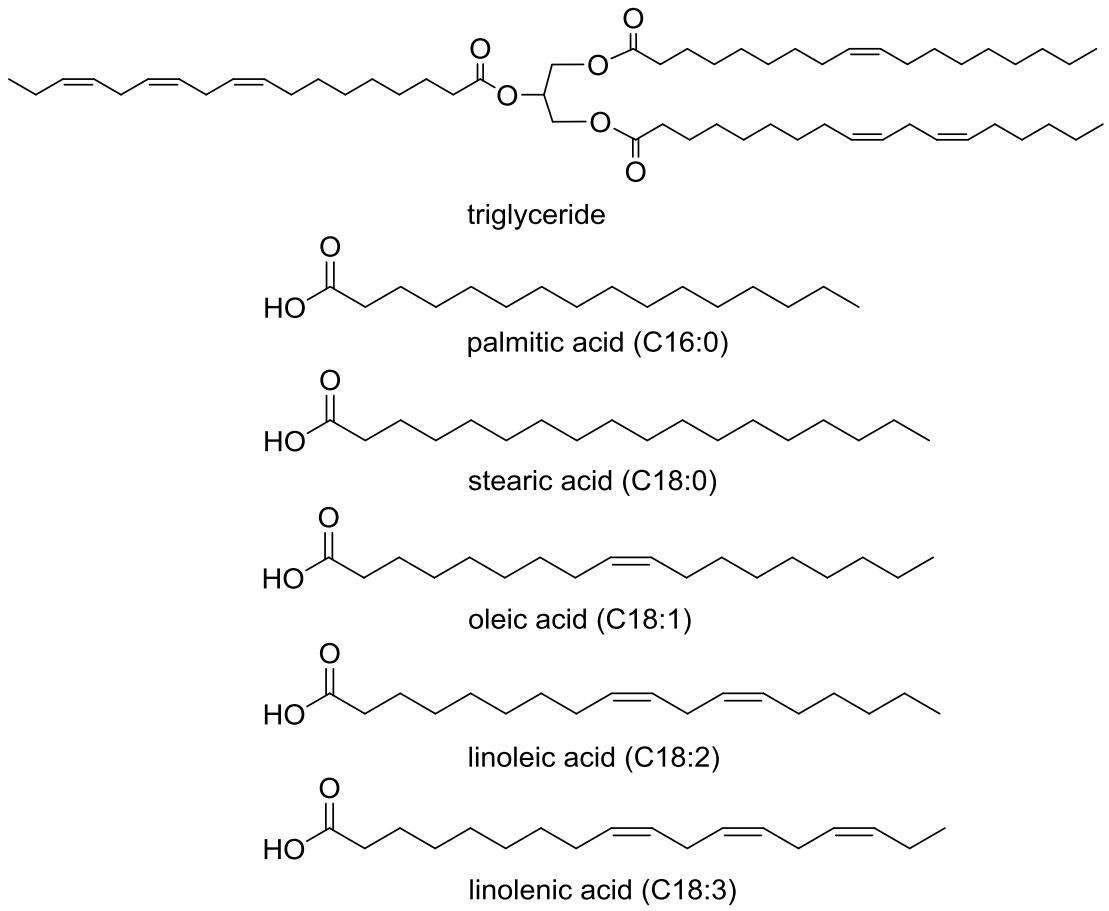

Figure 1.2. Structures of triglyceride and five most important fatty acids

The industrial exploitation of VOs is mostly based on the chemical modification of the carboxyl and/or unsaturation carbon groups present in fatty acids.[10-12] One of the most important parameters affecting the physical and chemical properties of fatty acid and VO is the number of double bonds, or the degree of unsaturation, which is measured by the iodine value (I.V.). Based on the iodine values, VOs can be divided into three

types: drying oils (I.V. > 130, such as linseed oil); semi-drying oils (100 < I.V. < 130, such as soybean oil) and non-drying oils (I.V. < 100, such as palm oil).[13] For a thermosetting polymers application, VOs with higher I.V. are desirable, which means more functional groups that facilitate more highly crosslinked structures for better thermal and mechanical strengths. One must bear in mind that saturated chains possessing no double bonds show no reactivity for polymerization except through the ester carboxyl.

Table 1.1 Typical properties and fatty acid compositions of common vegetable oils[14-18]

VO	Saturated		Unsaturated			Double Bonds[a]	Iodine Value[b]
	palmitic	stearic	oleic	linoleic	linolenic		
Canola	4	2	61	21	9	3.9	110-126
Cottonseed	22	3	19	54	1	3.9	90-119
Corn	11	2	25	60	1	4.5	102-130
Linseed	5	4	22	17	52	6.6	168-204
Olive	14	3	71	10	1	2.8	75-94
Palm	44	4	39	10	-	1.8	44-58
Peanut	11	2	48	32	-	3.4	80-106
Soybean	11	4	23	53	8	4.6	117-143
Sunflower	6	4	42	47	1	4.7	110-143

* Note: percentages may not add to 100% due to rounding and/or presence of other minor fatty acid contents, which are not listed; [a] Average number of double bonds per triglyceride; [b] I.V. = grams of iodine consumed by 100 g of oil samples

Vegetable oils and their derivatives have been exploited in many ways to synthesize various polymeric materials,[13, 19-23] such as oxypolymerized oils, polyesters,

polyamides, epoxies and polyurethanes (Figure 1.3). Although VOs possess double bonds, the radical initiated polymerization of common, non-conjugated VOs have received little attention due to the low reactivity of the internal double bonds and to the chain transfer processes that occur at their adjacent, allylic positions in fatty acid chains.[21]

VOs, however, especially highly unsaturated drying oils, can react with atmospheric oxygen to form a crosslinked structures through radical combination and radical addition mechanisms.[24] These polymeric materials found application in air oxidative drying paints, varnishes and other coating processes that date back to the days of cave paintings (ca. 30,000 yr ago).[25] Viscous liquid polymers of "bodied oil" or "air blown oils" are oligomers of oils that have been prepared from simply thermally heating of soybean oils with or without air-blowing, respectively. Such processes also result in the formation of numerous oxidation products such as alcohols, carboxylic acids, aldehydes and ketones.[26]

Polyester alkyd (*i.e.*, alcohol-acid) resins are historically among the oldest polymers derived from VOs and have been widely used in a variety of commercial coating applications. They are prepared by the transesterification of polyols with polyacids/anhydride and VOs/fatty acids. After initial esterification, the viscosity is further increased by heating to a high temperature through further esterification and crosslinking reactions. Depending on the oil percentage present in the mixture, the resulting alkyd resin can be classified as oil-free (0%), short oil (<45%), medium oil (45-55%) or long oil (>55%) alkyd.[27]

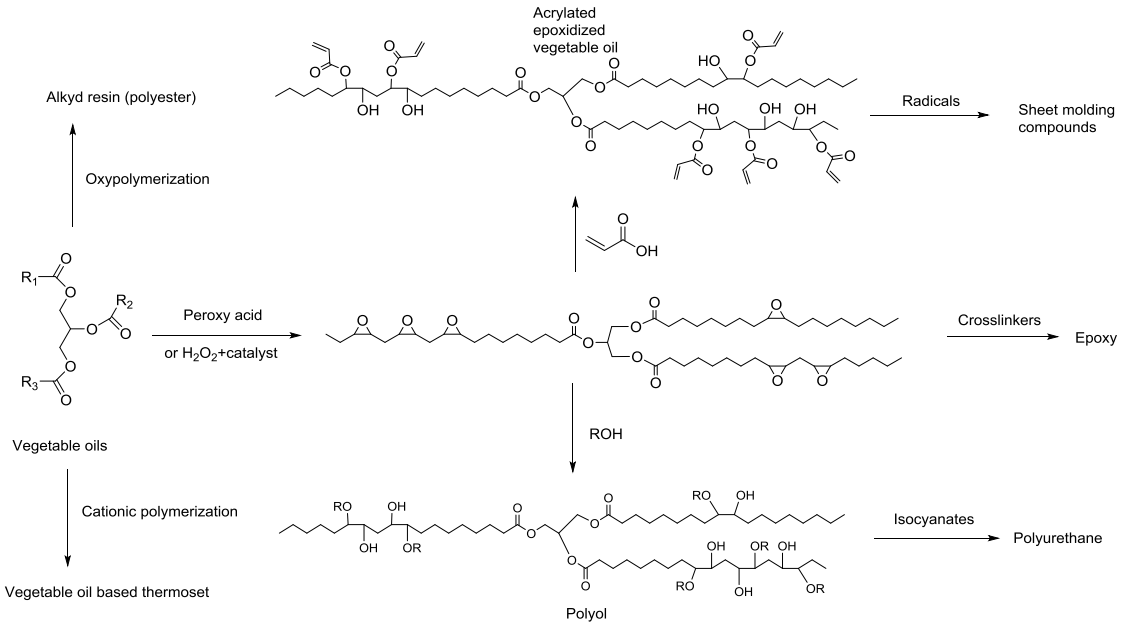

Figure 1.3. General routes for synthesis of VO-based polymers

The internal double bonds of VOs are rich in electrons thus are susceptible to cationic polymerization. Using $BF_3{\cdot}Et_2O$ as initiation catalyst, cationic polymerization of VOs has been conducted by Larock and co-workers.[18, 21, 28] To further improve the thermal and mechanical performance and reduce heterogeneity, copolymerization with vinyl monomers such as styrene, divinyl benzene is necessary, and has resulted in polymers ranging from soft rubbers to hard plastics, depending on the comonomer ratios.[29]

Instead of directly polymerizing neat VOs, monomers can be synthesized through chemical transformation or functionalization of VOs before polymerization. Several types of triglyceride functionalization can be obtained at active sites, *i.e.*, double bond and/or ester groups. The epoxidation of double bonds using peroxy acids to prepare epoxidized vegetable oils (EVO), such as epoxidized soybean oil (ESO) or epoxidized

linseed oil (ELO), is one of the most industrially important functionalizations of VOs because the highly reactive epoxy groups can be utilized as monomer or be readily transformed into other polymerizable functionalities. For instance, polyols for polyurethane can be prepared by a ring opening reaction of epoxy groups to form alcohols.[19, 30-32] Acrylated epoxidized soybean oil (AESO) is another important functionalization of EVO through an epoxy ring opening with acrylic acid. The AESO can be blended with other reactive diluent comonomers such as styrene and then cured by a free radical or cationic initiated polymerization. The formed thermoset has found application as sheet molding compound with mechanical properties comparable to commercially available unsaturated polyester and vinyl ester resins.[14, 33-35]

Direct polymerization of EVOs to prepare epoxy thermoset polymers has been conducted since 1950s; however, EVO has received only limited success so far as an epoxy monomer because of the low reactivity of internal epoxy with common, nucleophilic curing agents, such as polyamines and anhydrides. Moreover, the inherently aliphatic nature and residual, saturated fatty acid component in VO feedstocks lead to less tightly crosslinking structures and polymeric materials that lack the necessary rigidity and strengths required for structural applications. EVO are, therefore, mostly used as secondary plasticizers or stabilizers for poly(vinyl chloride) or as reactive diluents for oil-base coatings with lower strength requirement.

2. OBJECTIVE OF THIS RESEARCH

Traditional EVO materials have been shown not only to have potential advantages but also distinct disadvantages toward high performance epoxy thermoset materials. I hypothesize that the properties and performance of EVO monomers are a function of the EVO chemical structure, oxirane content and residual unsaturation. The main objective of the work is to develop new VO-base epoxy monomers, polymers and composites materials with improved properties. The following studies were planned to attain the objective:

1. Synthesize VO-based epoxy monomers using glycidation and double bond epoxidation chemistry to produce monomers of controlled reactivity, oxirane content and chemical structure including residual saturation, and characterize these monomers using standard techniques.
2. Investigate the curing and thermal mechanical behaviors of the VO-based epoxy monomers with various curing agents such as anhydrides, polyamines and cationic catalysts. The structure-property relationship of VO-based epoxy thermosets will be especially emphasized.
3. Blend the VO-based epoxy monomers with commercial available epoxy resins such as diglycidyl ether of bisphenol-A (DGEBA), to improve polymers thermal and mechanical properties. Study the effect of structure of aromatic DGEBA and its concentration on the curing characteristics, thermal and mechanical performance.
4. Manufacture of VO-based epoxy composites using nano-reinforcements or long fiber-reinforcements to further improve performance of VO-based polymers and potentially for a high strength structural applications.

3. REFERENCES

1. M. N. Belgacem and A. Gandini, *Monomers, Polymers and Composites from Renewable Resources*, Elsevier, Oxford, UK, 2008.
2. A. Gandini, *Macromolecules*, 2008, **41**, 9491-9504.
3. C. K. Williams and M. A. Hillmyer, *Polymer Reviews*, 2008, **48**, 1-10.
4. L. Montero de Espinosa and M. A. R. Meier, *European Polymer Journal*, 2011, **47**, 837-852.
5. M. A. R. Meier, J. O. Metzger and U. S. Schubert, *Chemical Society Reviews*, 2007, **36**, 1788-1802.
6. M. A. Mosiewicki and M. I. Aranguren, *European Polymer Journal*, 2013, **49**, 1243-1256.
7. "SoyStats 2013," http://soystats.com/, accessed May 2014.
8. "The AOCS Lipid Library," http://lipidlibrary.aocs.org/market/index.html, accessed May 2014.
9. "Food and Agriculture Organization of United Nations," http://faostat3.fao.org/faostat-gateway/go/to/download/Q/QD/E, accessed May 2014.
10. H. Baumann, M. Bühler, H. Fochem, F. Hirsinger, H. Zoebelein and J. Falbe, *Angewandte Chemie International Edition in English*, 1988, **27**, 41-62.
11. J. O. Metzger, European Journal of Lipid Science and Technology, 2009, **111**, 865-876.
12. Ursula Biermann, W. Friedt, S. Lang and W. Luhs, *Angew.Chem.Int.Ed*, 2000, **39**, 2206-2224.
13. N. Karak, *Vegetable oil-based polymers: Properties, processing and applications*, Woodhead Publishing Limited, Philadelphia, PA, USA, 2012.
14. S. N. Khot, J. J. Lascala, E. Can, S. S. Morye, G. I. Williams, G. R. Palmese, S. H. Kusefoglu and R. P. Wool, *Journal of Applied Polymer Science*, 2001, **82**, 703-723.
15. F. Seniha Güner, Y. YagcI and A. Tuncer Erciyes, *Progress in Polymer Science*, 2006, **31**, 633-670.
16. C. Scrimgeour, in *Bailey's Industrial Oil and Fat Products*, John Wiley & Sons, Inc., 2005.
17. F. Gunstone, The Chemistry of Oils and Fats: Sources, Composition, Properties and Uses, Blackwell Publishing Ltd, Oxford, UK, 2004.
18. Y. Xia and R. C. Larock, *Green Chemistry*, 2010, **12**, 1893-1909.

19. M. Desroches, M. Escouvois, R. Auvergne, S. Caillol and B. Boutevin, *Polymer Reviews*, 2012, **52**, 38-79.

20. M. Galià, L. M. de Espinosa, J. C. Ronda, G. Lligadas and V. Cádiz, *European Journal of Lipid Science and Technology*, 2010, **112**, 87-96.

21. Y. Lu and R. C. Larock, *ChemSusChem*, 2009, **2**, 136-147.

22. V. Sharma and P. P. Kundu, *Progress in Polymer Science*, 2006, **31**, 983-1008.

23. V. Sharma and P. P. Kundu, *Progress in Polymer Science*, 2008, **33**, 1199-1215.

24. R. van Gorkum and E. Bouwman, *Coordination Chemistry Reviews*, 2005, **249**, 1709–1728.

25. M. R. Van De Mark and K. Sandefur, *Inform*, 2005, **16**, 478-481.

26. I. Mihail and P. S. Zoran, in *Soybean - Applications and Technology*, ed. T.-B. Ng, INTECH, 2011.

27. P. Deligny and N. Tuck, in *Surface Coating*, ed. P. Oldring, John Wiley and Sons, London, UK, Second Edition edn., 2000, vol. 2.

28. Y. Xia, R. L. Quirino and R. C. Larock, *Journal of Renewable Materials*, 2013, **1**, 3-27.

29. F. Li, J. Hasjim and R. C. Larock, *Journal of Applied Polymer Science*, 2003, **90**, 1830-1838.

30. S. Miao, P. Wang, Z. Su and S. Zhang, *Acta Biomaterialia*, 2014, **10**, 1692–1704.

31. Z. S. Petrović, *Polymer Reviews*, 2008, **48**, 109-155.

32. D. P. Pfister, Y. Xia and R. C. Larock, *ChemSusChem*, 2011, **4**, 703-717.

33. A. Campanella, J. J. L. Scala and R. P. Wool, *Journal of Applied Polymer Science*, 2011, **119**, 1000-1010.

34. J. Lu, S. Khot and R. P. Wool, *Polymer*, 2005, **46**, 71-80.

35. J. Lu and R. P. Wool, *Journal of Applied Polymer Science*, 2006, **99**, 2481-2488.

PAPER

I. TOWARDS GREEN: A REVIEW OF RECENT DEVELOPMENTS IN BIO-RENEWABLE EPOXY RESINS FROM VEGETABLE OILS

Rongpeng Wang and Thomas Schuman

Department of Chemistry, Missouri University of Science and Technology, Rolla, MO 65409 USA

ABSTRACT

Polymers based on vegetable oil (VO) have the potential to replace or augment the traditional, petroleum-based polymers. Epoxidized vegetable oils (EVO) are one form of epoxy monomer that are derived from raw VO. They are widely used as plasticizers and intermediates for polyols of bio-based polyurethane or unsaturated polyesters. A comprehensive review covers epoxy thermoset polymers prepared from EVO and analogous, fatty acid derived epoxy monomers resins. The scope, performance, and limitations with respect to utilization of such materials in various applications are highlighted. The utility of EVO monomers is enabled or limited by their reactivity and by the physical properties of their resulting polymers. The effects of the chemical structures of VO-based epoxy, various catalysts, and comonomers on the properties of thermoset polymers are especially emphasized.

1. INTRODUCTION

Epoxy resin is compound or pre-polymer normally containing more than equivalent of oxirane per mole of compound. Oxirane, also known as epoxy, is highly reactive due to the strained ring and polar bond structure and can afford a large variety of chemical reactions. Epoxy resins can react with themselves, through anionic or cationic homopolymerization, or with a variety curing agents, often called hardeners or crosslinkers. Common curing agents include polyamines, anhydrides, or phenols. An enormous numbers of epoxy formulations fitting various applications are possible through a down-selection of the epoxy resin, curing agent, additive(s) and curing conditions. The cured epoxy resins exhibit excellent thermal and mechanical strength, outstanding chemical resistance, high adhesive strength and low shrinkage. Since the first commercial debut in about the 1940s, epoxy resins have become one of the most important monomers for synthesizing thermoset polymers and are widely used in coatings, adhesives and composites.[1]

Epoxy resins can be roughly divided into three classes: aliphatic, cycloaliphatic and aromatic. By far, the diglycidyl ether of bisphenol A (DGEBA) structure, which is made from the condensation reaction of bisphenol A (BPA) and epichlorohydrin (EPCH), is the most common, commercially available epoxy resin. EPCH is traditionally produced from propylene in a multi-step process. Glycerol, which is an effluent byproduct from the biodiesel industry, can also be used to produce EPCH and has been recently commercialized (Figure 1).[2] Since BPA is classified as an endocrine disruptor, which may lead to negative impact on human health, several countries have banned BPA using in infant bottles and considerable research has been focused on using compounds

derived from wood/lignin,[3-6] rosin,[7-12] tannins,[13, 14] sugar,[15, 16] cardanol,[17] or itaconic acid[18, 19] to replace BPA and, at the same time, to contribute toward sustainable development in the polymer industry as bio-based thermoset polymers. However, some of these epoxies still have unresolved issues such as limited production, low purity, complex structure and lack of structural control, hydrophilicity, brittleness, and/or unknown toxicity. The efficient and economical synthesis of a bio-based epoxy is a challenge and still strongly dependent on future developments.[20]

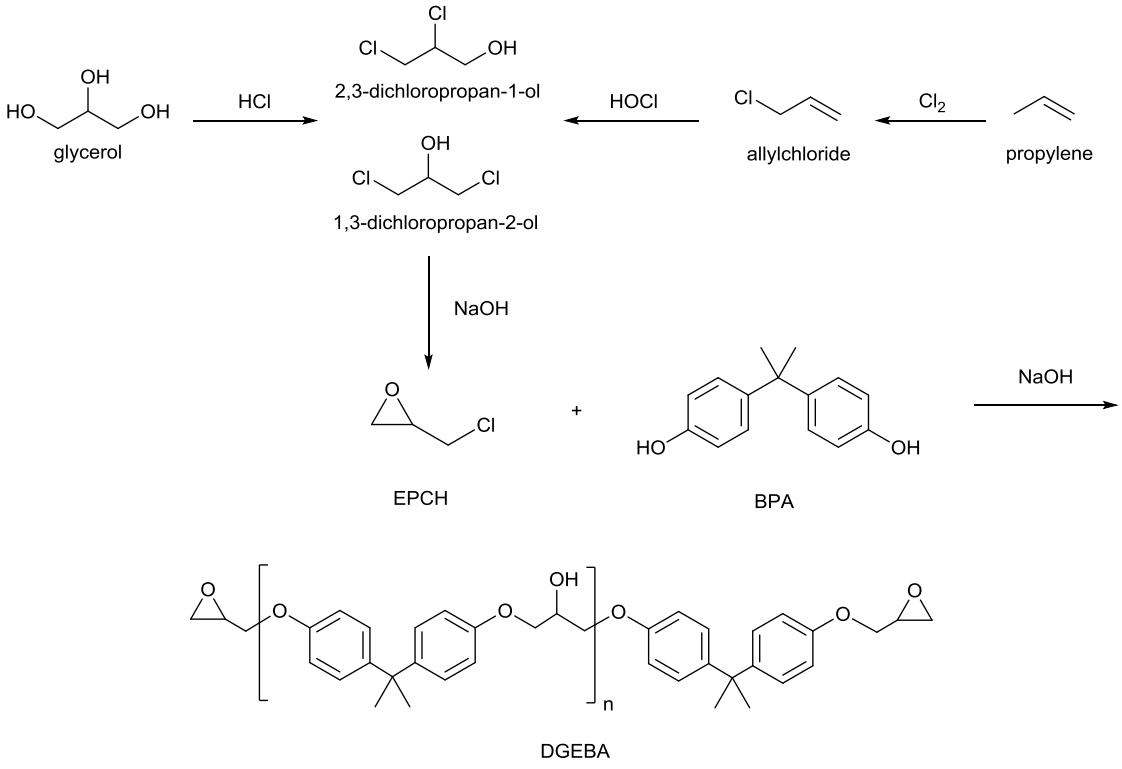

Scheme 1. Synthesis of epichlorohydrin and DGEBA epoxy resin.

2. EPOXIDIZED VEGETABLE OILS

Apart from renewability, availability and relatively low and stable prices, vegetable oils (VOs) such as soybean or linseed oil, of diverse chemical structure and high synthetic potential, could be attractive and feasible resources in the synthesis of bio-based chemicals.[21, 22] VOs are major agricultural commodities with total production about 159 million tons in 2012. While their production was continuously increasing in recent years,[23] only a small portion of VOs are used as oleochemicals for surfactants, lubricants, coatings, paints and biodiesel. The industrial exploitation of VOs is mostly based on chemical modification of the carboxyl and carbon double bonds presented in triglyceride, *i.e.*, glycerol ester of fatty acid.

There are five dominating types of free fatty acids that range in length from 14 to 18 carbon atoms of 0 to 3 double bonds within the chain. The common unsaturated fatty acids are oleic, linoleic and linolenic acids that containing one (C18:1), two (C18:2) or three (C18:3) double bonds, respectively. The common saturated fatty acids are palmitic acid (C16:0) and stearic acid (C18:0). One must bear in mind that saturated fatty acids show no reactivity except through a telechelic carbonyl. Highly unsaturated fatty acids are desirable for thermoset polymer application since double bonds provide opportunity for property development through highly crosslinked structures, hence better thermal and mechanical strength.

Epoxidized vegetable oils (EVO) are a frequently studied polymer precursor in recent years.[22] Vernonia oil is a naturally occurring EVO that is obtained from the seeds of a plant native to Africa, *Vernonia galamensis*. The seeds contain up to 40 wt.% oil by weight, with typical fatty acid distributions averaging 6% oleic acid, 12% linoleic acid,

and 80% vernolic acid (Scheme 2).[24] Possessing low viscosity, vernonia oil has been used as reactive diluent in epoxy coating formulations[25] or in cationically cured blends with commercial epoxy.[26]

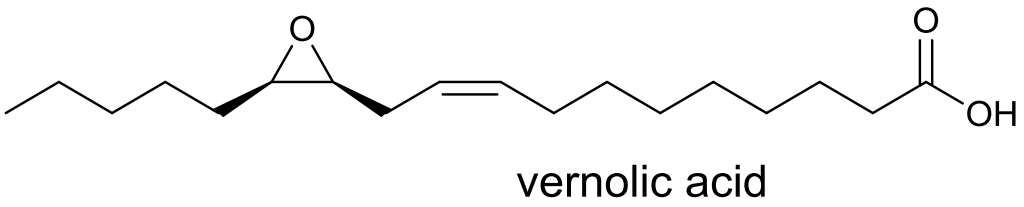

vernolic acid

Scheme 2. Structure of venolic acid in Vernonia oil.

Epoxidized soybean oil (ESO) and epoxidized linseed oil (ELO) are currently the only bio-renewable epoxies that reach industrial scale production. World annual production of EVOs is greater than 200,000 tons.[27] EVO can be prepared by the epoxidation of the double bond of fatty acids using peracids and such processes have been utilized since the 1940s.[28, 29] Performic acid or peracetic acid are commonly employed by the industry and are formed *in situ* from hydrogen peroxide and the corresponding acid in the presence of strong acid catalyst such as sulfuric acid (Scheme 3).[30] However, strong acids also catalyze the ring-opening reaction of the desired product, oxirane. In order to improve epoxidation selectivity and reduce side reactions, an acidic ion exchange resin,[31] heterogeneous transition metal catalyst[32] or enzyme[33, 34] have been used as a peracid catalyst for epoxidation of VOs. The latter has proved to be very effective for the epoxidation of VOs with extremely high yields and less side reaction. The epoxy content of VOs depends on the epoxidation methodology and origin

of the VO, *i.e.*, the extent of epoxidation and starting iodine value. The oxirane oxygen concentrations of ESO and ELO are approximately 7% and 9%, respectively.

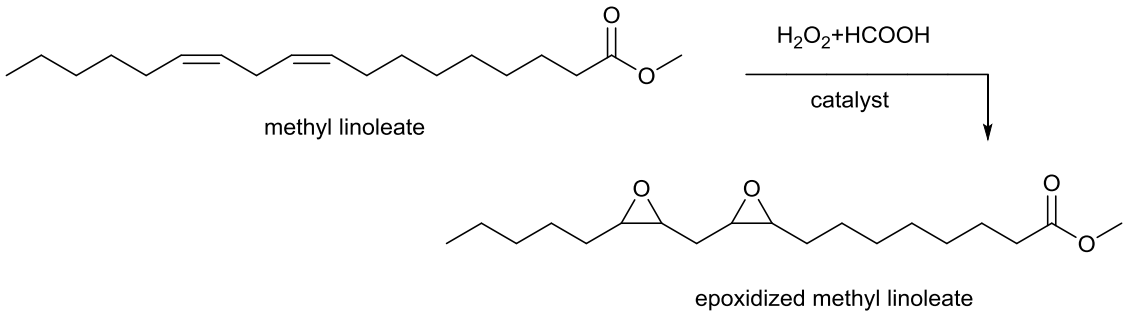

Scheme 3. Epoxidation of VOs or their fatty acid derivatives.

EVOs are industrially applied in polyvinyl chloride (PVC) plastics as a secondary plasticizer and scavenger for hydrochloric acid liberated during heat treatment of PVC. EVO offers promise as an inexpensive, renewable material (about $1500/ton in 2013) for many epoxy applications because EVOs share many of the characteristics of conventional petroleum-based epoxies. The epoxy group of EVO is versatile as a reactive intermediate to provide other functionalities suitable for polymer synthesis, *e.g.*, polyols for polyurethanes,[35] maleinized and/or acrylated VO as sheet molding compounds.[36] Such processes have been well established and are also commercialized. These applications, however, fall outside the scope of this review where only direct use of fatty acid-derived epoxy as monomers for preparing epoxy thermoset polymers is considered.

Despite their promise and versatility, EVO are not able to compete with analogous petroleum-based epoxy polymers in many structural applications. Direct use of EVO as an epoxy resin[37, 38] dates to the 1950s, but have since shown limited success.

EVOs lack a stiff, aromatic or cycloaliphatic structure which confers greater strength as found in other commercial epoxy thermoset polymers. Their internal, secondary carbon oxiranyl groups possess relatively much lower reactivity to common polyamine or anhydride curing agents.

In what could be regarded as a stalled field, strongly revitalization has occurred in recent years. Firstly, a "green chemistry" emphasis, also called "sustainable chemistry", has entered the field of polymer industry. For instance, the reputed RSC publishing journal *Green Chemistry*, which focuses on research of alternative/sustainable technologies, debuted in 1999. The utilization of natural, renewable products is considered one of the most important approaches to conduct green chemistry. Use of an EVO not only takes advantage of the synthetic potential of nature but can also reduce our environmental footprint through a reduction in consumption of non-renewable resources such as petroleum.

Secondly, the application of the EVOs has been actively widened. Various thermoset polymers have been synthesized from EVOs through properly choosing curing agents or curing conditions, through new formulation approaches in composites, coatings and toughening agents are being continuously developed, as will be detailed in later sections. Lastly, but most important, new epoxy monomers derived from VOs have been successfully synthesized that show more promise than common EVOs in terms of reactivity and thermal and mechanical strength. The new monomers are a strong step towards advanced applications, such as structural composites, made possible through improved structure, reactivity and proper choice of formulation conditions. Properties are the avenue by which to provide the opportunity for bio-based epoxy resins to replace

or supplement petroleum-based counterparts. Without sufficient properties, there can be no commercial opportunity.

3. VEGETABLE OIL DERIVED EPOXY MONOMERS

Commercial EVOs, as the major epoxy resins derived from VOs, have inherent problems that derive from their chemical structure, flexibility and hindered reactivity. Most thermoset polymers derived from EVO have very low glass transition temperature (T_g) and are mainly of a rubbery state, which inevitably limits their application. As a result, it has been of interest to synthesize VO-derived epoxies of enhanced polymerization rate and stiffer polymer backbone.

Functionalized oils have been prepared from linseed oils and 1,3-butadiene, cyclopentadiene or dicyclopentadiene through Diels-Alder reaction (Scheme 4). Epoxynorbornane linseed oils (ENLOs) were prepared using hydrogen peroxide under catalyst.[39, 40] The produced cycloaliphatic structure is expected to improve polymer tensile strength, toughness and T_g and well suited for cationic polymerization. However, the double bond conversion of linseed oil had to be limited, *e.g.*, < 30%, otherwise only high viscosity liquids or soft solids were obtained. Reactive diluents were required to reduce the viscosity of the formulation, accelerate the rate of cationic polymerization, and increase their final conversions.[41]

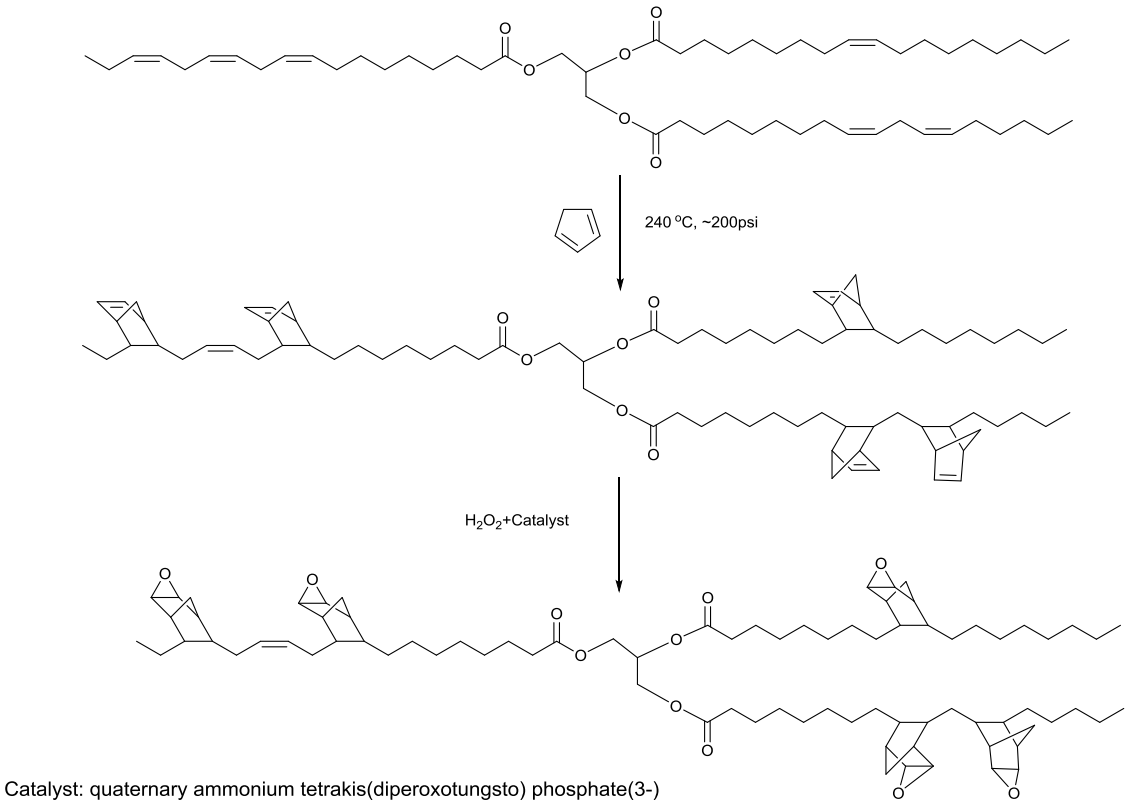

Scheme 4. Synthesis of ENLO which is derived from linseed oil and cyclopentadiene.

Epoxidized sucrose esters of fatty acids (ESEFAs), highly functional epoxy compounds with reasonably well-defined structures, have been synthesized by Webster and coworkers (Scheme 5).[42, 43] Anhydride cured ESEFAs showed better thermal and mechanical strength than those of EVO. ESEFAs still possess internal epoxy groups, which are less reactive with common anhydride and amine curing agents than a terminal epoxy analogous to DGEBA, internal epoxy groups are better used for cationic cured coating applications.[44] A drawback to the ESEFA approach is the relatively large viscosity increase compared to EVO that hampers some applications.

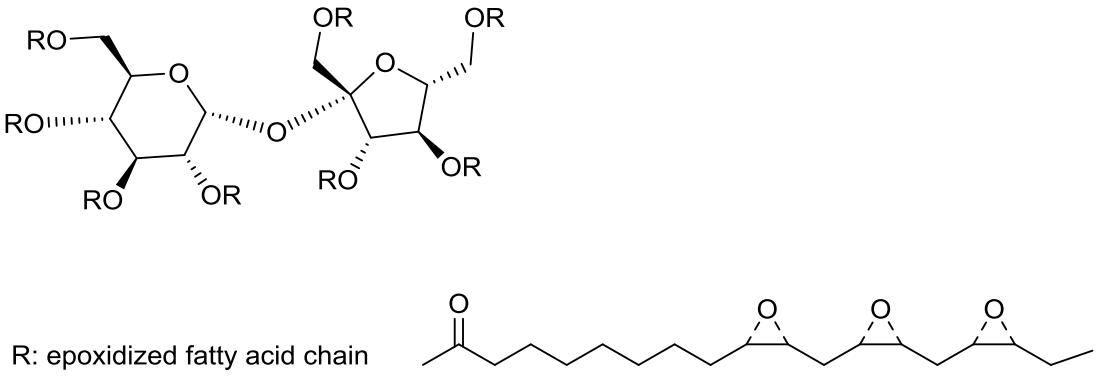

Scheme 5. Molecular structure of ESEFA.

Polyepoxides were derived from poly (vinyl ether of soybean oil fatty acid esters) (poly-VESFA) through transesterification of soybean oil with ethylene glycol vinyl ether (Scheme 6). The poly-VESFA has an increased number of fatty branches per molecule than native soybean oil thus the epoxidized poly-VESFA showed faster curing kinetics and improved T_g than ESO due to the higher number of epoxy groups per molecule.[45] The much higher viscosity, a reduced molecular mobility associated with a polymeric structure as compared with EVO, and presence of only internal epoxy limits epoxidized poly-VESFA toward coating applications.[46]

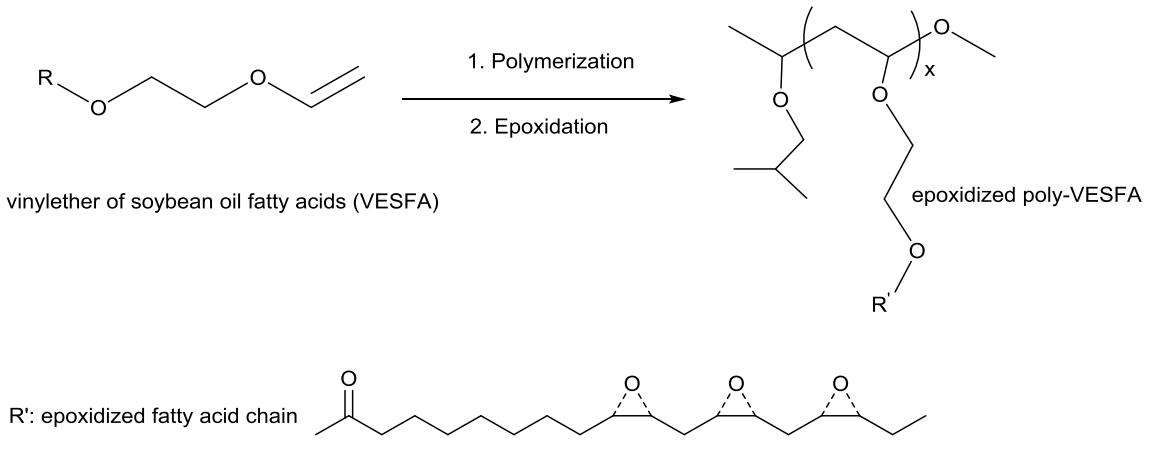

Scheme 6. Synthesis of epoxidized poly-VESFA.

Unlike the internal oxirane of monomers such as EVO, terminal epoxies such as glycidyl show improved reactivities during nucleophilic curing reactions. For instance, the terminal epoxy of epoxidized triglyceride esters of undecylenic acid (Scheme 7) have been synthesized and successfully used in the epoxy-amine or epoxy-anhydride curing.[47, 48] The prepared coating compounds also exhibited UV stability due to the predominance of aliphatic structures.[49] The epoxidation rate of the terminal electron-deficient alkenes in undecylenic acid by peracids is much lower than the internal double of natural fatty acids.[50-52]

Undecylenic acid is produced by pyrolytic cracking of castor oil under pressure. The non-natural fatty acid then must be reacted with glycerol to reform triglyceride ester and to increase crosslink density. The maximum 3 oxirane per epoxidized triglyceride ester of undecylenic acid molecule is still lower than that of ESO with about 4.5 oxirane per triglyceride. Cured thermosets polymers offer little advantage over the similar but more readily available ESO or ELO counterparts with the exception of minimized pendant alkyl chain content.

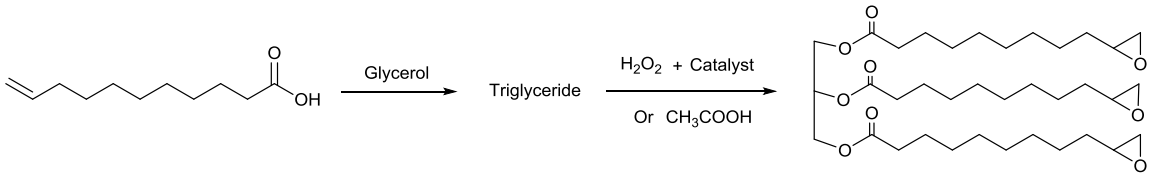

Scheme 7. Synthesis of epoxidized triglyceride ester of undecylenic acid.

Terminal epoxies of glycidyl esters synthesized from dimer or trimer fatty acids have been commercially available for some time.[53-55] Recently, both dicarboxylic acid and a tricarboxylic acid were synthesized by Huang *et al.*[56] using Diels-Alder addition

onto tung oil (eleostearic) fatty acid with acrylic acid and fumaric acid, respectively. The corresponding diglycidyl or triglycidyl esters were prepared using base and EPCH (Scheme 8). Both epoxies showed higher reactivities and improved performance compared to ESO. The triglycidyl ester version displayed comparable strength, modulus and T_g to a DGEBA control.

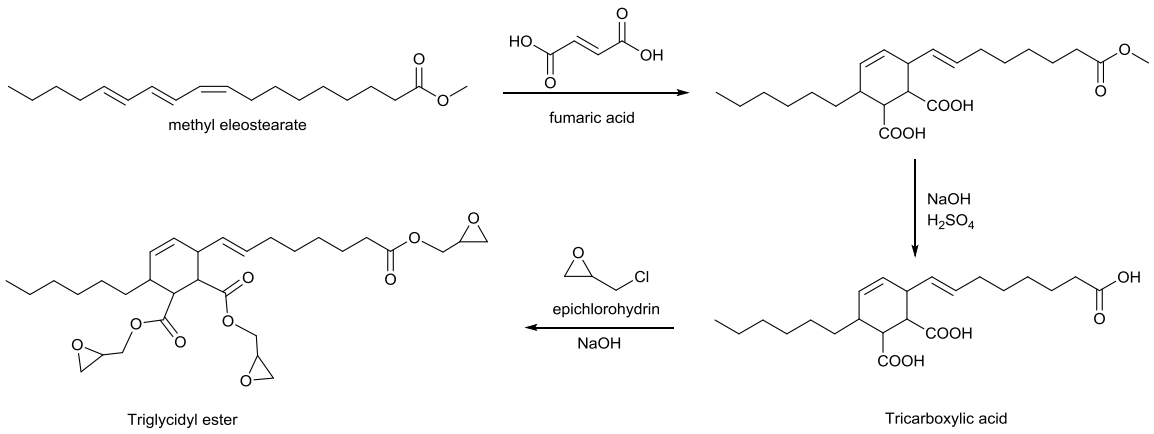

Scheme 8. Synthesis of triglycidyl esters derived from tung fatty acid and fumaric acid.

Using readily available soybean oil or its free fatty acids, a fatty glycidyl ester epoxy was synthesized by Wang and Schuman.[57] Versatility of transesterification and epoxidation reactions (Scheme 9) provide several routes toward synthesize the glycidyl esters of epoxidized fatty acids (EGS). EGS merits include higher oxirane content and lower viscosity than commercial ESO, ELO or DGEBA. A structure-property relationship study measured the effects of oxirane content and presence of saturated fatty acids on polymer properties. EGS had unreactive saturated fatty acid components removed. Upon curing cationically, neat EGS polymer displayed T_g well above room temperature. Yet much higher T_g, *e.g.*, greater than 100 °C, and improved mechanical

properties compared to other bio-based systems were obtained through selection of curing agents and catalysts.

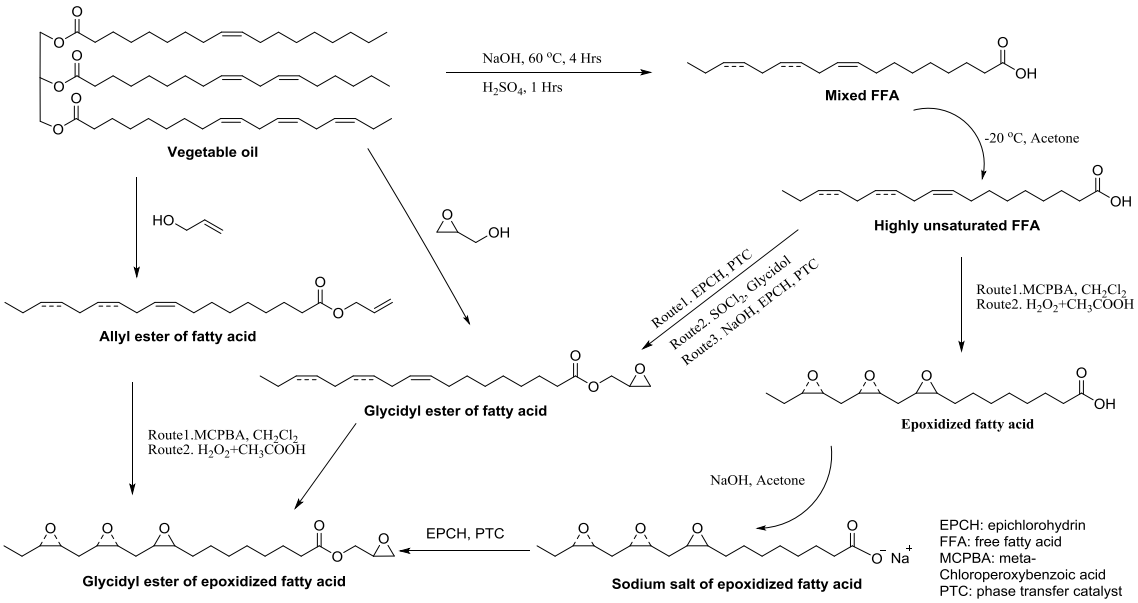

Scheme 9. Synthesis of glycidyl esters of epoxidized fatty acid (EGS, EGL).

4. CURING REACTIONS OF EPOXIDIZED VEGETABLE OILS

The polymeric materials of EVO are crosslinked networks of three dimensional structure through use of curing agents. There are two types of curing agents, catalytic and co-reactive. The catalytic curing agents initiate polymerization of the EVOs themselves, *i.e.*, through homopolymerization, whereas the co-reactive curing agent behaves as a comonomer for EVO. The curing process is bond formation through a combination of step-growth and/or chain-growth mechanisms. Due to the polarity of C-O bonds, the electron deficient carbon of oxirane constitutes an active site for nucleophilic reactions while the electron rich oxygen atom can afford an electrophilic

reaction site. The rate of curing is dependent on temperature, curing agent and thus mechanism, as well as the type and number of epoxy groups present in the chemical structure.

Despite a large volume of literature on the reactivity of EVO that can be in conflict, there is a consistency in its general conclusions: due to the sterically hindered and electron donating alkyl substituents, the rate of reaction of EVO with nucleophilic curing agents is lower compared to glycidyl (terminal) epoxy, while the rate is higher with electrophilic curing agents. For instance, EVOs react especially sluggishly with common polyamine curing agents.[48, 58] It is not/or uncommon for some EVOs to show no or reduced degree of curing due to the low reactivity and/or low oxirane content. In many ways, the curing behaviors of EVOs are analogous to the commercial cycloaliphatic epoxies rather than the DGEBA. Polyacids and their derivative anhydrides, plus the cationic catalysts, are commonly used curing agents for EVOs.

4.1. ADDITION WITH POLYAMINES

Polyamines are very frequently used curing agents for epoxy resins. The overall reaction rate of amines with epoxy resin is influenced by structure and electronic properties of the amine. The nucleophilic reactivity of amines generally follows the order: aliphatic > cycloaliphatic > aromatic. Where the EVO molecules have long, flexible, and aliphatic structure, cycloaliphatic or aromatic amines can compensate for this shortcoming through their rigid structures. Cyclic curing agents favor applications with high thermal and mechanical strength requirements[59-61] but require higher curing temperature and longer reaction time.[62]

The main reaction of polyamines with epoxy is through a step-growth polymerization mechanism without formation of byproducts (Scheme 10). A primary amine with two active hydrogens can consume two epoxy groups while a secondary amine will only consume one. A tertiary amine group, which has no active hydrogen, is not bond forming with epoxy but instead behaves as a catalyst to accelerate epoxy-amine reactions. Thus, curing with polyamines is an auto catalytic process. However, polyamines are less efficient curing agents for EVO because of a lower reactivity of internal epoxy as mentioned above. Accelerator or high temperature is required to cure EVO even for nucleophilic aliphatic amine, which can cure DGEBA at room or low temperature. In addition, esters groups will react with primary amine and form alcohols and amides, *i.e.*, via ester-aminolysis reaction.[63] Epoxy monomers may be also attacked by the hydroxyl group of the reaction product especially under high temperature, a source of uncertainty during formulation.

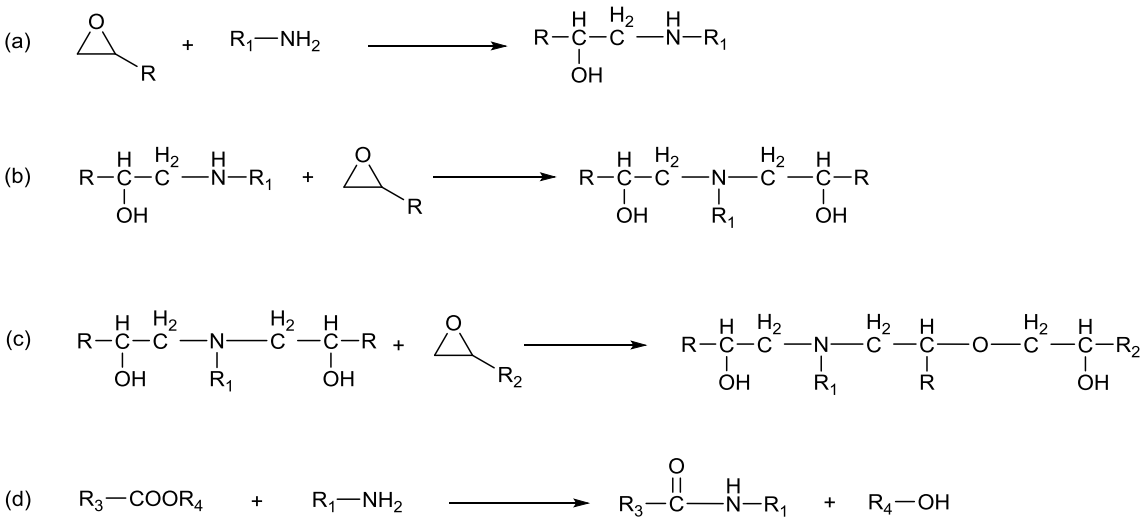

Scheme 10. Mechanism of primary amine cure of an epoxy resin: (a) through a primary amine; (b) through a secondary amine; (c) through hydroxyl group generated from reactions a and b; and (d) ester-aminolysis reaction.

Autocatalytic curing behaviors were observed by Manthey *et al*.[64, 65] in curing epoxidized hemp oil (EHO) with triethylenetetramine (TETA) and/or isophorone diamine (IPD), the addition of IPD was found to increase the curing rate of the EHO with TETA. A modified Kamal autocatalytic model indicated a decrease of reaction order with increase in temperature and a negative activation energy (E_a) was also observed. The authors believed this was due to an unidentified competitive reaction at higher temperature. Two different mechanisms, depending on the temperature for the epoxidized methyl oleate (EMO) and aniline system, were postulated by del Río *et al.*[66] The mechanism was autocatalytic at lower temperatures and non-autocatalytic at higher temperatures which favored an ester aminolysis reaction and lead to thermoset polymers of poor quality.

The Reaction mechanism of EVO with polyamines has been determined by Fourier transform infrared spectroscopy and nuclear magnetic resonance. Wang *et al.*[67] found only one of two adjacent epoxy groups in the same fatty acid chain takes part in the ring-opening reaction due to the steric hindrance. While internal epoxies have higher reactivity with primary amines than ester groups, partially crosslinked ESO structures were broken by aminolysis reactions. Secondary amines are unreactive with ester groups. Miao *et al.*[68] also found that some ESO epoxy groups showed low reactivity especially after partially curing with isopropanol amine. Lu[69] found the secondary amine of bis (4-aminocyclohexyl) methane (PACM) was left unreacted in the cured ESO network, which lead to lower crosslink density and the extent of aminolysis side reaction was decreased by lower amine concentrations.

The fact that hydroxyl compounds, water, alcohol, phenol, acid, *etc*., can accelerate the reaction between epoxides and amine compounds is widely recognized in commercial epoxy formulations. Hydroxyl groups catalyze the reaction through the formation of a trimolecular complex, which facilitates nucleophilic attack of the amino group.[70] Interestingly, these strategies are less applied toward EVO-amine curing systems. In contrast, Lewis acids have been used to catalyze EVO-amine reactions.

Harry-O'kuru[71] found the ring opening of internal epoxy in EVO with dibutylamine under anhydrous $ZnCl_2$ catalysis was facile and the reaction proceeded smoothly at moderate temperatures with only trace amounts of amide by-product. Stannous octoate also can significantly reduce the onset and peak exothermic temperature of ELO curing with 4,4'-methylenedianiline.[48] BF_3-amine has been used to accelerate reaction of ESO with cycloaliphatic and aliphatic amines.[69, 72] The chemistry of the Lewis acid catalyzed cure process is rather complex, both step-growth and chain growth mechanisms are operative. Besides the amine curing reaction, homopolymerization of epoxides and ester aminolysis may also take place depending on curing agents and curing conditions.

4.2. ADDITION WITH ANHYDRIDES

Anhydride reagents are the principal curing agents for EVO due to their improved reactivity with internal epoxy. The reaction of anhydrides with epoxy groups is complex and several competing reactions take place at the same time.[73] However, without accelerator the reaction is both slow and incomplete. Anhydride is first initiated by hydroxyl (Scheme 11a) and the newly formed carboxyl group reacts with an epoxy group to form a hydroxyl diester (Scheme 11b). The hydroxyl diester can react with anhydride

to generate another carboxyl group for reaction propagation (Scheme 11c). The hydroxyl-epoxy reaction existed especially at high temperature (Scheme 11d). If directly using polyacids as a curing agent, the initial mechanistic steps are not necessary as the reaction can be initiated by the protonation of epoxy groups followed by attack of carboxylic acid in a stepwise manner. At high temperature the esterification between carboxylic acid and hydroxyl groups will occur (Scheme 11e) and generated water can hydrolyze the epoxy groups (Scheme 11f).[74] Under alkaline catalysis such as with tertiary amine or imidazole, the carboxylate ion, which is generated by deprotonation of the acid at the beginning of the reaction, will act as a nucleophile in the epoxy ring-opening reaction. While etherification and condensation esterification reactions require the presence of unreacted epoxide or carboxyl groups, the former reaction is faster and the latter generally requires higher temperature.[75]

Unlike epoxy-acid curing, Lewis base-catalyzed epoxy-anhydride reactions proceed much faster through a chain-growth manner including initiation, propagation, and termination or chain transfer steps.[76] The initiation mechanism with tertiary amines or imidazoles is not well understood and appears complex. The suggested curing mechanism[1] follows: Base accelerators catalyze curing reactions by the generation of carboxyl anions with anhydride (Scheme 11g). The carboxylate ion then acts as a nucleophile in the ring-opening of the epoxide, resulting in an alkoxide (Scheme 11h). The alkoxide anion in turn ring-opens an anhydride group to generate a carboxylate anion (Scheme 11i).[77] Continuation of these alternating steps results in a polyester. Etherification between epoxy and alkoxide anion is less likely.[78]

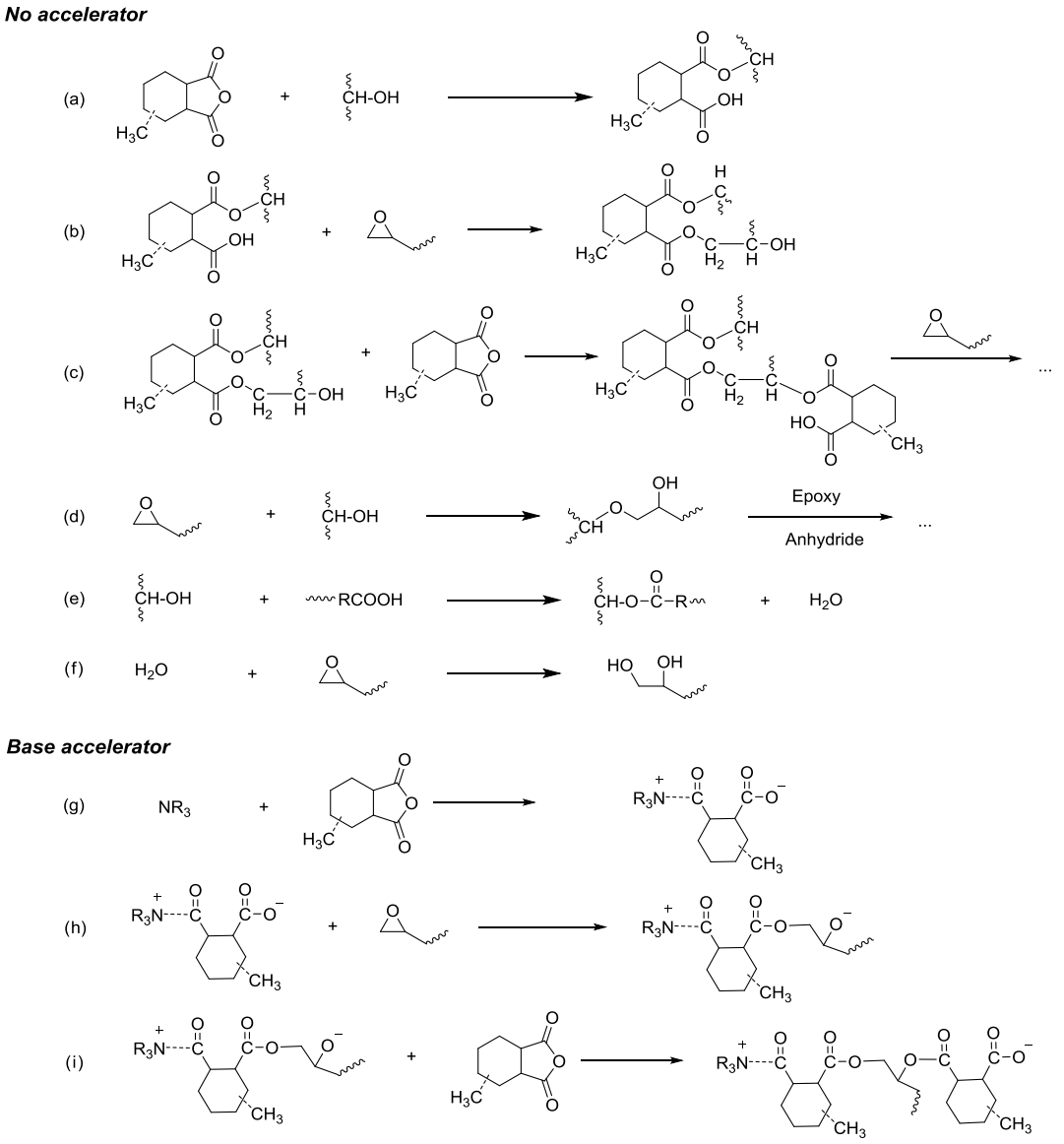

Scheme 11. Proposed reaction mechanisms of anhydride with epoxy.

Boquillon and Fringant[79] modeled the cure kinetics of an ELO-tetrahydropthalic anhydride system catalyzed with 2-methylimidazole using differential scanning calorimetry (DSC) and an *n*th-order rate equation. The curing reaction of their system followed first-order kinetics at extents of cure above 0.7. Liang and Chandrashekhara[80] studied the catalyzed soya epoxy-anhydride curing system where the curing showed

autocatalytic behavior. The overall reaction order was approximately 2 based on the Kamal's autocatalytic model using the DSC and rheology results. Using the same model, Tan *et al*.[81] studied a methylhexahydrophthalic anhydride cured ESO system in the presence of 2-ethyl-4-methylimidazole (EMI) catalyst. The EMI content and curing temperature showed significant influences on reaction rate constant and reaction order. The overall reaction order ranged from 1.5-3.0 and the E_a were decreased with increase in EMI catalyst concentration.

Kinetic analysis of a similar 1-methyl imidazole catalyzed ELO-methyl nadic anhydride system by iso-conversion methods found that E_a increased at the beginning of the curing and decreased as crosslinking proceeded.[82] The increased E_a might be due to the slow initiation mechanism by catalyst and the decrease in E_a by gelation and vitrification or autocatalysis. The curing kinetics of EMO and epoxidized biodiesel of sunflower and linseed oils origin with cis-1,2-cyclohexanedicarboxylic anhydride catalyzed by triethylamine was investigated by Nicolau *et al*.[83] Their results indicated E_a was related to the oxirane content and to locations of the oxirane in the fatty acid structure. The oxirane at (C9–C10), which is closed to ester group, showed higher E_a than those of oxirane at positions C12–C13 or C15–C16. The difference may be due to steric hindrance.

4.3. CATIONIC POLYMERIZATION

Catalytic ring opening of EVO by Lewis acids is well known[84] and improves reactivity compared to either polyamines or anhydrides alone. Boron trihalides, super acids, have been widely used for cationic cure of EVO. Due to high reactivity and concomitant difficulty in handling, these catalysts are generally added as latent

complexes, which are inert under normal conditions, such as ambient temperature, but release active species upon external stimulation, such as with heating or photoirradiation. A boron trifluoride ethylamine complex ($BF_3{\cdot}NH_2C_2H_5$) is used extensively in commercial epoxy formulations. Catalytic polymerization of ESO by boron trifluoride diethyl etherate ($BF_3{\cdot}OEt_2$) and superacid of fluoroantimonic acid hexahydrate ($HSbF_6{\cdot}6H_2O$) has been well developed by Liu *et al*.[85-88] The biodegradable polymers prepared by this method find application in personal care/health care upon further chemical functionalization.

Due to the various advantages, such as lack of oxygen inhibition and "dark" reaction post-polymerization (occurring after ceasing photo irradiation), photo-induced cationic curing of epoxy resins is a rapidly growing method for the application of coatings, inks and adhesives.[89] The newly developed photo-initiated systems by Tehfe *et al*.[90] showed high efficiency even when induced in air via solar irradiation. Photosensitive onium salts, such as aryliodonium or triarylsulfonium salts of group VA elements, are promising photoinitiators in curing EVO.[91] The photolysis of onium salts produces a mixed radical-cation species upon UV irradiation. The superacid species will activate epoxy as oxonium ion, which is attacked by other epoxies and propagates as a chain-growth mechanism (Scheme 12).

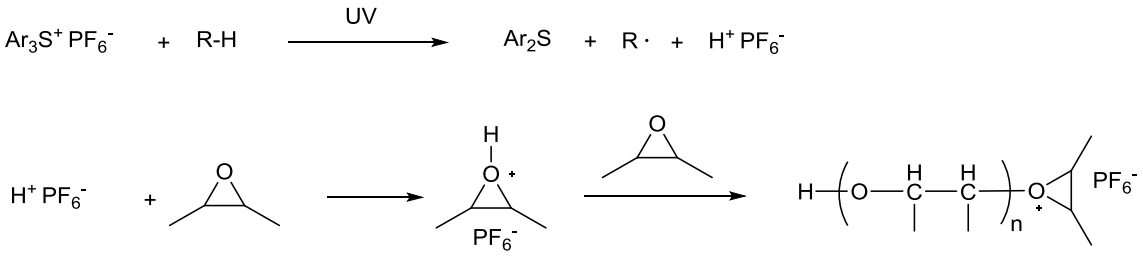

Scheme 12. Proposed mechanism for photoinitiated cationic polymerization of epoxy.

Crivello[26] reported the curing rate of strong acids derived from photo-initiator followed the order: HSbF6 > HAsF6 > HPFB, since with lower nucleophilicity of the counter anion SbF_6^- the tendency for chain termination is minimized.[92] The rate of the cationic photopolymerization of EVO could be enhanced by the addition of hydroxyl groups or presence of moisture (humidity), which can reduce the E_a and shift the curing toward an activated monomer mechanism due to the higher nucleophilicity of a hydroxyl compared to an epoxide (Scheme 13).[93] Ortiz[94] reported that alcohol or water promotes a more rapid transfer of protonated oxonium species to monomer to speed up the entire propagation process. Due to the presence of both epoxy and hydroxyl groups, epoxidized castor oil (ECO) has been shown to have better reactivity than ELO or ESO when using diaryliodonium salt photoinitiators.[95] However, too much hydroxyl groups or water can also act as a chain transfer agent thus retarding the chain growth process and leading to softer polymer structures.[96, 97]

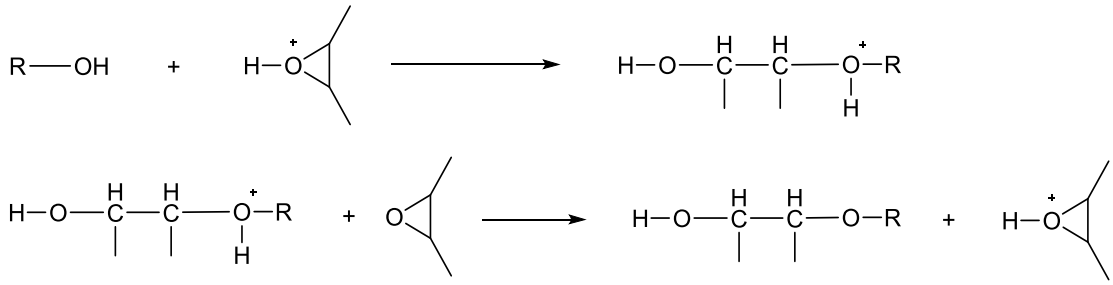

Scheme 13. Proposed acceleration mechanism of hydroxyl to cationic polymerization of epoxy.

Park *et al*.[98-100] used N-benzylpyrazinium hexafluoroantimonate (BPH) and N-benzylquinoxalinium hexafluoroantimonate (BQH) as thermally latent catalysts to cure

ESO and ECO. The BQH showed comparable curing activity for ECO at slightly lower temperature than that of BPH. Compared to ESO, ECO polymerization initiated at lower temperature when using the BPH catalyst. The authors also proposed that an observed variation in thermal and physical properties of resulting polymers was due to activities of the catalysts.

ENLOs showed higher curing rates than ELO during UV-initiated cationic polymerization, but were still slower than polymerization of cycloaliphatic epoxide, 3,4-epoxycyclohexylmethyl-3,4 epoxycyclohexane carboxylate. The lower reactivity of ENLOs compared to cycloaliphatic epoxide was attributed to a greater steric hindrance present in the epoxybornyl groups and to a higher viscosity.[40] During cationic photopolymerization, the relative reactivity of the oxiranes was found to be not as important as viscosity of the reacting system. The polymerization rate was observed to be diffusion controlled where adding diluents such as divinyl ethers can markedly accelerated the curing rate and overall conversion rate of epoxy.[41]

4.4. MISCELLANEOUS CURING AGENTS

Epoxy can also be polymerized in anionic fashion for precise control of molecular weight and polydispersity as well as chain functionality.[101] Tertiary amines, imidazoles, and ammonium salts, are commonly used anionic catalysts for epoxy resin homopolymerization although their induced curing mechanisms are very complex and not universally accepted.[102] Boonkerd *et al*.[103] successfully synthesized a bio-based elastomer using post-living anionic polymerization of poly(butadienyl)lithium and ESO; however, the strongly nucleophilic anions preferentially cleaved ester groups rather than inducing ring-opening of epoxy. Due to a higher oxirane content, ESO is more reactive

than EMO for anionic epoxy ring-opening polymerization. While a pyridine-initiated epoxy reaction between ESO and 4-methylpyridine and poly(4-vinylpyridine) has been reported by Öztürk and Küsefoğlu,[104] no homopolymerization of the epoxy groups as initiated by pyridine was observed. Instead, pyridine addition followed by rearrangement to a pyridone derivative was observed.

Del Rio *et al*.[105] used coordination catalysts to polymerize EMO. Two main polymerization mechanisms, cationic and the ionic-coordinative, were observed with the former being predominant. Yielded polymers were a mixture of cyclic and linear structures with different end groups depending on the initiator used but a higher molecular weight was obtained than with conventional cationic catalysts. Transesterification side reactions lead to the formation of branched structures containing ester groups in the main chain. The prepared polymers could be used as polyether polyols for polyurethane applications.

Dicyandiamide (DICY) is one of the most popular curing agents for DGEBA. Zhao *et al*.[106] reported rapid cures of either neat ESO or ESO-DGEBA blends using DICY at 190 °C or 160 °C, respectively. Carbonyldiimidazole was used as an accelerator. The optimum stoichiometric molar ratio of epoxy : DICY was found to be 3 : 1. The first two epoxy units reacted with the amine groups of DICY to produce secondary alcohol and secondary amine. The produced secondary amine will not attack another internal epoxy and the remaining epoxy unit was linked to the DICY nitrile group.

5. POLYMER STRUCTURE AND PROPERTY

A good understanding of structure–property relationships is critical when designing VO based epoxy thermosets for various applications.[57] However, elucidating a VO based thermoset polymer structure is quite difficult due to the heterogeneous content of monomers and of the cured polymers. For instance, the fatty acid composition of VO varies not only from plant to plant but also within oils of the same plant. Unreacted monomers, dangling chains, and intra-crosslinking are common for VO-based thermoset polymers.[107-110] The structure and distance between the crosslinked positions, in terms of crosslink density, are an important characteristic when describing the structure of thermoset polymers. Dynamic mechanical analysis has been widely used to calculate crosslink density based on the rubber network elasticity theory. The T_g, which is unique for each epoxy system, also reflects crosslink density where it is generally observed that an increased crosslink density increases T_g. That cured VO resins range from soft rubbers to hard plastics mainly depends on not only the chemistries and structures of epoxy monomer but also the curing agent. Other factors include polymerization conditions, monomer ratios, and catalyst, *e.g.*, as described in previous examples.

5.1. EPOXY RESINS

For VO-based epoxy monomers, the types of epoxy structure and oxirane content greatly influence the thermoset polymer thermal and physical properties.[99, 111] A terminal epoxy and/or high oxirane content can lead to rapid gelation and high crosslink density.[42, 48] EVOs of low oxirane values either are not reactive or impart waxy properties of poor strength to the polymer system.[37] The effect of oxirane content of ESO on the mechanical properties of anhydride cured polymers were investigated by Tanrattanakul

and Saithai.[112] The mechanical properties such as tensile modulus, strength or toughness, and tear strength of the ESO thermoset polymers are controlled by the crosslink density and chain flexibility. Fully epoxidized ESO monomers of the highest oxirane content had cured polymers with the lowest elongation at break but higher storage modulus, thermal stability and T_g than less epoxidized, lower oxirane content counterparts. Due to a rich linolenic content, ELO possesses the highest oxirane content among common EVOs. Thus cured ELO thermosets generally haven shown higher crosslink densities, T_gs, and moduli.[113]

A series of epoxy resins with different structures, oxirane contents and contents of saturated fatty acid were synthesized by Wang and Schuman[57] in order to examine structure-property relationships. Both anhydride cured ESO and ELO showed broader T_g regions that indicate a broader distribution of chain environments and more heterogeneous polymer structures due to less reactivity of internal oxirane and presence of saturated fatty acids. The T_gs of either methylhexahydrophthalic anhydride (MHHPA) or BF_3-amine cationically cured thermoset polymers were observed to increase fairly linearly with oxirane value (Scheme 14). Linseed oil based epoxies, such as ELO and EGL, had much higher T_g compared to their respectively ESO or EGS counterparts of lower oxirane content. Removal of saturated components greatly increased the T_g. A 30 and 20 °C increase in polymer T_g was observed for MHHPA cured EGS and EGL compared to EGS-S and EGL-S, respectively. Such trends were also observed in crosslink density measurements as a significant increase of crosslink density upon removal of the saturated components. Due to the loss of glycerol as a crosslink site and liberated saturated fatty acid esters, the addition of an unreactive function group to ester

end, *e.g.*, an allyl (EAS) or methyl group (EMS), generated even lower T_g and polymer crosslink density though the oxirane values are similar to those of ESO. The results reiterate the reported, very low T_g of an epoxidized biodiesel polymer.[114]

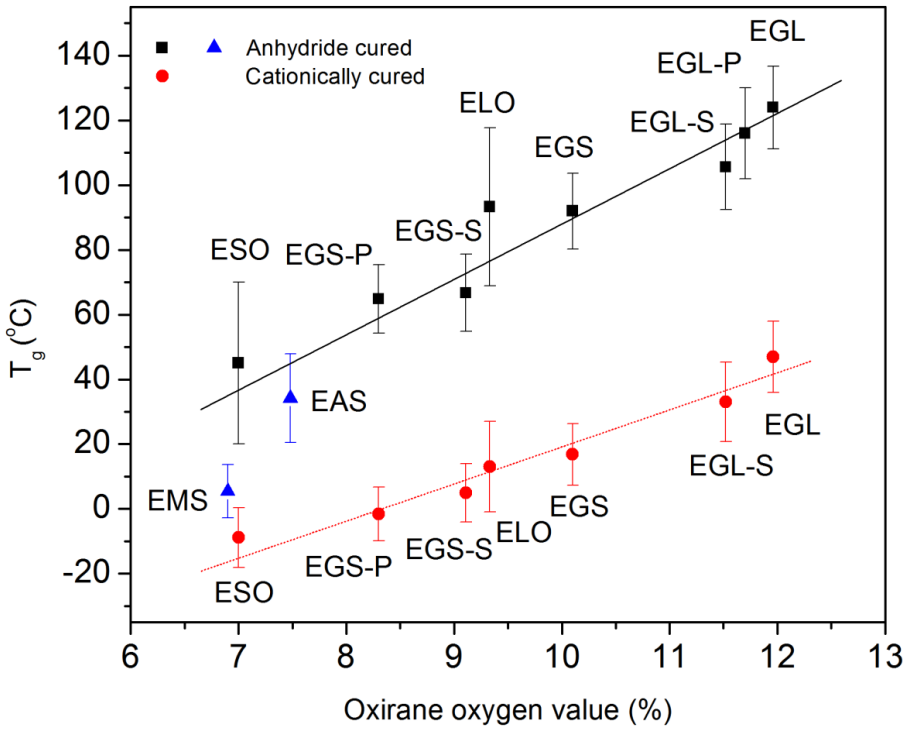

Scheme 14. Measured T_g as a function of oxirane content [-P: partially epoxidized; -S: monomer where saturated fatty ester content was not removed.] NOTE: vertical "error bars" are indicating a breadth of the glass transition and polymer heterogeneity.[57]

5.2. CURING AGENTS

The influence of the curing agent is just as critical to the final properties of thermoset polymers as the epoxy resin component. Since curing agent will become part of the crosslinked network structure, special attention should be paid to structure and stoichiometry. Lu[69] found that aromatic polyamines were unable to react with ESO. Polymer produced by aliphatic TETA was rubbery with a T_g of 15 °C. Cycloaliphatic

polyamines, such as PACM, reacting with the same ESO monomer enhance the T_g to 58 °C, where the highest flexural strength was achieved at a ESO/PACM molar ratio of 0.53:1. Juangvanich[72] also found that the reaction of diaminodiphenyl sulfone or 4,4'-methylenedianiline with ESO did not occur even at high temperatures. Aromatic amine, *e.g.*, p-phenylenediamine, reacted to a smaller extent compared to that of curing with a more nucleophilic aliphatic amine. An imperfect network was formed when using p-phenylenediamine as a curing agent due to the intramolecular crosslinking.

Anhydride is one of the most important curing agents for EVO. Gerbase *et al.*[115] investigated the mechanical and thermal behavior of ESO cured with various anhydrides in the presence of tertiary amine accelerators. Thermosets showed higher T_g, storage modulus, and crosslink densities when the system was cured with the more rigid phthalic, hexahydrophthalic, or maleic anhydrides than more flexible dodecenylsuccinic or succinic anhydrides. Similar results were also reported by Rösch.[116] Due to the effects of steric factors and the rigidity of the formed diester segment, ELO cured by phthalic anhydride and methyl-endomethylenetetrahydrophthalic anhydride in the presence of 2-methylimidazole showed lower crosslinking densities than those cured with cis-1,2,3,6-tetrahydrophthalic anhydride.[79]

In addition to the structure of anhydride, a variation in stoichiometric ratios of epoxy/anhydride was also found to have significant effect on the resulting of network structure and performance of thermosets. From the epoxy-anhydride polyesterification curing mechanism,[117-119] the maximum crosslinking degree, storage modulus, and T_g may be achieved at a stoichiometric ratio R=1.0. However, in practical formulation, less than stoichiometric ratios are commonly used to achieve balanced properties and also account

for competitive reactions such as epoxy homopolymerization. The reaction of ELO with cis-1,2,3,6-tetrahydrophthalic catalyzed by imidazole indicated complete conversion at the stoichiometric ratio of R=0.8. The increase in anhydride to R=0.8 caused an increase in T_g and stiffness but at a sacrifice of chain mobility. The T_g was reduced for R>1 due to reduced crosslink density.[79]

5.3. CATALYSTS

Due to the low reactivity of EVO during nucleophilic curing reactions, a choice of catalyst and its amount are critically important that strongly influence crosslink density, network morphology/structure, and ultimate performance.[77, 120] Lewis acid catalysts are commonly used for the EVO-amine curing reaction, *e.g.*, stannous octoate catalyst in an ELO and 4,4'-methylenedianiline curing system.[48] The onset and peak temperature of the reaction exotherm were significantly reduced while the polymer T_g was increased more than 20 °C. Tertiary amine, imidazole, and quaternary ammonium salts are commonly used catalysts for polyacids or anhydride curing of EVO.

The use of imidazoles has advantages compared with tertiary amines in improving the T_g,[121] which may due to a reaction of imidazole with the epoxy.[122] Supanchaiyamat *et al.*[75] reported that the mechanical and thermal properties of diacid cured ELO films were significantly influenced by the type of amine catalyst selected. Both 1-methylimidazole and 4-dimethylaminopyridine (DMAP) can significantly enhance the mechanical properties of the resulting films. For DMAP, etherification may occur due to good nucleophilicity. The curing speed is highly sensitive to the catalyst amount, where the optimum DMAP catalyst concentration was 1 wt.% of total ELO and crosslinkers. Further increase of the DMAP concentration decreased the Young's modulus.

In 2-ethyl-4-methyl imidazole (EMI) catalyzed ESO-MHHPA curing system, Tan and Chow[123] found the rate of polyesterification, the degree of conversion, T_g, storage modulus and crosslink density were improved at higher EMI concentrations. However, a continued increase in the catalyst concentration lead to rapid gelling but reduced conversion due to hindered monomers/oligomers diffusion.[79] Tan and Chow[124] also compared the type and concentration of catalysts on the fracture mechanics of MHHPA cured ESO thermoset polymers. The improvement in fracture toughness with catalyst concentration was due to an increase of degree of cure, while extreme crosslink densities lead to catastrophic brittle fracture and low fracture toughness. For EMI catalyst, fracture toughness increased with an increase in concentration of EMI whereas a reduction of fracture toughness was observed when using tetraethylammonium bromide as catalyst and its concentration exceeded 0.5 wt.%.

6. POLYMER BLENDS OF EPOXIDIZED VEGETABLE OILS

As mentioned above, an EVO can be polymerized with a variety of curing agents. The cured thermoset polymers, however, generally show low thermal/mechanical performance and crosslinking density due to their flexible structure and lower reactivity compared to DGEBA and cycloaliphatic epoxy. Commercially available epoxies such as DGEBA and cycloaliphatic epoxies possess stiffer structures thus EVOs can be blended with these petroleum-based epoxy monomers to mutually improve mechanical and thermal properties. EVOs generally have lower viscosity, so EVOs or their derivatives can be used as reactive diluents for DGEBA resins, which are relatively high viscosity liquids or solids, to decrease overall cost and improve the processability. Due to a less

homogeneous structure, ESO is less efficient in reducing the viscosity of epoxy resin compared to many petroleum-based reactive diluents.

Strictly speaking, EVOs are not always "reactive." There can be an especially large difference in the reactivities of EVO and DGEBA and heterogeneous structures, such as phase inversion, may form and inevitably lead to a significant decrease in performance of cured polymer. Therefore, few to no reports of high concentration (> 50 wt.%) in DGEBA exist because low oxirane content and an unreactive saturated component in EVO both lead to a lower crosslink density upon cure and the saturated fatty chains affect miscibility between EVO and the DGEBA. Compositions with low EVO diluent content mostly preserve the undiluted polymer thermal and mechanical properties, *e.g.*, of neat petroleum-based epoxy polymer. The blends can, though improve impact strength of the pure epoxy polymer, which may be brittle (*e.g.*, see Section 6.3).

6.1. STRUCTURE AND MORPHOLOGY

Epoxy monomer blends that contained EVO have produced heterogeneous structures such as phase separation or semi-miscibility[125] due to different reactivity of the epoxies as a function of the concentration of monomers and curing conditions. In addition, the initial miscibility/compatibility between epoxy monomers also plays an important role toward the formation of heterogeneous structures. The Flory-Huggins equation combined with Hilderbrand solubility parameters was used to assess the compatibility of DGEBA with ESO and EGS.[57] Compared to ESO, the solubility parameter of EGS monomer was more similar to that of DGEBA compared to ESO, EGS monomer of lower molecular weight and higher reactivity produced EGS-DGEBA blends

with improved homogeneity and mechanical strength compared to analogous ESO-DGEBA systems.

ESO less efficiently dissolves into and plasticizes, the rigid DGEBA matrix but still becomes part of the crosslinked structure at low concentration. At higher ESO concentrations *e.g.*, > 70 wt.%, a faster gelation of DGEBA occurring at low degree of conversions of ESO can lead to a phase separation or defect structures. Transparent ESO-DGEBA blends can still be produced by catalyst selection or choice of curing condition (Scheme 15). A transparent morphology does not necessarily indicate homogeneity.

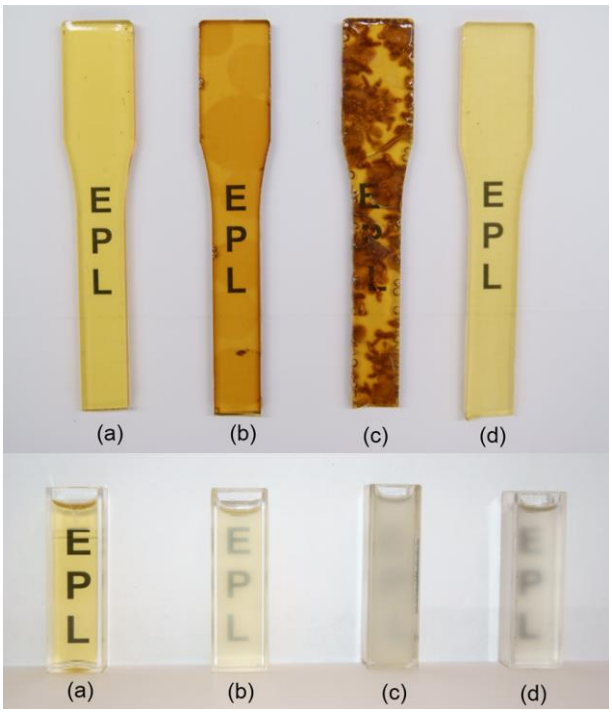

Scheme 15. Physical appearance of MHHPA cured EGS/ESO-DGEBA polymers and uncured monomer blends: (a) EGS-DGEBA (90:10); (b) ESO-DGEBA(90:10) precured at 145°C for 10 min; (c) ESO-DGEBA (90:10) without procuring; and (d) pure ESO inducted for 12 hrs.

Transparent ESO-DGEBA blends cured by methyltetrahydrophthalic anhydride were prepared by Altuna.[126] Despite optical clarity, phase separations at 40 wt.% and 60 wt.% ESO concentration were observed by SEM or through a change in intensity of the transmitted light. The phenomenon was ascribed to a match of refractive index between the dispersed ESO phase and the continuous phase. In a similar system but with methyl nadic anhydride as curing agent, Chen *et al.*[127] observed phase separated structures at only a 20 wt.% ESO concentration by SEM. The two-phase structure was explained a result of different reaction rates of ESO and DGEBA under the applied curing conditions. Transparent ESO-DGEBA blends of single glass transition were observed by Karger-Kocsis *et al.*[128] Atom force microscope inspection of the plasma etched samples clearly indicated a two-phase structure of dispersed domain size of about 100 nm, *i.e.*, smaller in size than the wavelength of visible light.

Due to the even lower reactivity of EVO with amine curing agents than anhydrides, compared to that of DGEBA, an EVO component in EVO-DGEBA blends is either not reactive or proceeds via different reaction mechanisms. Therefore, heterogeneous structures such as phase separation are more common than in anhydride polymerizations but are still related to the EVO structure, concentration, and reaction process and conditions. Using epoxidized crambe oil as epoxy monomer and 4,4'-diaminodiphenylmethane amine curing agent, Raghavachar *et al.*[129] found the epoxidized crambe oil was only partially compatible with the DGEBA and formed a two-phased structure after direct mixing and curing. ESO of molecular weight lower than epoxidized crambe oil is more compatible with DGEBA.

Using TETA as curing agent, a plasticizing effect was observed when directly mixing ESO into DGEBA and polymerized. Phase separation could be induced by two-stage mixing where ESO was first reacted with TETA to form pre-polymers.[130] Similar research was also conducted by Sarwono *et al.*[131] in epoxidized palm oil (EPO)-DGEBA system crosslinked by xylylenediamine. Directly mixing 10 wt.% EPO into DGEBA or EPO pre-polymers reacted with amine less than 2 hrs showed opacity, *i.e.*, phase separation. More transparent blends were obtained by synthesizing EPO pre-polymers, reacting longer than 2 hrs at 120 °C. Frischinger and Dirlikov[132] prepared liquid rubber pre-polymer of EVO with amine as rubbery particles of 15 to 30 wt.%, randomly distributed in a rigid DGEBA matrix. Phase inversion was observed at higher, intermediate rubber contents of 30 to 35 wt.%. However, homogeneous morphologies were also observed at either lower or higher rubber contents, *i.e.*, > 70 wt.%. Authors concluded that the particle size and concentration of phase inversion depended on the miscibility between the rubbery and DGEBA phases that was regulated by the nature of the EVO pre-polymer.

6.2. THERMAL AND MECHANICAL PROPERTIES

Although a polymer blend is a simple idea, in combining the advantages of EVO and petroleum-based epoxies a combination is not always successful. As with earlier discussions, lower reactivity and oxirane content generally shift the onset and peak reaction temperature higher. At the same time, a decrease of reaction heat or an increase in E_a has been observed.[128] Unreactive EVO monomers and/or an inherently flexible structure plasticize the rigid epoxy matrix such as DGEBA.[133] At high EVO concentration, the polymerization may occur in two stages to form heterogeneous

structures. EVO components can not only reduce the crosslink density but also can behave as a weak point or flaw under application of load where fracture is prematurely initiated by stress concentration at structural weak points. Adding EVO into petroleum-based epoxies has been frequently observed to decrease mechanical strength, T_g, thermal stability, and chemical resistance.[134]

The concentration of EVO in polymer blends, cost, and acceptable property loss are important considerations during epoxy formulation. To retain optimum properties, the concentration of ESO was limited. An addition of < 40 wt% ESO into DGEBA produced storage modulus and T_g compared to neat DGEBA polymers, but with a 38 % increase in impact strength and without loss of transparency.[126] An abrupt decrease in T_g and flexural strength/modulus at high ESO concentrations, *e.g.*, > 50 wt%, were observed by Wang and Schuman.[57] The properties appear predominately controlled by the ESO part, *i.e.*, to form heterogeneous structure of less synergy between ESO and DGEBA. A non-linear transition of properties and lack of synergy between epoxy monomers was observed in anhydride cured ESO-DGEBA system. The Gordon-Taylor equation was applied to account for the T_g-composition relationship of this system. The interaction between ESO and DGEBA was only of medium strength.[135]

The optimum EVO concentration was also related to the structure of EVO, especially oxirane content. Heat distortion temperature (HDT) and tensile strength of EVO-DGEBA polymer blends were almost identical for either ESO or epoxidized lard oil up to 20 wt.% level. Since the oxirane content of ESO was much higher, at higher EVO concentrations the HDTs and strength of the epoxidized lard oil blends decreased more rapidly than the ESO.[38]

EPO is richer in saturated fatty acids and thus possesses lower oxirane content and more plasticizing effect than those of ESO. EPO-DEGBA blends showed significantly reduced T_g with an increase of EPO concentration. Polymer blends also showed higher coefficients of thermal expansion and tan δ due to increased free volume and chain flexibility in the crosslinked networks.[136] To retain thermal and mechanical performance a low EPO concentration, $\leq$ 10 wt.%, is necessary.[131]

ELO shows the highest oxirane contents among common EVOs. Miyagawa *et al.*[137] observed that crosslink densities, T_gs, and storage moduli of MHHPA cured diglycidyl ether of bisphenol F (DGEBF) systems remained relatively constant or were only very slightly decreased at up to 70 wt.% ELO loading and then started increasing again upon further increase in the ELO content. This abnormal phenomenon was ascribed to higher oxirane content of ELO such that more curing agent was required for proper formulation. In addition, ELO is rich in linolenic acid content that facilitates dense crosslinked structures. Thus, it was found possible to replace petroleum-based epoxy with ELO while still maintaining high performance.

However, amine cured ELO-DGEBF systems show a completely different trend.[138] The crosslink densities, T_gs, and storage moduli of blends decreased continuously with an increase of ELO concentration. The reduction of storage modulus was especially significant and T_g was but close to room temperature for ELO concentrations of greater than 20 wt.%. The trend is due to the much lower reactivity of ELO with amine curing agent and unreacted ELO can plasticize the rigid DGEBF matrix. A decrease of reaction exotherm, thermal stability and mechanical strength of isophorone diamine cured DGEBA with increase in epoxidized rapeseed oils or ESO concentration

was also reported by Czub[139, 140] where polymer blends of high EVO contents were highly flexible and properties were dominated by the EVO content.

Though cationic crosslinking of EVO generally shows higher reactivity than curing with amine or anhydride, it results in rubbery polymers since all the networks are composed of flexible fatty acid components. The addition of stiffer petroleum-based epoxies, cycloaliphatic or DGEBA can increase the EVO hardness and modulus.[141, 142] Adding EVO into DGEBA as a diluent not only reduces the viscosity but can shift polymerization temperature lower since the cationic reactivity of EVO is higher than that of DGEBA. Decker *et al.*[91] found that the addition of 20 wt.% ESO accelerated the photoinitiated cationic curing process of DGEBA and formed a relatively tight polymer network of better chemical resistance. Park[100] found polymerization of ECO-DGEBA blends initiated using BPH as catalyst had maximum onset decomposition temperature at 10 wt.% ECO content due to an optimum network structure. However, further increases in the EVO content still lead to decreased T_g, thermal stability, and crosslink density and increased coefficient of thermal expansion.[143]

6.3. EPOXIDIZED VEGETABLE OIL AS TOUGHENING AGENT

Epoxy thermoset polymers may suffer low toughness or brittleness due to stiff structures with high crosslink densities. Various methods, include the addition of a either rigid or soft secondary phase, the chemical modification with a flexible backbone, or a lowering of the crosslink density of the polymer, have been attempted to improve epoxy toughness.[144] The addition of rubbery compounds to form phase-separated inclusions has been proved to be one of the most effective methods for toughening epoxy to avoid major deterioration of thermal and mechanical properties. The toughening mechanism is

generally thought due to increased shear yielding of the rubber phases at low strain rate and cavitation at high strain rates.[145]

EVOs ability to form heterogeneous phases with petroleum-based epoxies has been found beneficial as reactive toughening agents in epoxy or other engineering plastics.[146, 147] As mentioned above, for EVO-DGEBA polymer blends the mechanical and physical properties of an EVO toughened epoxy are closely related to the network structure in terms of the EVO compositions, phase morphology, crosslink density and the chains flexibility. Most polymerized EVO are of rubbery state but also depend on the curing system. A crosslinked EVO structure can efficiently absorb, transform and dissipate fracture energy through deformation of molecular networks analogous to common rubbery compounds. Researchers have shown that EVO polymers possessed better toughness than those of stiff, neat epoxies and that the incorporation of EVOs into epoxy can improve impact strength.[135, 139, 140, 148, 149]

Shabeer *et al*.[150] found the fracture toughness of anhydride cured DGEBA polymer was greatly improved more than 200% with substitution of 75 wt.% DGEBA with epoxidized allyl soyate (EAS). Increase in fracture toughness of the blend was attributed to lesser degree of crosslinking. A ductile fracture behavior at the high concentration of EAS resin was observed. However, improvement was also associated with greatly reduced storage modulus, T_g and crosslink density, *e.g.*, the T_g of 75 wt.% EAS blend was only 40.5 °C compared to a 90 °C of neat DGEBA polymer. Anhydride cured ELO-DGEBF showed single phased structure and no apparent improvement in toughness up to 50 wt.% ELO. A further increase in ELO content even resulted in a decrease of fracture toughness and Izod impact strength[137] while a 30 wt.% ESO showed

improvement in toughness due to phase separation of rubbery ESO particles within the rigid DGEBF matrix.[151]

Tan and Chow[152] indicated the plasticizing effect of EPO, which is rich in saturated components, improved the fracture toughness of DGEBA by enhancing flexibility through cavities occupied by unreacted EPO that increase resistance to deformation, crack initiation and propagation. The crosslink density and water absorption capability of the EPO-DGEBA polymer decreased with increase in the loading of EPO but other thermal and mechanical properties were not disclosed. Under thermally latent catalysis, Jin and Park[153] showed the Izod impact strength of a 60 wt.% ESO blend was 58% higher than the neat DGEBA but the flexural strength was also reduced more than 40%.

Amine polymerized ESO with 4,4'-tetradiglycidy diaminodiphenol methane resulted in a two-phased structure due to the incompatibility between epoxy monomers. The critical stress intensity factor was improved by 54 % at 10 wt.% ESO content. The flexural strength was also increased but thermal stability, crosslink density and T_g of the blends were slightly decreased with addition of ESO due to the incomplete curing reaction of ESO in the blend system.[154] An amine cured ELO-DGEBF showed improved Izod impact than neat DGEBF although no clear phase separation was observed, the crosslink densities and storage moduli of polymer blends were decreased, the T_g dropped almost 50 % for only 30 wt.% ELO, this probably due to the plasticizing effects of less reactive ELO.[138]

When directly mixing EVO into epoxy resulted in a single phased structure, the improvement in toughness was less impressive and was commonly associated with

decreased crosslink density, T_g, modulus of elasticity, and yield stress.[155] On the other hand, introduction of EVO liquid rubber pre-polymers into the epoxy resin has obvious advantages toward preparation of two-phase thermoset polymer over directly incorporating ESO monomer.[130] Through proper choice of curing profile, a two-phased structure can be formed. The impact strength of DGEBA can be markedly improved at a relatively low concentration of EVO with marginal sacrifice of thermal and mechanical properties.

Two-phase thermoset polymer that consisted randomly distributed small ESO rubbery particles (0.1-5 μm) in a rigid epoxy matrix were prepared by Frischinger and Dirlikov.[156] The liquid rubber pre-polymers were prepared from a stoichiometric mixture of ESO and 4,4'-diaminodiphenylmethane amine. The diamine molecules at the interface can react with epoxy groups of both DGEBA and EVO thus forming a strong interfacial bond between the two phases where no ejection or disbonding of rubbery particles was observed under shear deformation. These EVO rubber toughened epoxy showed slightly lower T_g and Young's modulus but remarkably improved toughness comparable to commercial, carboxyl-terminated butadiene-acrylonitrile rubber toughening agents.

Ratna[130] compared the effects of direct mixing (single stage) versus pre-polymer mixing (two stage) on amine cured DGEBA-ESO thermoset polymer morphology and resulting thermal, flexural and impact properties. A two stage mixing showed milder decreases in T_g and flexural and tensile strength than single stage mixing, in which high ESO concentrations usually lead to drastic reductions in these resulting properties. Network polymers made by a single stage process showed only a modestly increased impact energy as a consequence of nearer single-phase morphology. A significant

increase in impact energy was obtained for modified networks made by the two stage process at 20 wt.% ESO of phase separated morphology.[157]

7. EPOXIDIZED VEGETABLE OIL PAINTS AND COATINGS

Due to versatility, excellent adhesion to a wide range of substrates, and corrosion and chemical resistance, epoxy resins are widely used in coating applications.[78] EVOs have promise as alternatives or supplements to petroleum-based epoxies for a combination of attributes: low viscosity, low cost, and epoxy functionality. Use of EVOs in coatings not only provides the sustainable chemical content but also offers a way to reduce volatile organic compounds and, as just discussed, improve flexibility or toughness of epoxy coatings.[158-161] However, the challenge for neat EVO polymer coatings is to improve their mediocre mechanical and thermal performance, especially of polymer moduli and T_gs, which to date have prevented further market penetration. Copolymerization with petroleum-based monomers of rigid structure and/or an application of inorganic compounds to form blended or nanocomposites coatings, respectively, are frequently applied strategies to enhance EVO coating properties.[46, 92, 162, 163]

With similar reactivity towards cationic polymerization and stiffer structure, cycloaliphatic epoxy such as 3,4-epoxycyclohexylmethyl-3,4-epoxyhexane carboxylate is commonly used as comonomer with EVOs in coating applications. High-solids, cationically cured coatings based on cycloaliphatic epoxy resin, ESO and polyols were prepared by Raghavachar *et al.*[158] that had useful film properties as general-purpose coatings. A blend with 10 wt.% ESO gave a coating with similar performance as the cycloaliphatic epoxy control. With further increases in the ESO content, the hardness of

the coatings was decreased but was regulated by the structure of epoxy and polyol or adjustment in the epoxy/polylol ratio.

Coatings derived from epoxidized *Mesua ferrea L.* seed oil and DGEBA were prepared by Das and Karak.[160] The results indicate that the EVO not only reduced the viscosity of the DGEBA but also enhanced performance of the polymer. The performance of 50 wt.% epoxidized seed oil was further enhanced by formation of a nanocomposite using organically modified nanoclay. From 2.5 wt.% to 5 wt.% clay improved the alkali resistance of the prepared coating.

Ultraviolet (UV) initiated cationic polymerization of EVOs has been the subject of intensive research due to the convenience of curing at room temperature and fast curing rate.[39, 89, 91, 95] Bio-based coatings prepared by Thames and Yu[164] exhibited excellent adhesion, impact resistance, UV stability, gloss retention, and corrosion resistance properties. Vernonia oil or ESO that were blended with cycloaliphatic epoxy were used as epoxy resin and cationically UV initiated. The incorporation level of EVOs was formulated by their compatibility with other coating ingredients. Although both EVOs were compatible with cycloaliphatic epoxy at high concentrations the EVO epoxy blends were only partial compatible and formed hazy formulations with polyols or UV initiators. The pencil hardness and tensile strength of coating films decreased but the gloss retention was increased. Optimum properties in hardness, gloss and gloss retention were obtained at a 10 wt.% of EVO in the coatings.

Clear coatings containing ESO and cycloaliphatic epoxy resin were formulated by Gu *et al*.[165] using onium tetrakis (pentafluorophenyl) gallate catalyst. The gallate catalyst showed better solubility and reactivity towards the nonpolar monomer than common UV

initiation catalysts diaryliodonium or triarylsulfonium salts. Up to 50-60 wt.% ESO could be added to formulations without compromising the mechanical properties of the cured coatings.

Despite a current lack of optimum thermal and physical strength for commercial coating applications, high EVO based or pure EVO content coatings would be desirable for their high bio-renewable content. Goals for EVO development include improvement of T_g, hardness, moduli and strength. Inorganic-organic hybrids films have been synthesized from EVO and titania or silicon based or combined precursors.[166-171] These hybrid films generally showed improved properties, such as hardness, adhesion, chemical resistance, tensile strength and T_g, but strongly depended on the type and concentration of inorganic contents. Overloading the inorganic component lead to decreased fracture toughness and elongation at break. A sharp transition from ductile to brittle material when loading with inorganic precursors has been observed.[171]

8. COMPOSITES FROM EPOXIDIZED VEGETABLE OILS

Considerable attention has been focused on the development of VO-based composites due to their sustainable characteristics, greatly improved stiffness, modulus and strength.[172-175] A composite approach greatly expands the potential application of VO-based polymeric materials, where some have been successfully commercialized and have behaved well as promising alternatives to petroleum-based materials in transport and construction applications[176]. Recent development is more toward high performance bio-based materials and “green” composites for value-added and structural applications.[177-179] Based on the reinforcement type, EVO-based composites can be grossly divided into fiber reinforced polymer composites (FRP) and nanocomposites.

The fibers either natural or synthetic, can be continuous or chopped (short strand) of macroscopic scale. The particle size and surface area per volume of nanocomposites provides reinforcement at the nanoscopic level.

8.1. FIBER REINFORCED COMPOSITES

The mechanical strength of a FRP is dependent primarily upon the properties of the continuous phase reinforcement, while the matrix phase supports and binds the reinforcement together and distributes stress to the reinforcement. When designing a composite for a structural application, the polymer matrix must be strong enough to efficiently transfer stress amongst the reinforcement without initiation of cracks, *i.e.*, of sufficiently high crosslink density and of T_g higher than the temperature of its intended work environment. Since most pure EVO polymers generally show lower crosslink density and T_g, even below room temperature, polymer blends of EVO with DGEBA have been frequently applied as polymer matrices for FRC.

Some research has shown that EVO were best limited as minor component in blends, *i.e.*, < 30 wt.% because the solely EVO component could not provide the mechanical and thermal properties desired for an FRC.[61, 180] Pure EVO or high EVO content (*e.g.*, > 50 wt.%) based polymer matrices for high performance composites applications are rare and more suited for non-structural applications.[181-184]

Glass fibers are one of the most widely used reinforcement materials in epoxy composites because of their availability, low cost, high modulus and excellent adhesion to the matrix resin. Espinoza-Perez *et al*.[61] manufactured glass fiber reinforced composites using a hand lay-up method. PACM cured EVO-commercial epoxy blend was used as matrix. The 30 wt.% EVO blended composite thermal and mechanical

performance was slightly lower than the composites without EVO but were comparable with those of the anhydride cured ones.

EAS, ESO and EMS have been applied in bio-composite manufacturing using pultrusion processing but these epoxies were limited to being a minor component in blends, *e.g.*, ≤ 30 wt.% of the epoxy blend.[185, 186] Greater mechanical properties were demonstrated for EAS than those of ESO or EMS due to an improved oxirane content and better reactivity. A further increase of EAS replacement content, up to 50 wt.%, was also attempted. While the T_g of the composite was decreased from 78 °C to 52 °C, the impact strength was improved.[187] The pulling force of pultrusion manufacturing was significantly reduced due to good lubricity provided by the oily bio-based component which apparently came from the saturated and unreactive component of EAS.

Using anhydride cured pure EGS, a blend of EGS-DGEBA, or a pure DGEBA as polymer matrix, glass fiber reinforced composites were fabricated from the matrices via vacuum assisted resin transfer molding.[188] The EGS-based composite showed mechanical properties comparable to that of the DGEBA counterparts in terms of flexural strength/modulus and impact strength. Only a slightly reduced T_g and thermal stability were observed. This high performance bio-based composite has good potential to replace petroleum-based epoxy resin as a value-added product form VOs.

Cellulosic fibers such as flax, hemp, or jute are also promising reinforcements for polymers composites due to their availability, high specific strength, low cost and the environmental friendliness[189]. VO-based polymer composites reinforced by cellulose are often called as “green” composites, since both matrix resins and reinforcements are from bio-renewable resources.[178] However, these composites tend to have lower mechanical

strength than similar composites reinforced with glass fibers. Due to the hydrophilic character of cellulosic fibers, surface modification of was required to improve the adhesion or compatibility between cellulose and polymer matrices.[190, 191]

Hemp fiber reinforced ELO composites were manufactured by Boquillon[192] using a hot pressing method. DMA results indicated the storage modulus at rubbery region increased from 17 MPa for the neat resin to 850 MPa for 65 vol.% fiber content composites; however, a reduced composite T_g at high fiber content was also observed. The adsorption of anhydride hardener on the hemp fiber surface leads to an off-stoichiometric reaction between epoxy and anhydride. Reduction of T_g was also observed in flax fiber reinforcement of ELO composites by Fejos *et al*.[193] that was ascribed to a chemical reaction between the hydroxyl groups of fibers and anhydride hardener.

Flax fiber reinforced composites were manufactured by Liu *et al*.[194] using a compression molding method. The polymer matrix was an amine cured ESO and 1,1,1-tris(p-hydroxyphenyl) ethane triglycidyl ether blend (THPE-GE). The flexural and tensile modulus increase with fiber content but decreased at higher fiber loadings due to the increased fiber-fiber interactions and dispersion problems. So the optimum fiber content was about 10 wt.%. A high percentage of THPE-GE in the blend was essential to achieve high thermal and mechanical strength composites. Longer fiber composites had better mechanical properties than shorter fibers.

Manthey *et al*.[180] manufactured jute fiber reinforced bio-composites in which amine cured EVO and DGEBA blends were used as matrix. The epoxidized hemp oil (EHO) composites displayed marginally higher mechanical strength than those of their

ESO counterparts and both composites mechanical performance decreased with increased ESO or EHO loading. A significant reduction in strength occurred above 30 wt.% bioresin concentration.

8.2. NANOCOMPOSITES

Polymer nanocomposites have attracted interest over past few years for their ability to generate improved thermal and mechanical strength, light weight and optical transparency at relatively low particle concentrations, *e.g.*, ≤5 wt.%.[195] Various nanomaterials including nanoclay,[196, 197] carbon nanotubes,[198] silica,[199] polyhedral oligomeric silsesquioxane[200] and alumina[201] have been used in EVO based polymer nanocomposites. Among these, organo modified montmorillonite clay platelets (OMMT) are inexpensive but highly efficient reinforcement fillers for polymer nanocomposites. With extremely large surface area and high aspect ratio of nanoclay platelets, strong interfacial interactions between polymer and nanoclay play a key role in confinement of polymer chain mobility under stress. Polymer properties can be substantially improved.[202, 203] Therefore, the major challenge encountered during the preparation of polymer clay nanocomposites is proper dispersion of the clay into the polymer matrix on a nanometric scale to achieve exfoliated, intercalated or mixtures of these structures.

Wang and Schuman[204] reported nanocomposite morphologies and thermal and mechanical strength as a function of clay concentration and dispersion technique. Mechanical shear mixing method led to an intercalated structure of undisrupted tactoids. High speed shear mixing combined with ultrasonication reduced the platelet tactoids toward much smaller scale and exfoliation, which in turn provided better properties compared to a shear mixing method alone. Compared to neat polymer, only 1 wt.% of

clay dispersed by ultrasonication improved the nanocomposite tensile strength and modulus by 22% and 13%, respectively. In other words, tensile modulus could be increased up to 34% by 6 wt.% clay without any sacrifice of strength. The T_g was also increased by 4-6 °C depending on the OMMT concentration.

Tan *et al.*[63] studied anhydride cured ESO nanocomposites. OMMT from 1-5 wt.% concentration was dispersed into ESO by ultrasonication. The surface modifier of OMMT and imidazole co-catalyze the epoxy-anhydride curing reaction and, with an exfoliated structure, the tensile strength of nanocomposite was increased with an increase in OMMT loading up to 4 wt.%. Tensile modulus, T_g and thermal stability of the ESO were also increased after adding OMMT but the fracture toughness and elongation at break were reduced due to improved stiffness and crosslink density. In a similar anhydride cured ESO-clay nanocomposite system, Tanrattanakul and Saithai[112] indicated that exfoliation was prone to occur only at low OMMT content and higher clay concentrations lead to intercalated structures with aggregations.

Miyagawa *et al.*[205, 206] reported nanocomposites of anhydride cured blend of DGEBF and ELO. Clay nanoplatelets were almost completely exfoliated and homogeneously dispersed in the epoxy network after ultrasonication dispersion. The resulting nanocomposites showed higher storage modulus than the neat polymer to offset a reduced storage modulus caused by replacement of DGEBF by ELO. However, the Izod impact strength did not change after adding clay while the heat distortional temperature and T_g were lower due to the plasticizing effect of modifier of OMMT. The nanocomposite was used as matrix for carbon fiber reinforced polymer composite,[207] results indicated that the interlaminar shear strength of composite was improved after

adding 5 wt.% intercalated clay but the exfoliated clay nanoplatelets were less effective in preventing the crack propagation.

More significant improvements in strength have been observed for EVO based nanocomposites of low T_g. Nanocomposite tensile strength and modulus were increased more than 300% for 8 wt.% OMMT has been reported by Liu *et al.*[208] The TETA was used as a curing agent for ESO, and the OMMT was dispersed in ESO by ultrasonication to form an intercalated structure. The T_g was increased from 11.8 °C of neat polymer to 20.7 °C with 5 wt.% clay. Higher OMMT concentrations lead to a properties reduction due to clay aggregation.

Shabeer *et al.*[209] synthesized nanocomposites using EAS and anhydride. Two types of dispersion technique, pneumatic and ultrasonication, were carried out to disperse the OMMT into EAS. The nanoclay was readily exfoliated into the resin due to a clay interaction and reaction with the anhydride. Tensile testing showed that the OMMT improved the tensile modulus and strength by 625% and 340%, respectively. These significant improvements in strength were explained by a strong interaction of epoxy with the clay platelets and the much higher modulus for clay platelets than flexible polymer chains. However, the T_g of the polymer, which was below room temperature, was further decreased with increased clay loadings and are best suited for non-structural applications.

SUMMARY

The current major commercial application of EVO is as a stabilizer and plasticizer. EVO has already shown versatility as an epoxy monomer material resource and a variety of epoxy thermoset polymers ranging from flexible rubbers to rigid plastics

have been synthesized from different EVOs by a number of different polymerization methods. Some of the thermoset polymers have possessed comparable properties to petroleum-based counterparts and have shown promise as replacements or supplements to commercially available epoxy monomer materials.

However, inherently less reactive internal epoxy groups and flexible carbon chain structures in EVO has prevented their applications as high performance thermoset polymers for structural applications. A remaining opportunity is a supplement for petroleum-based commercial epoxy monomers as matrix materials for coatings, composites or as nanocomposites. The future trend in this area has been increasing the percentage of bio-based content but to optimize overall performance through structure-property studies. Developing new, VO-derived epoxy monomers with higher reactivity and oxirane functionality provides opportunity to expand EVO as green materials. As novel VO-based epoxy resins, EGS have shown improved properties than other EVO structures but only when saturated content is reduced. They are at an experimental stage toward commercialization.

The versatility of epoxy formulation is not only dependent on the epoxy monomer alone but also on a combined effect of the curing agent, comonomer and polymerization conditions. Effective EVO curing systems of short polymerization time and lower curing temperature are highly desired. EVO will be of continued interest with regard to environmental and renewable/sustainable efforts through industrial application but only if the material meets customer performance requirements in reactivity, compatibility, polymer mechanical, thermal, and environmental stability properties with minimal or no tradeoffs and at a competitive cost. The review has summarized the issues of reactivity,

compatibility, and properties as a function of EVO chemical structure. The continuing challenge is to create new cost-effective EVO derived structures that improve upon existing performance levels.

REFERENCES

1. H. Q. Pham and M. J. Marks, in *Encyclopedia of Polymer Science and Technology*, John Wiley & Sons, Inc., 2002.
2. E. Santacesaria, R. Tesser, M. Di Serio, L. Casale and D. Verde, *Industrial & Engineering Chemistry Research*, 2009, **49**, 964-970.
3. H. Kishi, Y. Akamatsu, M. Noguchi, A. Fujita, S. Matsuda and H. Nishida, *Journal of Applied Polymer Science*, 2011, **120**, 745-751.
4. H. Kishi, A. Fujita, H. Miyazaki, S. Matsuda and A. Murakami, *Journal of Applied Polymer Science*, 2006, **102**, 2285-2292.
5. T. Koike, *Polymer Engineering & Science*, 2012, **52**, 701-717.
6. G. Sun, H. Sun, Y. Liu, B. Zhao, N. Zhu and K. Hu, *Polymer*, 2007, **48**, 330-337.
7. A. M. Atta, R. Mansour, M. I. Abdou and A. M. El-Sayed, *Journal of Polymer Research*, 2005, **12**, 127-138.
8. A. M. Atta, R. Mansour, M. I. Abdou and A. M. Sayed, *Polymers for Advanced Technologies*, 2004, **15**, 514-522.
9. X. Q. L. Liu, W. Huang, Y. H. Jiang, J. Zhu and Z. C. Z., *eXPRESS Polymer Letters*, 2011, **6**, 293-298.
10. K. Huang, J. Zhang, M. Li, J. Xia and Y. Zhou, *Industrial Crops and Products*, 2013, **49**, 497-506.
11. X. Liu and J. Zhang, *Polymer International*, 2010, **59**, 607-609.
12. S. Carlotti, S. Caillol, C. Mantzaridis, A.-L. Brocas, G. Cendejas, A. Llevot, A. Remi and H. Cramail, *Green Chemistry*, 2013, **15**, 3091-3098.
13. H. Nouailhas, C. Aouf, C. Le Guerneve, S. Caillol, B. Boutevin and H. Fulcrand, *Journal of Polymer Science Part A: Polymer Chemistry*, 2011, **49**, 2261-2270.
14. S. Benyahya, C. Aouf, S. Caillol, B. Boutevin, J. P. Pascault and H. Fulcrand, *Industrial Crops and Products*, 2014, **53**, 296-307.
15. J. Łukaszczyk, B. Janicki and M. Kaczmarek, *European Polymer Journal*, 2011, **47**, 1601-1606.
16. X. Feng, A. J. East, W. B. Hammond, Y. Zhang and M. Jaffe, *Polymers for Advanced Technologies*, 2011, **22**, 139-150.

17. F. Jaillet, E. Darroman, A. Ratsimihety, R. Auvergne, B. Boutevin and S. Caillol, *European Journal of Lipid Science and Technology*, 2013, **116**, 63-73.

18. S. Ma, X. Liu, Y. Jiang, Z. Tang, C. Zhang and J. Zhu, *Green Chemistry*, 2013, **15**, 245-254.

19. S. Ma, X. Liu, L. Fan, Y. Jiang, L. Cao, Z. Tang and J. Zhu, *ChemSusChem*, 2014, **7**, 555-562.

20. R. Auvergne, S. Caillol, G. David, B. Boutevin and J.-P. Pascault, *Chemical Reviews*, 2013, **114**, 1082-1115.

21. L. Montero de Espinosa and M. A. R. Meier, *European Polymer Journal*, 2011, **47**, 837-852.

22. M. A. R. Meier, J. O. Metzger and U. S. Schubert, *Chemical Society Reviews*, 2007, **36**, 1788-1802.

23. "Food and Agriculture Organization of the United Nations," http://faostat3.fao.org/faostat-gateway/go/to/download/Q/QD/E, accecssed April 2014.

24. N. Mann, S. Mendon, J. Rawlins and S. Thames, *Journal of the American Oil Chemists' Society*, 2008, **85**, 791-796.

25. P. Muturi, D. Wang and S. Dirlikov, *Progress in Organic Coatings*, 1994, **25**, 85-94.

26. J. V. Crivello and R. Narayan, *Chemistry of Materials*, 1992, **4**, 692-699.

27. F. Gunstone, *The Chemistry of Oils and Fats: Sources, Composition, Properties and Uses*, CRC Press LLC, Boca Raton, FL, 2004.

28. D. Swern, *Chemical Reviews*, 1949, **45**, 1-68.

29. K. Mark Rüsch gen and W. Siegfried, in *Recent Developments in the Synthesis of Fatty Acid Derivatives*, AOCS Publishing, 1999, pp. 157-181.

30. V. V. Goud, A. V. Patwardhan, S. Dinda and N. C. Pradhan, *Chemical Engineering Science*, 2007, **62**, 4065-4076.

31. S. Sinadinović-Fišer, M. Janković and Z. Petrović, *J Amer Oil Chem Soc*, 2001, **78**, 725-731.

32. G. J. H. Buisman, A. Overeem and F. P. Cuperus, in *Recent Developments in the Synthesis of Fatty Acid Derivatives*, AOCS Publishing, 1999, pp. 128-140.

33. T. Vlček and Z. Petrović, *J Amer Oil Chem Soc*, 2006, **83**, 247-252.

34. *Recent Developments in the Synthesis of Fatty Acid Derivatives*, AOCS Publishing, 1999.

35. Z. S. Petrović, *Polymer Reviews*, 2008, **48**, 109-155.

36. J. Lu, S. Khot and R. P. Wool, *Polymer*, 2005, **46**, 71-80.

37. L. Gelb, W. Ault, W. Palm, L. Witnauer and W. Port, *J Am Oil Chem Soc*, 1959, **36**, 283-286.

38. L. Gelb, W. Ault, W. Palm, L. Witnauer and W. Port, *Journal of the American Oil Chemists' Society*, 1960, **37**, 81-84.

39. K. Zou and M. D. Soucek, *Macromolecular Chemistry and Physics*, 2005, **206**, 967-975.

40. J. Chen, M. D. Soucek, W. J. Simonsick and R. W. Celikay, *Polymer*, 2002, **43**, 5379-5389.

41. Z. Zong, M. D. Soucek, Y. Liu and J. Hu, *Journal of Polymer Science Part A: Polymer Chemistry*, 2003, **41**, 3440-3456.

42. X. Pan, P. Sengupta and D. C. Webster, *Biomacromolecules*, 2011, **12**, 2416-2428.

43. X. Pan, P. Sengupta and D. C. Webster, *Green Chemistry*, 2011, **13**, 965-975.

44. T. Nelson, T. Galhenage and D. Webster, *Journal of Coatings Technology and Research*, 2013, 1-12.

45. S. Alam, H. Kalita, A. Jayasooriya, S. Samanta, J. Bahr, A. Chernykh, M. Weisz and B. J. Chisholm, *European Journal of Lipid Science and Technology*, 2014, **116**, 2-15.

46. S. Alam and B. Chisholm, *Journal of Coatings Technology and Research*, 2011, **8**, 671-683.

47. G. Lligadas, J. C. Ronda, M. Galià and V. Cádiz, *Journal of Polymer Science Part A: Polymer Chemistry*, 2006, **44**, 6717-6727.

48. J. D. Earls, J. E. White, L. C. López, Z. Lysenko, M. L. Dettloff and M. J. Null, *Polymer*, 2007, **48**, 712-719.

49. J. Earls, J. White, M. Dettloff and M. Null, *Journal of Coatings Technology and Research*, 2004, **1**, 243-245.

50. J. M. Fraile, J. I. García, D. Marco and J. A. Mayoral, *Applied Catalysis A: General*, 2001, **207**, 239-246.

51. K. Kamata, K. Sugahara, K. Yonehara, R. Ishimoto and N. Mizuno, *Chemistry – A European Journal*, 2011, **17**, 7549-7559.

52. S. G. Yang, J. P. Hwang, M. Y. Park, K. Lee and Y. H. Kim, *Tetrahedron*, 2007, **63**, 5184-5188.

53. US 3859314 A, 1975.

54. US3075999 A, 1963.

55. US2940986 A, 1960.

56. K. Huang, P. Zhang, J. Zhang, S. Li, M. Li, J. Xia and Y. Zhou, *Green Chemistry*, 2013, **15**, 2466-2475.

57. R. Wang and T. Schuman, *eXPRESS Polymer Letters*, 2013, **7**, 272-292.

58. H. Q. Pham and M. J. Marks, in *Ullmann's Encyclopedia of Industrial Chemistry*, Wiley-VCH Verlag GmbH & Co. KGaA, 2000.

59. P. Lu, J. O. Stoffer, R. A. Babcock and L. R. Dharani, 220th ACS National Meeting.

60. J. Zhu, K. Chandrashekhara, V. Flanigan and S. Kapila, *Journal of Applied Polymer Science*, 2004, **91**, 3513-3518.

61. J. D. Espinoza-Perez, B. A. Nerenz, D. M. Haagenson, Z. Chen, C. A. Ulven and D. P. Wiesenborn, *Polymer Composites*, 2011, **32**, 1806-1816.

62. G. López Téllez, E. Vigueras-Santiago, S. Hernández-López and B. Bilyeu, *Designed Monomers & Polymers*, 2008, **11**, 435-445.

63. A. Gandini, T. M. Lacerda and A. J. F. Carvalho, *Green Chemistry*, 2013, **15**, 1514-1519.

64. N. W. Manthey, F. Cardona, T. Aravinthan and T. Cooney, *Journal of Applied Polymer Science*, 2011, **122**, 444-451.

65. N. W. Manthey, F. Cardona and T. Aravinthan, *Journal of Applied Polymer Science*, 2012, **125**, E511-E517.

66. V. del Río, M. P. Callao and M. S. Larrechi, *International Journal of Analytical Chemistry*, 2011, **2011**.

67. Z. Wang, X. Zhang, R. Wang, H. Kang, B. Qiao, J. Ma, L. Zhang and H. Wang, *Macromolecules*, 2012, **45**, 9010-9019.

68. S. Miao, S. Zhang, Z. Su and P. Wang, *Journal of Applied Polymer Science*, 2013, **127**, 1929-1936.

69. P. Lu, University of Missouri-Rolla, 2001.

70. M. Partansky A, in *Epoxy Resins*, AMERICAN CHEMICAL SOCIETY, 1970, vol. 92, pp. 29-47.

71. R. E. Harry-O'kuru, S. H. Gordon and A. Biswas, *Journal of the American Oil Chemists' Society*, 2005, **82**, 207-212.

72. N. Juangvanich, University of Missouri-Rolla, 2003.

73. X. Fernàndez-Francos, X. Ramis and À. Serra, *Journal of Polymer Science Part A: Polymer Chemistry*, 2014, **52**, 61-75.

74. F. I. Altuna, V. Pettarin and R. J. J. Williams, *Green Chemistry*, 2013.

75. N. Supanchaiyamat, P. S. Shuttleworth, A. J. Hunt, J. H. Clark and A. S. Matharu, *Green Chemistry*, 2012, **14**, 1759-1765.

76. J.-P. Pascault, H. Sautereau, J. Verdu and R. J. J. Williams, *Thermosetting polymers*, Marcel Dekker, New York, 2002.

77. S. G. Tan and W. S. Chow, *eXPRESS Polymer Letters*, 2011, **5**, 480-492.

78. C. A. May, *Epoxy Resins: Chemistry and Technology, Second Edition,*, M. Dekker, New York, 1988.

79. N. Boquillon and C. Fringant, *Polymer*, 2000, **41**, 8603-8613.

80. G. Liang and K. Chandrashekhara, *Journal of Applied Polymer Science*, 2006, **102**, 3168-3180.

81. S. G. Tan, Z. Ahmad and W. S. Chow, *Industrial Crops and Products*, 2013, **43**, 378-385.

82. A. Mahendran, G. Wuzella, A. Kandelbauer and N. Aust, *Journal of Thermal Analysis and Calorimetry*, 2012, **107**, 989-998.

83. A. Nicolau, D. Samios, C. M. S. Piatnick, Q. B. Reiznautt, D. D. Martini and A. L. Chagas, *European Polymer Journal*, 2012, **48**, 1266-1278.

84. A. J. Clark and S. S. Hoong, *Polymer Chemistry*, 2014.

85. Z. Liu, K. M. Doll and R. A. Holser, *Green Chemistry*, 2009, **11**, 1774-1780.

86. Z. Liu and S. Z. Erhan, *Journal of the American Oil Chemists' Society*, 2009, **87**, 437-444.

87. Z. Liu and A. Biswas, *Applied Catalysis A: General*, 2013, **453**, 370-375.

88. B. K. Sharma, Z. Liu, A. Adhvaryu and S. Z. Erhan, *Journal of Agricultural and Food Chemistry*, 2008, **56**, 3049-3056.

89. L. Fertier, H. Koleilat, M. Stemmelen, O. Giani, C. Joly-Duhamel, V. Lapinte and J.-J. Robin, *Progress in Polymer Science*, 2013, **38**, 932-962.

90. M.-A. Tehfe, J. Lalevée, D. Gigmes and J. P. Fouassier, *Macromolecules*, 2010, **43**, 1364-1370.

91. C. Decker, T. Nguyen Thi Viet and H. Pham Thi, *Polymer International*, 2001, **50**, 986-997.

92. W. D. Wan Rosli, R. N. Kumar, S. Mek Zah and M. M. Hilmi, *European Polymer Journal*, 2003, **39**, 593-600.

93. Y.-S. Li, M.-S. Li and F.-C. Chang, *Journal of Polymer Science Part A: Polymer Chemistry*, 1999, **37**, 3614-3624.

94. R. A. Ortiz, D. P. López, M. d. L. G. Cisneros, J. C. R. Valverde and J. V. Crivello, *Polymer*, 2005, **46**, 1535-1541.

95. S. Chakrapani and J. V. Crivello†, *Journal of Macromolecular Science, Part A*, 1998, **35**, 691-710.

96. M. Soucek and J. Chen, *Journal of Coatings Technology*, 2003, **75**, 49-58.

97. A. Hartwig, K. Koschek and A. Lühring, in *Adhesion*, Wiley-VCH Verlag GmbH & Co. KGaA, 2006, pp. 205-216.

98. S.-J. Park, F.-L. Jin, J.-R. Lee and J.-S. Shin, *European Polymer Journal*, 2005, **41**, 231-237.

99. S.-J. Park, F.-L. Jin and J.-R. Lee, *Macromolecular Rapid Communications*, 2004, **25**, 724-727.

100. S.-J. Park, F.-L. Jin and J.-R. Lee, *Macromolecular Chemistry and Physics*, 2004, **205**, 2048-2054.

101. A.-L. Brocas, C. Mantzaridis, D. Tunc and S. Carlotti, *Progress in Polymer Science*, 2013, **38**, 845-873.

102. I. E. Dell'Erba and R. J. J. Williams, *Polymer Engineering & Science*, 2006, **46**, 351-359.

103. K. Boonkerd, B. K. Moon, M. C. Kim and J. K. Kim, *Journal of Elastomers and Plastics*, 2013.

104. C. Öztürk and S. H. Küsefoğlu, *Journal of Applied Polymer Science*, 2011, **121**, 2976-2984.

105. E. Del Rio, M. Galià, V. Cádiz, G. Lligadas and J. C. Ronda, *Journal of Polymer Science Part A: Polymer Chemistry*, 2010, **48**, 4995-5008.

106. C. H. Zhao, S. J. Wan, L. Wang, X. D. Liu and T. Endo, *Journal of Polymer Science Part A: Polymer Chemistry*, 2014, **52**, 375-382.

107. J. La Scala and R. P. Wool, *Polymer*, 2005, **46**, 61-69.

108. A. Zlatanić, Z. S. Petrović and K. Dušek, *Biomacromolecules*, 2002, **3**, 1048-1056.

109. Z. S. Petrović, W. Zhang and I. Javni, *Biomacromolecules*, 2005, **6**, 713-719.

110. M. Carme Coll Ferrer, D. Babb and A. J. Ryan, *Polymer*, 2008, **49**, 3279-3287.

111. M. Samper, V. Fombuena, T. Boronat, D. García-Sanoguera and R. Balart, *Journal of the American Oil Chemists' Society*, 2012, 1-8.

112. V. Tanrattanakul and P. Saithai, *Journal of Applied Polymer Science*, 2009, **114**, 3057-3067.

113. J. R. Kim and S. Sharma, *Industrial Crops and Products*, 2012, **36**, 485-499.

114. Q. B. Reiznautt, I. T. S. Garcia and D. Samios, *Materials Science and Engineering: C*, 2009, **29**, 2302-2311.

115. A. Gerbase, C. Petzhold and A. Costa, *Journal of the American Oil Chemists' Society*, 2002, **79**, 797-802.

116. J. Rösch and R. Mülhaupt, *Polymer Bulletin*, 1993, **31**, 679-685.

117. D. d. S. Martini, B. A. Braga and D. Samios, *Polymer*, 2009, **50**, 2919-2925.

118. A. P. Gupta, S. Ahmad and A. Dev, *Polymer-Plastics Technology and Engineering*, 2010, **49**, 657 - 661.

119. J. M. España, L. Sánchez-Nacher, T. Boronat, V. Fombuena and R. Balart, *Journal of the American Oil Chemists' Society*, 2012, **89**, 2067-2075.

120. S. G. Tan and W. S. Chow, *Journal of the American Oil Chemists' Society*, 2010, **87**, DOI 10.1007/s11746-11010-11748-x.

121. N. Bouillon, J.-P. Pascault and L. Tighzert, *Journal of Applied Polymer Science*, 1989, **38**, 2103-2113.

122. M. J. Abdekhodaie, Z. Liu, S. Z. Erhan and X. Y. Wu, *Polymer International*, 2012, **61**, 1477-1484.

123. S. Tan and W. Chow, *Journal of the American Oil Chemists' Society*, 2011, **88**, 915-923.

124. S. G. Tan and W. S. Chow, *Iranian Polymer Journal*, 2012, **21**, 353-363.

125. S. Qureshi, A. Manson J, C. Michel J, W. Hertzberg R and H. Sperling L, in *Characterization of Highly Cross-linked Polymers*, American Chemical Society, 1984, vol. 243, pp. 109-124.

126. F. I. Altuna, L. H. Espósito, R. A. Ruseckaite and P. M. Stefani, *Journal of Applied Polymer Science*, 2011, **120**, 789-798.

127. Y. Chen, L. Yang, J. Wu, L. Ma, D. Finlow, S. Lin and K. Song, *Journal of Thermal Analysis and Calorimetry*, 2013, **113**, 939-945.

128. J. Karger-Kocsis, S. Grishchuk, L. Sorochynska and M. Z. Rong, *Polymer Engineering & Science*, 2013, n/a-n/a.

129. R. Raghavachar, R. J. Letasi, P. V. Kola, Z. Chen and J. L. Massingill, *Journal of the American Oil Chemists' Society*, 1999, **76**, 511-516.

130. D. Ratna, *Polymer International*, 2001, **50**, 179-184.

131. A. Sarwono, Z. Man and M. A. Bustam, *Journal of Polymers and the Environment*, 2012, **20**, 540-549.

132. I. Frischinger and S. Dirlikov, in *Interpenetrating Polymer Networks*, American Chemical Society, 1994, vol. 239, pp. 517-538.

133. F. R. Mustata, N. Tudorachi and I. Bicu, *Industrial & Engineering Chemistry Research*, 2013, **52**, 17099-17110.

134. F. Mustata, N. Tudorachi and D. Rosu, *Composites Part B: Engineering*, 2011, **42**, 1803-1812.

135. A. P. Gupta, S. Ahmad and A. Dev, *Polymer Engineering & Science*, 2011, **51**, 1087-1091.

136. S. G. Tan and W. S. Chow, *J Therm Anal Calorim*, 2010, **101**, 1051–1058.

137. H. Miyagawa, A. K. Mohanty, M. Misra and L. T. Drzal, *Macromolecular Materials and Engineering*, 2004, **289**, 629-635.

138. H. Miyagawa, A. K. Mohanty, M. Misra and L. T. Drzal, *Macromolecular Materials and Engineering*, 2004, **289**, 636-641.

139. P. Czub, *Macromolecular Symposia*, 2006, **245-246**, 533-538.

140. P. Czub, *Macromolecular Symposia*, 2006, **242**, 60-64.

141. E.-A.-C. Demengeot, I. Baliutaviciene, J. Ostrauskaite, L. Augulis, V. Grazuleviciene, L. Rageliene and J. V. Grazulevicius, *Journal of Applied Polymer Science*, 2010, **115**, 2028-2038.

142. A. Remeikyte, J. Ostrauskaite and V. Grazuleviciene, *Journal of Applied Polymer Science*, 2013, **129**, 1290-1298.

143. F.-L. Jin and S.-J. Park, *Polymer International*, 2008, **57**, 577-583.

144. R. Bagheri, B. T. Marouf and R. A. Pearson, *Polymer Reviews*, 2009, **49**, 201-225.

145. A. F. Yee and R. A. Pearson, *J Mater Sci*, 1986, **21**, 2462-2474.

146. J. C. Munoz, H. Ku, F. Cardona and D. Rogers, *Journal of Materials Processing Technology*, 2008, **202**, 486-492.

147. G. Zhan, L. Zhao, S. Hu, W. Gan, Y. Yu and X. Tang, *Polymer Engineering & Science*, 2008, **48**, 1322-1328.

148. S. G. Tan, Z. Ahmad and W. S. Chow, *Polymer International*, 2014, **63**, 273-279.

149. F. I. Altuna, V. Pettarin, L. Martin, A. Retegi, I. Mondragon, R. A. Ruseckaite and P. M. Stefani, *Polymer Engineering & Science*, 2013, n/a-n/a.

150. A. Shabeer, S. Sundararaman, K. Chandrashekhara and L. R. Dharani, *Journal of Applied Polymer Science*, 2007, **105**, 656-663.

151. H. Miyagawa, M. Misra, L. T. Drzal and A. K. Mohanty, *Polymer Engineering & Science*, 2005, **45**, 487-495.

152. S. G. Tan and W. S. Chow, *Polymer-Plastics Technology and Engineering*, 2010, **49**, 900-907.

153. F.-L. Jin and S.-J. Park, *Materials Science and Engineering: A*, 2008, **478**, 402-405.

154. S.-J. Park, F.-L. Jin and J.-R. Lee, *Materials Science and Engineering: A*, 2004, **374**, 109-114.

155. M. A. Sithique, S. Ramesh and M. Alagar, *International Journal of Polymeric Materials*, 2008, **57**, 480-493.

156. I. Frischinger and S. Dirlikov, in *Toughened Plastics I*, American Chemical Society, 1993, vol. 233, pp. 451-489.

157. D. Ratna and A. K. Banthia, *Journal of Adhesion Science and Technology*, 2000, **14**, 15-25.

158. R. Raghavachar, G. Sarnecki, J. Baghdachi and J. Massingill, *Journal of Coatings Technology*, 2000, **72**, 125-133.

159. M. Y. Shah and S. Ahmad, *Progress in Organic Coatings*, 2012, **75**, 248-252.

160. G. Das and N. Karak, *Progress in Organic Coatings*, 2009, **66**, 59-64.

161. S. Ahmad, F. Naqvi, E. Sharmin and K. L. Verma, *Progress in Organic Coatings*, 2006, **55**, 268-275.

162. M. D. Soucek, A. H. Johnson and J. M. Wegner, *Progress in Organic Coatings*, 2004, **51**, 300-311.

163. N. Jiratumnukul and R. Intarat, *Journal of Applied Polymer Science*, 2008, **110**, 2164-2167.

164. S. F. Thames and H. Yu, *Surface and Coatings Technology*, 1999, **115**, 208-214.

165. H. Gu, K. Ren, D. Martin, T. Marino and D. Neckers, *Journal of Coatings Technology*, 2002, **74**, 49-52.

166. D. M. Bechi, M. A. d. Luca, M. Martinelli and S. Mitidieri, *Progress in Organic Coatings*, 2013, **76**, 736-742.

167. M. Luca, M. Martinelli, M. Jacobi, P. Becker and M. Ferrão, *Journal of the American Oil Chemists' Society*, 2006, **83**, 147-151.

168. M. A. de Luca, M. Martinelli and C. C. T. Barbieri, *Progress in Organic Coatings*, 2009, **65**, 375-380.

169. D. Becchi, M. Luca, M. Martinelli and S. Mitidieri, *Journal of the American Oil Chemists' Society*, 2011, **88**, 101-109.

170. T. Tsujimoto, H. Uyama and S. Kobayashi, *Macromolecular Rapid Communications*, 2003, **24**, 711-714.

171. Z. Zong, J. He and M. D. Soucek, *Progress in Organic Coatings*, 2005, **53**, 83-90.

172. A. O'Donnell, M. A. Dweib and R. P. Wool, *Composites Science and Technology*, 2004, **64**, 1135-1145.

173. P. H. Henna, M. R. Kessler and R. C. Larock, *Macromolecular Materials and Engineering*, 2008, **293**, 979-990.

174. Y. Lu and R. C. Larock, *Macromolecular Materials and Engineering*, 2007, **292**, 1085-1094.

175. R. L. Quirino, Y. Ma and R. C. Larock, *Green Chemistry*, 2012, **14**, 1398-1404.

176. R. P. Wool and X. S. Sun, *Bio-Based Polymers and Composites*, Elsevier Academic Press, 2005.

177. M. A. Mosiewicki and M. I. Aranguren, *European Polymer Journal*, 2013, **49**, 1243-1256.

178. E. Zini and M. Scandola, *Polymer Composites*, 2011, **32**, 1905-1915.

179. A. K. Mohanty, M. Misra and G. Hinrichsen, *Macromolecular Materials and Engineering*, 2000, **276-277**, 1-24.

180. N. W. Manthey, F. Cardona, G. Francucci and T. Aravinthan, *Journal of Reinforced Plastics and Composites*, 2013, **32**, 1444-1456.

181. J. V. Crivello, R. Narayan and S. S. Sternstein, *Journal of Applied Polymer Science*, 1997, **64**, 2073-2087.

182. Z. S. Liu, S. Z. Erhan, J. Xu and P. D. Calvert, *Journal of Applied Polymer Science*, 2002, **85**, 2100-2107.

183. A. Retegi, I. Algar, L. Martin, F. Altuna, P. Stefani, R. Zuluaga, P. Gañán and I. Mondragon, *Cellulose*, 2012, **19**, 103-109.

184. Z. S. Liu, S. Z. Erhan and P. D. Calvert, *Composites Part A: Applied Science and Manufacturing*, 2007, **38**, 87-93.

185. J. Zhu, K. Chandrashekhara, V. Flanigan and S. Kapila, *Composites Part A: Applied Science and Manufacturing*, 2004, **35**, 95-101.

186. K. Chandrashekhara, S. Sundararaman, V. Flanigan and S. Kapila, *Materials Science and Engineering: A*, 2005, **412**, 2-6.

187. S. Sundararaman, A. Shabeer, K. Chandrashekhara and T. Schuman, *Journal of Biobased Materials and Bioenergy*, 2008, **2**, 71-77.

188. R. Wang and T. Schuman, in *245th ACS National Meeting & Exposition*, New Orleans, Louisiana, 2013.

189. F. P. La Mantia and M. Morreale, *Composites Part A: Applied Science and Manufacturing*, 2011, **42**, 579-588.

190. Z. Liu, S. Z. Erhan, D. E. Akin, F. E. Barton, C. Onwulata and T. A. McKeon, *Composite Interfaces*, 2008, **15**, 207-220.

191. P. Tran, D. Graiver and R. Narayan, *Journal of Applied Polymer Science*, 2006, **102**, 69-75.

192. N. Boquillon, *Journal of Applied Polymer Science*, 2006, **101**, 4037-4043.

193. M. Fejős, J. Karger-Kocsis and S. Grishchuk, *Journal of Reinforced Plastics and Composites*, 2013, **32**, 1879-1886.

194. Z. Liu, S. Z. Erhan, D. E. Akin and F. E. Barton, *Journal of Agricultural and Food Chemistry*, 2006, **54**, 2134-2137.

195. S. Sinha Ray and M. Bousmina, *Progress in Materials Science*, 2005, **50**, 962-1079.

196. H. Uyama, M. Kuwabara, T. Tsujimoto, M. Nakano, A. Usuki and S. Kobayashi, *Macromolecular Bioscience*, 2004, **4**, 354-360.

197. H. Uyama, M. Kuwabara, T. Tsujimoto, M. Nakano, A. Usuki and S. Kobayashi, *Chemistry of Materials*, 2003, **15**, 2492-2494.

198. H. Miyagawa, A. K. Mohanty, L. T. Drzal and M. Misra, *Nanotechnology*, 2005, **16**, 118.

199. G. Zhan, X. Tang, Y. Yu and S. Li, *Polymer Engineering & Science*, 2011, **51**, 426-433.

200. G. Lligadas, J. C. Ronda and M. Galia`, *Biomacromolecules*, 2006, **7**, 3521-3526.

201. H. Miyagawa, A. Mohanty, L. T. Drzal and M. Misra, *Industrial & Engineering Chemistry Research*, 2004, **43**, 7001-7009.

202. J. Lu, C. K. Hong and R. P. Wool, *Journal of Polymer Science Part B: Polymer Physics*, 2004, **42**, 1441-1450.

203. Y. Lu and R. C. Larock, *Biomacromolecules*, 2006, **7**, 2692-2700.

204. R. Wang, T. Schuman, R. R. Vuppalapati and K. Chandrashekhara, *Green Chemistry*, 2014, **16**, 1871-1882.

205. H. Miyagawa, M. Misra, L. T. Drzal and A. K. Mohanty, *Journal of Polymers and the Environment*, 2005, **13**, 87-96.

206. H. Miyagawa, M. Misra, L. T. Drzal and A. K. Mohanty, *Polymer*, 2005, **46**, 445-453.

207. H. Miyagawa, R. J. Jurek, A. K. Mohanty, M. Misra and L. T. Drzal, *Composites Part A: Applied Science and Manufacturing*, 2006, **37**, 54-62.

208. Z. Liu, S. Z. Erhan and J. Xu, *Polymer*, 2005, **46**, 10119-10127.

209. A. Shabeer, K. Chandrashekhara and T. Schuman, *Journal of Composite Materials*, 2007, **41**, 1825-1849.

II. VEGETABLE OIL-DERIVED EPOXY MONOMERS AND POLYMER BLENDS: A COMPARATIVE STUDY WITH REVIEW

Rongpeng Wang and Thomas Schuman*

Department of Chemistry, Missouri University of Science and Technology, Rolla, MO 65409, USA

**Correspondence to*: Thomas Schuman (tschuman@mst.edu)

ABSTRACT

Glycidyl esters of epoxidized fatty acids derived from soybean oil (EGS) and linseed oil (EGL) have been synthesized to have higher oxirane content, more reactivity and lower viscosity than epoxidized soybean oil (ESO) or epoxidized linseed oil (ELO). The EGS and ESO, for comparison, were used neat and in blends with diglycidyl ether of bisphenol A (DGEBA). Thermosetting resins were fabricated with the epoxy monomers and either BF3 catalyst or anhydride. The curing behaviors, glass transition temperatures, crosslink densities and mechanical properties were tested. The results indicated that polymer glass transition temperatures were mostly a function of oxirane content with additional influence of glycidyl versus internal oxirane reactivity, pendant chain content, and chemical structure and presence of saturated components. EGS provided better compatibility with DGEBA, improved intermolecular crosslinking and glass transition temperature, and yielded mechanically stronger polymerized materials than materials obtained using ESO. Other benefits of the EGS resin blend systems were significantly reduced viscosities compared to either DGEBA or ESO-blended DGEBA counterparts. Therefore, EGS that is derived from renewable sources has improved

potential for fabrication of structural and structurally complex epoxy composites, *e.g.*, by vacuum-assisted resin transfer molding.

KEYWORDS

thermosetting resins, mechanical properties, thermal properties, biopolymers, epoxy

1. INTRODUCTION

Since petroleum resources are ultimately limited, polymers based on vegetable oils are of great interest because they are renewable and could significantly contribute to a more sustainable development [1, 2]. Vegetable oils such as linseed and tung oil are drying oils, which can self-crosslink under atmospheric oxygen, have long been used in the coating industry [3]. Semi-drying oils like soybean oil are of plentiful supply and therefore of relatively low cost, have also attracted great interest for the preparation of polymers or resins [4]. In recent years, with the rising cost of fossil raw materials and environmental issues, polymers derived from soybean oil have demonstrated strong cost/performance competitiveness in many market applications [5]. However, the ability to obtain structures of sufficient mechanical or thermal properties has remained a challenge.

For instance, direct radical or cationic polymerization of vegetable oils is structurally difficult due to the non-conjugated, internal double bonds and only viscous liquid polymers with low molecular weight are formed [6]. On the other hand, polymers ranging from soft rubbers to hard plastics have been prepared by the cationic copolymerization of soybean oil blended with divinylbenzene (DVB). Styrene was added to reduce the heterogeneity of the crosslinked structures caused by incompatibility

between monomers and the modulus of polymer was dependent on the styrene and, particularly, the DVB content [7].

Epoxidation of vegetable oils using peracids, such as epoxidized soybean oil (ESO) and epoxidized linseed oil (ELO), is one of the most important and useful exploitations of double bonds since epoxides are reactive intermediates that are also readily converted to other functional groups through ring-opening reactions. Sheet molding compound (SMC) resins have been made from epoxidized soybean oil modified with unsaturated functional groups like acrylic acid or maleic anhydride where styrene was employed as a comonomer to reduce the viscosity of the resin [8, 9]. The SMC was obtained via common radical polymerization fashion. Allyl alcohol ring-opened ESO has been copolymerized with maleic anhydride (MA) to prepare thermosets by esterification and free radical polymerization. The resulting glass transition temperatures (T_g) and mechanical strengths were dependent on the loading of MA [10]. Soy based polyols derived from ESO have also been widely used to produce polyurethanes that are comparable in many aspects with polyurethanes obtained from petrochemical polyols [11].

ESO can be crosslinked into thermosetting polymers by various curing agents [12]. However, due to lower oxirane content and sluggish reactivity of the internal oxirane, the cured ESO polymers normally have low crosslinking density. Poorer thermal and mechanical properties result from both partially unreacted ESO and saturated fatty acid (FA) chains that reduce reactivity and self-plasticize. Most ESO industrial uses are thus limited to nonstructural, additive applications such as plasticizers or stabilizers for poly (vinyl chloride) [13], oil-base coatings [14] with low strength requirements [15].

Though the mechanical strength of cured ESO can be improved with the addition of nano-reinforcements [16], or fiber reinforcement [17], an inherently low T_g inevitably limits practical applications because T_g for a polymer must be appropriately higher than the temperature of its intended work environment to serve as a useful plastic [18]. When used as a matrix material in composites, the resin state is desired to be rigid/glassy, i.e., below its T_g, to effectively transfer energy to fibers [19].

ESO has a moderate viscosity so ESO or their derivatives can be used as reactive diluents for the partial replacement of diglycidyl ether of bisphenol A (DGEBA) resins, which are relatively high viscosity liquids or solids, to decrease the overall cost and improve the processability [20–22]. Generally, the mechanical strengths and thermal properties of ESO blended resins are not comparable to those of pure DGEBA epoxy resins, while their toughness can be better due to the introduction of a two phase structure [23–26]. However, due to the inhomogeneous structure, ESO is not as efficient in reducing the viscosity of epoxy resin compared to most petroleum based reactive diluents. A further increase in the ESO concentration inevitably leads to a significant decrease in performance of cured resin. There are few reports of high ESO replacement [20] because low oxirane content and the unreactive saturated component of ESO both lead to a low crosslink density upon cure and a poor miscibility exists between ESO and the DGEBA. There is an especially large difference in the reactivity of the internal oxirane in ESO and terminal oxirane in DGEBA and, as we will show, heterogeneous structures form during the curing reaction that leads to a phase separated materials of poorer mechanical /thermal performance.

More reactive terminal epoxy derived from chlorinated ESO has been reported and used as a matrix with DGEBA for glass fiber composites [27]. The dehydrochlorination under alkaline conditions will hydrolyze ester groups of triglycerides, even at room temperature. A triglyceride with terminal epoxy has been synthesized from 10-undecenoic acid and successfully used in epoxy-amine curing [28, 29], whereas 10-undecylenic acid, a derivative of castor oil, has only one terminal double bond so the epoxidized triglyceride ester of 10-undecylenic acid has a lower oxirane content compared to ESO. Large scale production also seems impractical [30]. Only those oils of poly-unsaturated FA content, especially soybean or linseed oils, that can produce dense oxirane functional resins are capable to produce satisfactory properties [12, 31–33]. Epoxidized vegetable oils (EVO) of low oxirane values either are not reactive or impart waxy, non-curing properties to the resin system.

Vegetable oils contain several actives sites amenable to chemical modification. The double bonds in FA chains and the ester groups in the glyceryl part are the most important. These active sites can be used to introduce reactive groups. ESO and aforementioned derivatives are most focused on the modification of FA chain. On the ester side, epoxidized methyl oleate [34], epoxidized methyl soyate, epoxidized allyl soyate [35], epoxidized sunflower oil biodiesel [36] and linseed oil epoxidized methyl esters [37] have been shown to have lower viscosity and more reactive compared to their ESO or ELO counterparts.

A caveat in the addition of functional groups, such as unreactive methyl or reactive allyl through transesterification, is a potential decrease of crosslinking density and final properties of cured resins upon breaking the oligomeric triglyceride structure.

FA chain ends at the ester become pendant after transesterification and are dependent on crosslinking to build molecular weight. Esters of saturated FAs may only behave as plasticizers [38]. Novel epoxy compounds such as epoxidized sucrose esters of fatty acids have been synthesized and crosslinked to prepare polyester thermosets [30, 39]. High modulus polymer was achieved due to the well-defined compact macromolecular structures and high oxirane functionality. Some applications may be hampered by their high viscosities.

Modified ELO synthesized through Diels–Alder reaction of dicyclopentadiene [40] or 1,3-butadiene [41] with linseed oil have been reported. The modified ELO resins still possessed internal oxirane and thus are more suitable for cationic cure. End users still seek economical bio-based epoxies that are competitive with petroleum-based epoxies [30].

Vegetable oils generally have variable levels of saturated FA content, for example, soybean oil normally has about 15% saturated FAs (~ 4.0 % stearic and ~ 11% palmitic) that varies with plant variety, growing regions, and weather. Saturated FAs have no functional groups within the FA chain that then act as dangling chains, low in reactivity, to plasticize the final polymer. The saturated chains are detrimental to the final properties of polymers [42, 43]. To improve reactivity and to increase hydroxyl number of soy based polyols, regionally selective enzymatic hydrolysis has been attempted to liberate saturated FAs, which were then removed by alkaline washing [44]. Total removal of saturated components is difficult and is also accompanied by partial hydrolysis of unsaturated FA esters. Conversion of oil triglyceride into free fatty acid (FFA) or FA derivatives allows separation of unsaturated and saturated components on

the basis of solubility through crystallization. The degree of unsaturation of FFA considerably changes the melting point and thus separation of mixtures of saturated and unsaturated FFAs can be readily achieved by proper choice of organic solvents and temperatures [45].

In this research, EGS were synthesized and examined. The goals were to remove and assess the role of the plasticizing effect of saturated components, to increase and assess the role of the oxirane content, and to minimize viscosity toward developing either a capable reactive diluent for commercial epoxy or a new commercial epoxy resin of its own right. The study gave us the opportunity to study how saturated component, oxirane type and oxirane content translate into curing, thermal and mechanical properties. We hypothesized that EGS as the ester of a terminal oxirane group (glycidyl), which is then readily accessible to nucleophilic attack, should further enable reactivity compared with the currently standard, commercial ESO and consequently reduce the molecular size and facilitate removal of the saturated FA components. We thus proposed to increase oxirane content. The goals and resin design were intended to provide a dense, intermolecular crosslinking structure and yield a more consistent thermosetting resin material with improved properties.

2. EXPERIMENTAL

2.1. MATERIALS

Refined, food grade soybean oil (Great Value™, Wal-Mart, Bentonville, AR, USA) was purchased. Linseed oil was purchased from Archer Daniels Midland Company (Red Wing, MN, USA). The major FA distributions [46] reported for soybean oil and linseed oil are listed in Table 1. ESO was obtained from Union Carbide Corporation

(Danbury, CT, USA). ELO was obtained from Arkema, Inc. (Philadelphia, PA, USA). Acetone, allyl alcohol, epichlorohydrin (EPCH), methylene chloride, methanol, meta-chloroperoxybenzoic acid (MCPBA), potassium hydroxide, sodium carbonate, sodium bicarbonate, sodium hydroxide, sodium sulfite, and anhydrous sodium sulfate were purchased from Fisher Scientific (St. Louis, MO, USA). Cetyltrimethylammonium bromide (CTAB), boron trifluoride mono -ethyl amine complex (BF_3-MEA), 2-ethyl-4-methyl - imidazole (EMI), hydrochloric acid and 4-methyl- 1,2-cyclohexanedicarboxylic anhydride (MHHPA) were purchased from Aldrich (St. Louis, MO, USA). Commercial DGEBA was supplied by Momentive (Deer Park, TX, USA) with trade name EPON™ Resin 828. Mold release agent Chemlease® 41-90 EZ was purchased from Chem-Trend, Inc. (Howell, MI, USA)

Table 1. Fatty acids profile in vegetable oils

Fatty Acid (x:y)	Palmitic (14:0)	Stearic (18:0)	Oleic (18:1)	Linoleic (18:2)	Linolenic (18:3)
Soybean Oil (%)	11	4	23	53	8
Linseed Oil (%)	5	4	19	15	57

Legend (x:y): x, number of carbon atoms; y, number of double bonds. Fatty acid contents do not add to 100% due to presence of minor fatty acid content.

2.2. CHEMICAL CHARACTERIZATION

Infrared spectra (IR) were measured with a Nicolet Nexus 470 E.S.P. spectrophotometer (Waltham, MA, USA). 1H NMR spectra were obtained on a Varian INOVA 400 MHz spectrometer (Palo Alto, CA, USA) using d6-DMSO as solvent. Iodine

value was assessed using ASTM Method D5554-95. Oxirane oxygen value was measured using AOCS Method Cd 9-57.

2.3. SOAP AND FREE FATTY ACID PREPARATION

Free fatty acids were made via acid neutralization of soap. Vegetable oil and water mixture (800 g, 50:50) was reacted with sodium hydroxide solution (200 g, 30 wt%) at 60°C for 4 hr to generate soap and then acidified with sulfuric acid (270 g, 30 wt%) to pH<2. The lower aqueous layer including sodium sulfate and glycerin was separated, washing the top FFA layer using 60 °C water. Finally the liquid organic FFA layer (339 g) was dried using anhydrous sodium sulfate. The iodine value of the soybean FFA was 133.

Freshly prepared FFA was dissolved in acetone based on the weight ratio of 1:6 and then purged with nitrogen gas, cooled to –20 °C for overnight. The formed crystals were removed by vacuum filtration. The procedure could be repeated several times until no further crystals were generated. For these studies, four times filtration were performed resulting in an iodine value for refined unsaturated soybean FFA of 150.

To a FFA/acetone solution (500 g) of weight ratio of 1:10, 110% of stoichiometric sodium hydroxide solution (18 mL, 10 M) based on amount of FFA (average molecular weight treated as 278 g/mol) was added dropwise. The neutralization reaction was continued for 4 hr under nitrogen gas to prevent air oxidation of the soap. The soap powder was readily filtered by vacuum filtration and then dried at 110 °C for 1.5 hr.

2.4. GLYCIDYL ESTERS OF EPOXIDIZED FATTY ACIDS PREPARATION

Dry soap (302 g) and EPCH (925 g) were heated to reflux. Phase transfer catalyst CTAB (7.3 g) at 2 equivalent-% per equivalent soap was then added. Reflux was

continued for 30 min, cooled and centrifuged, the clear solution was decanted to a flask. Excess EPCH was removed using *in vacuo* rotary evaporation. Oxirane oxygen value of prepared glycidyl ester was 4.4% (theoretical value of 4.7% for glycidyl oleate).

Glycidyl ester (341 g) and sodium carbonate (64 g) were mixed with methylene chloride (200 ml). MCPBA (367 g, 75 wt%) dissolved in methylene chloride at 0.1 g/ml concentration was added dropwise at a reaction temperature below 15 °C and then reacted for 4 hr to complete epoxidation. The reaction mixture was washed with 10 wt% sodium sulfite (200 g) and then by 10 wt% aqueous sodium bicarbonate (150 g). Methylene chloride was removed by *in vacuo* rotary evaporation and the product EGS (345 g) was dried over anhydrous sodium sulfate. Linseed oil based glycidyl esters of epoxidized fatty acids (EGL) were also prepared based on the above mentioned procedure. For EGSS/ EGL-S, saturated FFAs were not removed and remain in EGS/EGL. For EGS-P/EGL-P, FAs were partially epoxidized. Soybean oil based epoxidized methyl ester (EMS) and epoxidized allyl ester (EAS) were formed by standard alkaline transesterification with the corresponding alcohols and then epoxidized by MCPBA, *e.g.*, potassium hydroxide (2.2 g) was first crushed and dissolved in allyl alcohol (260 g), then poured into soybean oil (220 g). Mixtures were heated under reflux condition for 4 hrs. Workup included potassium hydroxide discharged by the addition of concentrated hydrochloric acid (3.9 g, 37 wt%), removal of the excess allyl alcohol using in vacuo rotary evaporation, washing of the allyl esters of soybean oil four times with distilled water to remove glycerin, salt, and any residual allyl alcohol, and then drying with anhydrous sodium sulfate and filtration to remove the sodium sulfate. The method

for epoxidation of allyl esters of soybean oil by MCPBA is the above-mentioned method for epoxidation of glycidyl esters.

2.5. THERMAL CHARACTERIZATION

2.5.1. Curing reactions

The weight ratios of EGS/ESO to DGEBA resin blend chosen for the present work were 0:100 (pure DGEBA), 10:90, 30:70, 50:50, 70:30; 90:10 and 100:0 (pure EGS/ESO). A stoichiometric ratio $r = 1.0$ of epoxy/anhydride was used for all samples and 1 wt% (based on epoxy part) of EMI were added to the blend. After mixing by a PowerGen 1000 homogenizer (Fisher Scientific, St. Louis, MO, USA) for 10 min, the mixture was degassed under vacuum for 30 min, then poured into a mold treated with mold release agent. Curing was performed at 145 °C for 15 hr for all blends except ESO-DGEBA (90:10) and pure ESO blend, which were inducted for 12 hr at room temperature, remixed, poured into the mold and cured at 125 °C for 15 hr. ESO required more stringent curing conditions due to the low reactivity and phase separation exhibited by ESO. Postcure for all samples was performed at 175 °C for 1 hr.

Two to three milligrams of mixture was hermetically sealed in an aluminum pan and cured on a model Q2000 differential scanning calorimetry (DSC) machine (TA Instruments, New Castle, DE, USA) by scanning temperature at a heating rate of 10°C/min from 40–250 °C to study the cure behavior of each formulation.

Neat epoxy monomers were also cationically cured. A 3 wt% (based on epoxy) of BF_3-MEA was mixed with monomer and cured at 150 °C for 3 hr followed by 185 °C for 1 hr.

2.5.2. Glass transition and degradation temperatures

DSC was used to determine the glass transition of cured resin. Samples were first preheated at 20 °C/min to 180°C to remove any previous thermal history, and then quenched to –40 °C. Heat flow was measured over a temperature range scanned from –40 to 180 °C at a heating rate of 20 °C/min. Universal Analysis 2000 software (TA Instruments, New Castle, DE, USA) was used to analyze the curve, inflection temperature (T_i) was reported as the glass transition temperature.

A model Q50 thermogravimetric analysis instrument (TGA, TA Instruments, New Castle, DE, USA) was used to determine the thermal degradation onset temperature of cured resin. Measurement was performed while scanning temperature from 30 to 750 °C at a heating rate of 10 °C/min under an ambient air flow environment.

2.6. SWELLING TEST

Approximately 0.2 g of the cured resins with a cubic shape (8 mm x 8 mm x 3 mm) were placed in toluene solvent until equilibrium was attained. To accelerate the swelling, samples were placed into a 45 °C oven to attain a constant weight, then equilibrated at room temperature for one week. The swollen samples were removed from the solvents, quickly blotted dry with paper towel, and weighed. The equilibrium swelling ratio [47] of the cured resin was calculated based on Equation (1):

$$Q = 1/v_2 = 1 + \frac{\left(\frac{m_s}{m_0} - 1\right) * \rho_{poly}}{\rho_{sol}} \quad (1)$$

where Q is the equilibrium swelling ratio of the polymeric network, v_2 is the volume fraction of polymer at equilibrium swelling, m_0 is the mass of the polymeric network

before swelling, m_s is the mass of the polymeric network at equilibrium swelling, and ρ_{sol} and ρ_{poly} are the densities of the solvent and polymeric network, respectively.

2.7. MECHANICAL TESTS

Tensile strengths and moduli were measured on a model 4469 Universal testing machine (Instron, Norwood, MA, USA) according to ASTM D638. All the tensile tests were performed at a crosshead speed of 10 mm/min. At least five specimens were tested for each different resin system. The flexural strengths and moduli were determined according to the ASTM method D790. The span was 50.8 mm, the crosshead speed was set at 12.7 mm/min.

2.8. PHYSICAL PROPERTIES

Viscosity was tested on a model LVDV-III+ Ultra Rheometer (Brookfield, Middleboro, MA, USA) at 25°C. Liquid density was determined using the pycnometer method. Specific gravity of solid samples was measured by immersion in water using a model XP 204S balance (Mettler-Toledo, Columbus, OH, USA) with density measurement kits.

3. RESULTS AND DISCUSSION

3.1. PREPARATION OF GLYCIDYL ESTERS OF EPOXIDIZED FATTY ACIDS

Figure 1 shows the synthetic route to EGS, generalized for oleic acid showing the process for a soybean triglyceride. Preparation of mixed FFAs from triglyceride is straightforward and well-developed. Methods of low temperature crystallization to remove the unsaturated FFAs are also well documented [48]. Most unsaturated FFAs are soluble in most organic solvents at temperature above 0 °C while the saturated FFAs,

which have higher melting points than unsaturated FFAs, are prone to form crystals/precipitates at low temperature in solvents like acetone or methanol. Although trace amounts of saturated FFAs remain unavoidably in the unsaturated FFAs after low temperature crystallization [49], further removal of saturated FA components was achieved after synthesis of glycidyl ester or EGS because glycidyl esters, or the epoxidized glycidyl esters, of unsaturated FAs are each liquid at room temperature and much lower in melting point than glycidyl esters of saturated FAs. The unsaturated esters are poorer solvents for saturated carbon chains, which are then more easily precipitated at room temperature. Although no FFA component analyses, like chromatography, were performed in this research, we believe the saturated components were minimized after three precipitations.

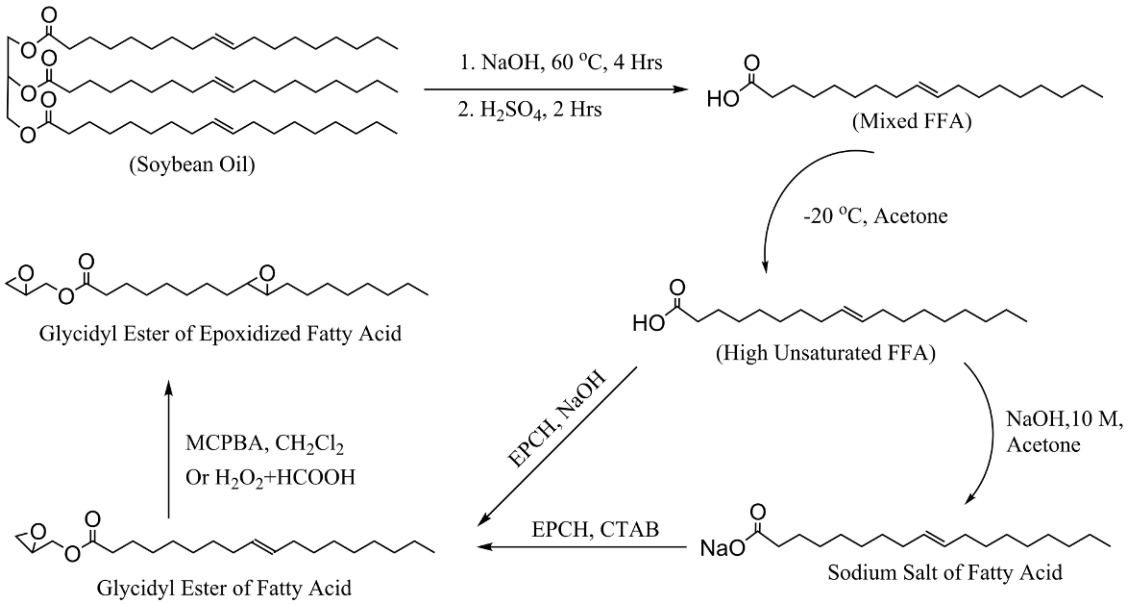

Figure 1. Synthetic route to EGS. (Vegetable oil and FAs are shown as simplified structures containing only oleic acid though they also contain other FAs. See Table 1)

Acetone was used as a low boiling, recoverable solvent to prepare soap. A slight excess of NaOH and higher concentration was preferable when preparing soap from FFA because unsaturated FFAs were prone to dissolve in acetone rather than react with base. Unsaturated FFA soaps are more soluble in water [50]. Carefully dried and finely powdered soaps resulted in greater yields of glycidyl esters of FAs [51].

A low solubility of soap in EPCH suggested that a phase transfer catalyst would be useful to accelerate the reaction. With CTAB catalyst, the consumption of soap was completed within half an hour under reflux condition. Glycidyl esters can also be prepared directly from FFA in EPCH medium but the yield and purity were lower than obtained by the soap process [50]. The epoxidation of glycidyl ester was carried out using MCPBA or *in situ* generated performic acid. The former was more efficient. Due to the low solubility of MCPBA in methylene chloride, large amounts of recoverable solvent was required for the epoxidation.

Figure 2 shows the FT-IR spectra of mixed FFA, soybean oil, glycidyl esters and EGS. The band at 3008 cm^{-1} was attributed to the C–H stretching of =CH in unsaturated FAs, such as oleic acid, linoleic acid or linolenic acid. New bands at 910 and 852 cm^{-1} were observed in the spectrum of glycidyl esters with the disappearance of the absorption at 937 cm^{-1} in the mixed-FFA spectrum that showed presence of glycidyl group. The conversion of double bonds to epoxy was confirmed by the disappearance of the 3008 cm^{-1} band observed in glycidyl esters and the concurrent appearance of absorption at 752 cm^{-1} in EGS.

Figure 3 shows the 1H NMR spectra of mixed-FFA, glycidyl ester and EGS, where linoleic acid is shown as a generalized compound for structural assignments. The

spectra showed no evidence of side reactions in preparing glycidyl esters using the soap process, nearly quantitative conversion of double bonds to epoxy groups, and no oxirane ring opening during the epoxidation of glycidyl esters to EGS using MCPBA, *i.e.*, showed complete conversion but a lack of side reactions.

General properties of EGS product compared to ESO and DGEBA is shown in Table 2.

Table 2. General physical properties of epoxy resins

Epoxy Resin	Oxirane oxygen (g/100g sample)	EEW (g/equivalent)	Viscosity at 25 ^{o}C (mPa·s)	Density (g/ml)
EGS	10.1	158	70	1.03
ESO	6.9	232	430	0.98
EGL	12.0	134	85	1.04
ELO	9.3	171	800	1.03
DGEBA	8.6	186	13000	1.16

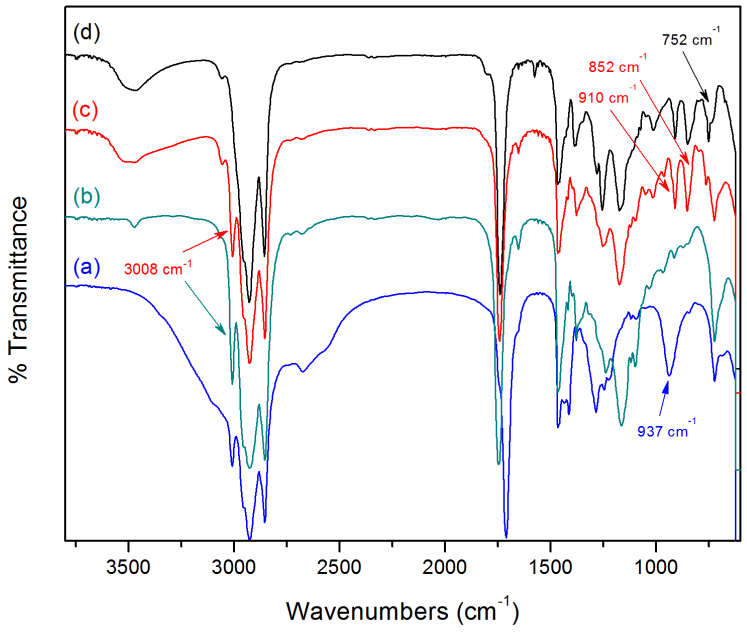

Figure 2. IR spectra (a): mixed-FFA (b): soybean oil (c): glycidyl esters (d): EGS

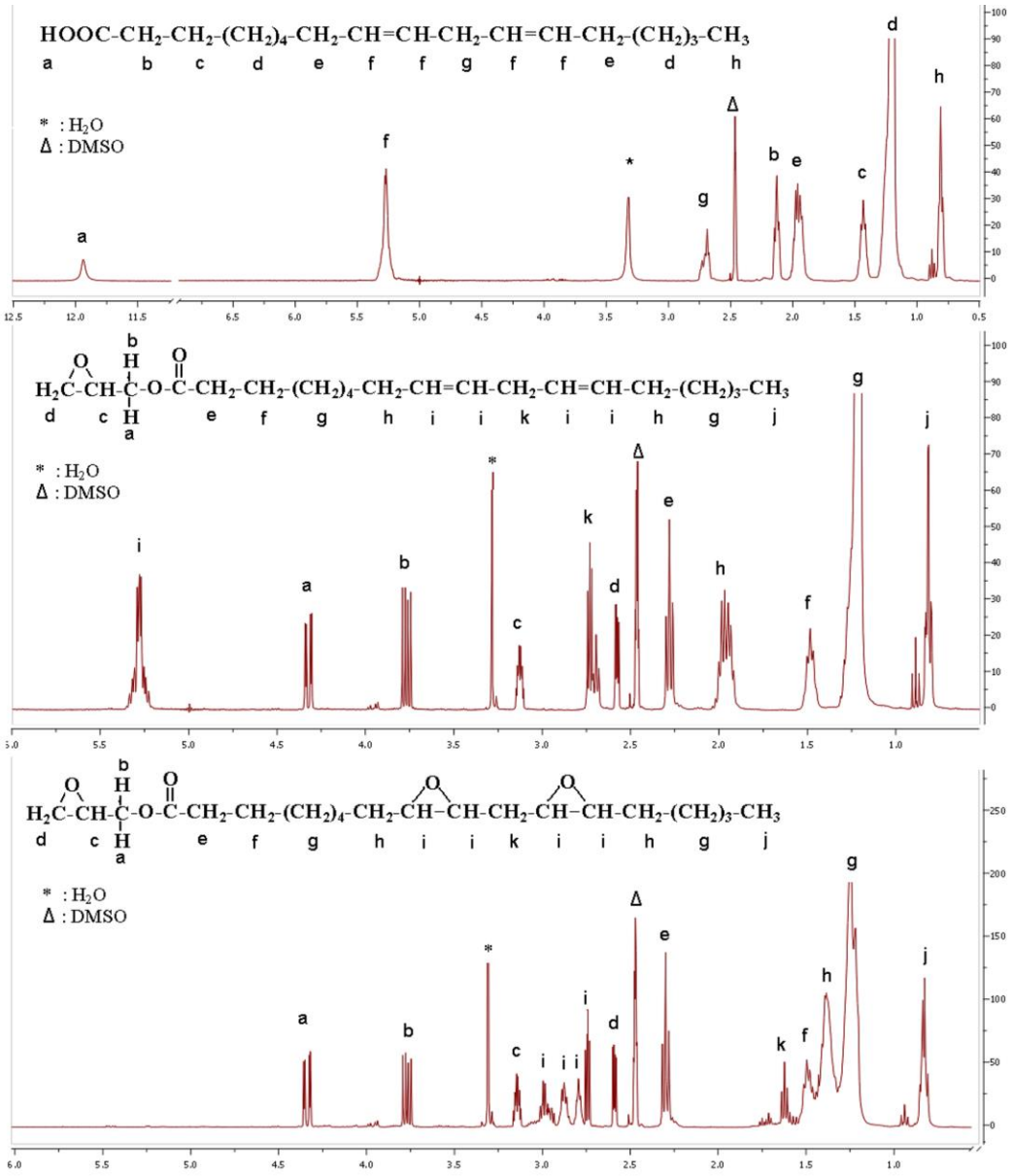

Figure 3. 1H NMR spectrum and structural assignments of a) FFA mixture; b) glycidyl ester of FFA mixture; and c) EGS monomer (see text for structural assignment details)

3.2. CURING REACTION

Differential scanning calorimetry was applied to study the curing behavior of the blended epoxy resins (Figure 4). The exothermic peaks were characteristic of the epoxy and anhydride curing reaction [52, 53]. Integration of the peaks allows the determination

of the enthalpy of curing reaction (ΔH), cure onset temperature (T_o) and peak exothermic (T_p).

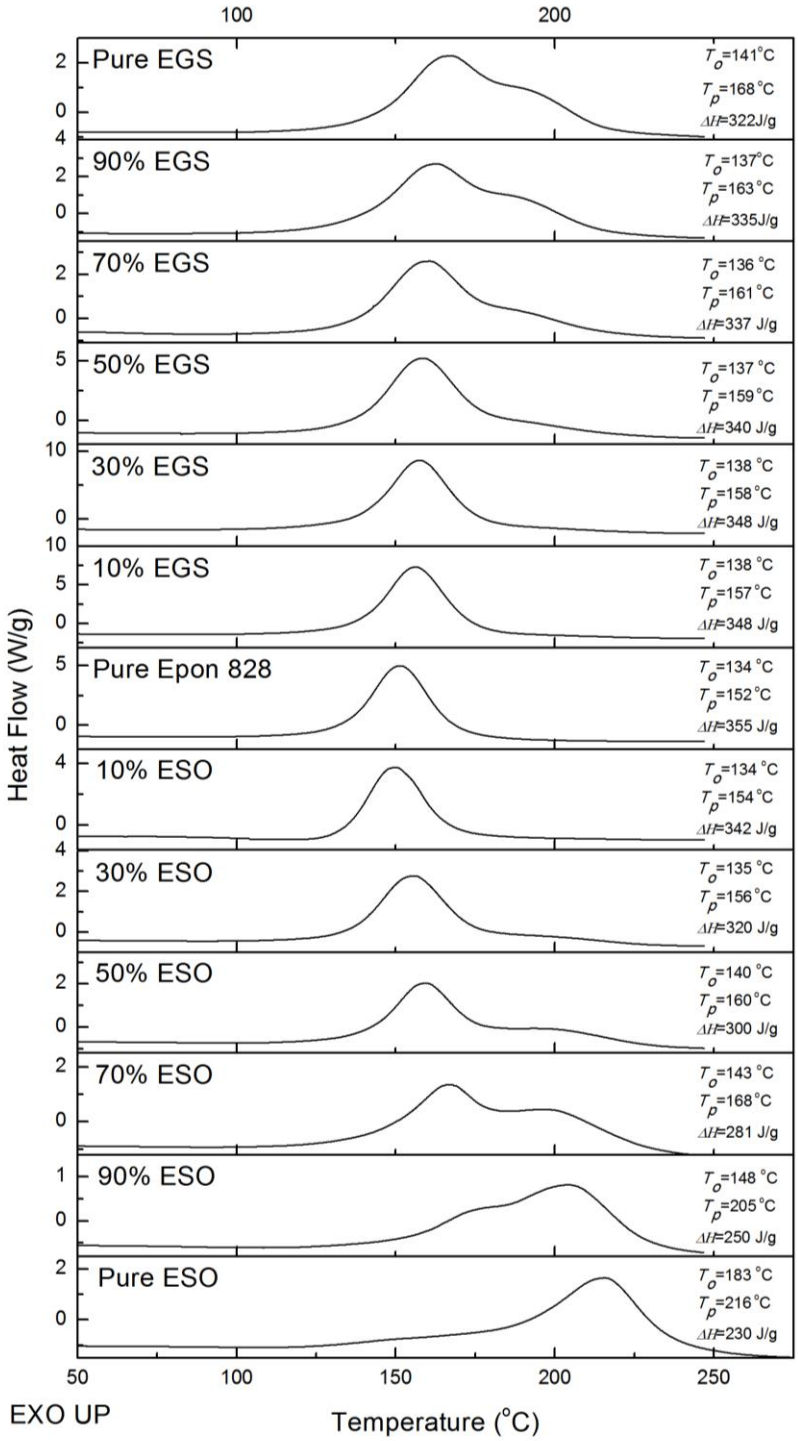

Figure 4. Dynamic thermograms of DGEBA-EGS/ESO-MHHPA systems

From Figure 4, the pure DGEBA and ESO reactions with MHHPA show single exothermic reaction peak at 152 °C and 216 °C, respectively. The higher predominance of the T_p value of ESO means a slower reaction rate, which was also confirmed by a lower ΔH value. A lower oxirane content of ESO and the internal oxiranes versus glycidyl functional groups react more sluggishly with MHHPA curing agent.

The addition of ESO to DGEBA leads to a shifting of T_p and T_o to higher values.With a decrease of ΔH value, two partially convoluted peaks were clearly observed that became pronounced for 50 wt% ESO or higher ESO concentrations, which suggested that there was decreasing ESO miscibility in the DGEBA. Immiscibility would lead to an inhomogeneous cure of the epoxy resin. Group reactivity also affects the polymerization reactions. ESO has internal, hindered oxiranes whereas DGEBA has glycidyl groups of less steric hindrance and greater reactivity than the internal oxirane.

The prepared EGS resin showed quite different and interesting curing behavior. The neat EGS showed two convoluted peaks, analogous to the blend of DGEBA and ESO, which is believed to be due to the inherently different reactivity of glycidyl and internal oxirane groups. The T_p and T_o values of EGS were more than 40 °C lower than ESO, which indicated EGS was much more reactive than ESO. Increased addition of EGS to DGEBA also lead to shifting of T_p to higher values but the T_o remained nearly constant. Only a 16°C increase of T_p was observed for 90 wt% EGS concentration compared to pure DGEBA while it was 54 °C for a 90 wt% ESO concentration.

The ΔH's [J/g] also followed a similar trend. The higher oxirane content of EGS and EGS blends, which bear glycidyl groups like pure DGEBA, would appear to facilitate a more homogenous three dimensional polymer structure upon curing compared

to ESO blends. Also of interest, a lower concentration of EGS/ESO, *e.g.*, 30 wt% EGS or below, or 10 wt% ESO, had little effect on the ΔH or T_p values compared to pure DGEBA cure, which may be related to homogeneity and compatibility with the DGEBA.

3.3. COMPATIBILITY

The DGEBA-ESO system generally has a heterogeneous structure [52] and, not surprisingly, a nonuniform crosslinked structure will lead to a poorer mechanical performance compared to a more homogeneous structure. Cured aromatic DGEBA polymers are much more rigid compared to cured aliphatic ESO, which behave as weak points or flaws when applying load. Fracture is initiated by the stress concentration at weak points. For instance, the mechanical properties of soybean oil/DVB plastics are significantly improved after increasing the uniformity of the crosslinked structure [7]. A heterogeneous polymer structure is mainly due to the reactivity differences between internal and terminal oxirane. Moreover, the miscibility/compatibility between the monomer-monomer and monomer-polymer structures should also play an important role during the formation of crosslinked structure. Solubility parameter is one method to assess the compatibility of epoxy resin with an additive or modifier [54]. To form a homogeneous structure, the monomers and copolymers should have similar solubility parameters in accordance with the general rule that chemical and structural similarity favors solubility, *i.e.*, 'like dissolves like'. Direct determination of polymer solubility parameters from heat of vaporization data is not possible because of their non-volatility [55].

Thus, Hildebrand solubility parameters were calculated based on the group contribution method [56]. The group contribution equation is given by Equation (2):

$$\delta = \frac{\rho \sum_i F_i}{M} \quad (2)$$

where δ is the calculated solubility parameter, $\Sigma_i F_i$ is the molar attraction constant summation over discreet i structural group present in the compound and ρ and M are the density and molar mass of the compound, respectively. For polymers, $\Sigma_i F_i$ is the sum of all the molar attraction constants in the repeat unit, ρ is the density of the polymer, and M is the molar mass of the repeat unit. For copolymers or polymer blends, following Equation (3) was used:

$$\delta_{mix} = \frac{\sum_i x_i V_i \delta_i}{\sum_i x_i V_i} \quad (3)$$

where x_i is mole fraction of component i, V_i is component i molar volume, and δ_i is component i solubility parameter. In this study, the solubility parameter of each resin was calculated based on Hoy or van Krevelen model [56]. All compounds structures are listed in Figure 5. For EGS, a total 2.3 epoxy groups were used for the calculation, which was calculated from titrated oxirane content. Calculated δ values are listed in Table 3.

Table 3. Calculated solubility parameters of monomer and cured matrix

δ $(MPa)^{1/2}$	EGS	DGEBA	ESO	MHHPA	DGEBA-MHHPA	EGS-MHHPA	ESO-MHHPA
δ (van Krevelen)	17.8	20.5	17.5	18.2	19.4	18.0	17.8
δ (Hoy)*	19.5 (18.6)	21.9 (21.1)	19.0 (18.4)	20.9	21.0	19.4	19.7

* Values in brackets are calculated based on linear ether functional group instead of cyclic oxirane.

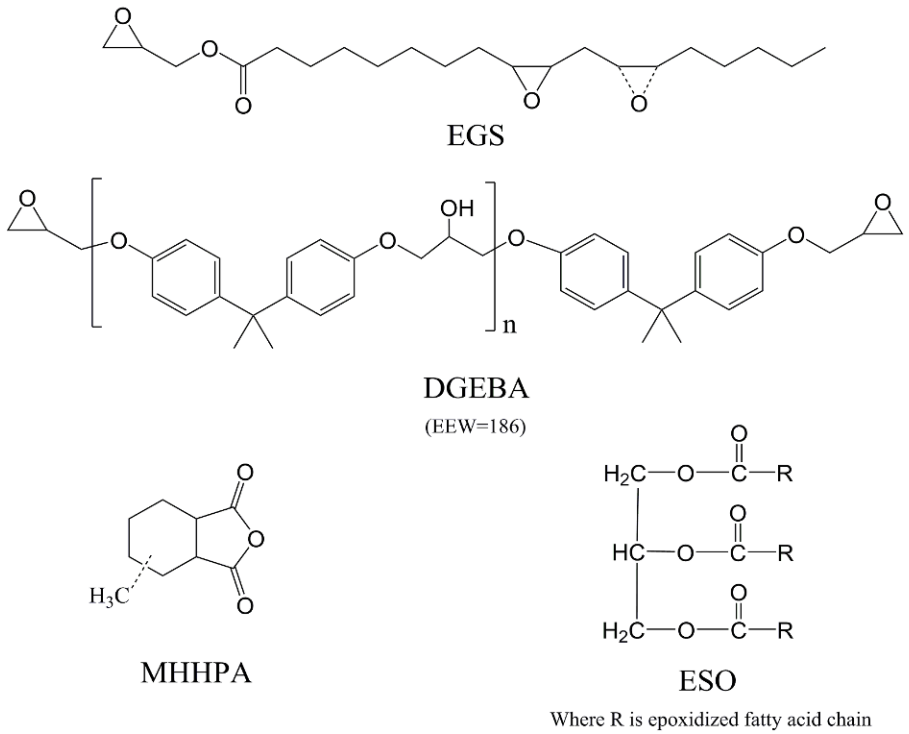

Figure 5. Compounds structure used for solubility parameters calculation

From Table 3, DGEBA, MHHPA and EGS have larger solubility parameters while ESO has the lowest solubility parameter in the blend system. Calculated values of DGEBA are close to the lower limits of the experimental values [13], which are often more reliable than upper-limit ones [57]. There are some differences in the calculated values using Hoy versus van Krevelen models because epoxy group and ether group have different values in Hoy's model. Epoxy groups should convert to ether/ester after curing reaction, so values based only on ether groups instead of epoxy were also listed in Table 3. There is a considerable difference in the values of MHHPA due to the large difference between the group contributions of the anhydride group quoted by Hoy and by van Krevelen. Only van Krevelen values were used for the further calculation because there

is evidence showing experimental values matched well with van Krevelen calculated values in the DGEBA-anhydride system [58].

It has been reported that ESO [59] or pre-polymerized ESO [60] is only partially miscible, *i.e.*, has phase separation, with the epoxy resins. The thermodynamic condition for polymer compatibility is that free energy change of mixing (ΔG_{mix}) should be small or negative, based on Flory-Huggins equation combined and Hildebrand solubility parameters [61]. ΔG_{mix} can be expressed by Equation (4):

$$\Delta G_{mix} = \phi_1 \phi_2 V(\delta_1 - \delta_2)^2 + RTV(\frac{\phi_1 \rho_1}{M_1} ln\phi_1 + \frac{\phi_2 \rho_2}{M_2} ln\phi_2) \quad (4)$$

where ϕ_n is the phase volume fraction, V is volume of lattice, ρ_i is the density of component i, M_i is the molecular weight of component i, R is gas constant and T is absolute temperature. The first term of the right side in Equation 4 are related to the enthalpy of mixing (ΔH_{mix}) and the second term is assigned to the entropy of mixing ($-T\Delta S_{mix}$). Since ϕ_1 and ϕ_2 are fractions, for a fixed DGEBA-EGS/ESO composition, ΔG_{mix} at constant temperature depends only on $\Delta\delta_i$ and ρ_i/M_i, which are determined by the chemical nature and molecular weight of the EGS/ESO/DGEBA, respectively. Proximity of δ_i between DGEBA and EGS/ESO and a low molecular weight EGS/ESO favors the mixing process. It is not then surprising that EGS of higher solubility parameter and lower molecular weight favors better compatibility with DGEBA than ESO.

We have noticed turbid blends indicating phase separation were formed only for high contents of DGEBA replacement by ESO (90 and 100 wt%, Figure 6b, 6c and 6d), especially when using EMI as accelerator. While using tertiary amine a more transparent

solution was formed but tertiary amine generally lead to lower T_g compared to using imidazole as accelerator [53]. These blends were prone to form cracked samples after curing and spots with dark brown or yellow colors were also observed (Figure 6b and 6c). We ascribed these to phase separation and internal stress due to incompatibility and low reactivity of ESO in these curing systems. The terminal oxirane of DGEBA is more reactive than the internal oxirane of ESO so gelation always occurs first in the DGEBA phase. At low ESO concentration, ESO is firstly dissolved and plasticizes the rigid DGEBA matrix but is finally cured by anhydride and becomes part of the crosslinked structure as two phase thermoset polymer. At high curing temperatures, the ΔG_{mix} is marginally negative and ESO is better compatible with DGEBA but slower to react. With the advancement of curing reaction the molecular weight of crosslinked DGEBA and ESO will increase, which will result in a decrease of ΔS_{mix}. At a certain stage ΔG_{mix} becomes positive and crosslinked ESO phase separates, which should be analogous to a phase separation of rubber in epoxy resin [62].

At higher ESO concentrations, due to a faster gelation rate of the glycidyl-DGEBA network occurring at low degree of conversions of ESO, internal stress can result after vitrification but which can be avoided by proper cure temperature profile [63]. Such internal stress and incompatibility can easily lead to crack initiation or defect structure as observed in Figure 6c. Prolonged induction via heated mixing of the ESO blend and carefully choosing the curing conditions led to more transparent polymers and uncracked samples that were used for further testing.

For EGS blends, due to the terminal oxirane as in DGEBA, EGS may remain part of the DGEBA matrix during curing where a more homogeneous crosslinked structure is

formed. An increase in oxirane value in EGS also boosts compatibility with the DGEBA system and may yield cured products with improved properties.

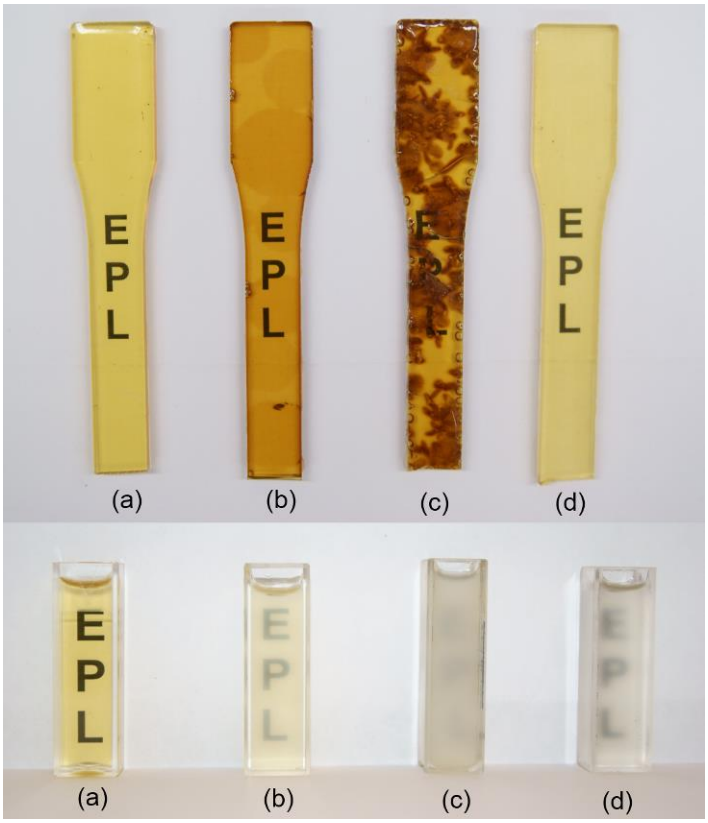

Figure 6. Physical appearances of MHHPA cured EGS/ESODGEBA polymers and uncured monomers blends (a): EGS-DGEBA (90:10); (b): ESO-DGEBA (90:10) precured at 145°C for 10 min; (c): ESODGEBA (90:10) without procuring; (d): Pure ESO inducted for 12 hrs

3.4. CROSSLINK DENSITY

Crosslink density is one of the most important factors determining the properties of cured thermoset resins and is typically reported as an average molecular weight (M_c) between crosslinks. The crosslink density increases as M_c decreases. Several methods are available for measuring the crosslink density of a thermoset. A common method is to measure the elastic modulus of the thermoset in the rubbery plateau region using dynamic mechanical analysis (DMA). Solvent swelling measurements are also used to determine

the crosslink density of epoxy resin [47, 64, 65]. Good agreement between M_c values from the swelling measurements based on the stoichiometry considerations has been reported [66]. A structure based on a stoichiometric curing condition was assumed because the dominant reaction in the present epoxy-anhydride-imidazole system is esterification while etherification of epoxy groups is much slower [67]. The M_c of the cured resin was calculated from equilibrium solvent swelling data based on the Flory–Rehner equation [47] (Equation (5)):

$$\upsilon = \frac{\rho_{poly}}{M_c} = \frac{ln(1-\upsilon_2) + \upsilon_2 + \chi{\upsilon_2}^2}{V_1(\frac{\upsilon_2}{2} - \upsilon_2^{\frac{1}{3}})} \quad (5)$$

where υ is the strand density, υ_2 is the volume fraction of polymer at equilibrium swelling as measured by swelling test (Equation (1)), V_1 is the molar volume of the solvent, and χ is the polymer-solvent interaction parameter, which is related to the solubility parameters via Equation (6):

$$\chi = 0.34 + \frac{V_1}{RT}(\delta_1 - \delta_2)^2 \quad (6)$$

where R is the gas constant, T is the absolute temperature, V_1 is the molar volume of the solvent, and δ_1 and δ_2 are the solubility parameters of solvent and polymer, respectively. δ_2 was calculated by Equation (3), and where for toluene δ_1 =18.3 $MPa^{1/2}$. The calculated and experimental results are listed in Table 4.

In ESO or EGS, the epoxy crosslink sites in the FA chains are located at the 9th and 10th carbons in the oleic acid and could be also at the 12nd and 13th carbons in linoleic acid, which leave the rest of the chain up through 18th carbon as an ineffective chain end in the crosslinked polymer (Figure 7). Furthermore, the presence of saturated palmitic or

stearic acids in ESO triglyceride structure also behave like pendant chain [42], so the inactive parts, *e.g.*, pendant chains and saturated FAs, in ESO and EGS constitute 34.8 and 18% of total mass, respectively. These maybe subtracted from the dry and swollen sample weights to obtain a corrected M_c^*, because end-linked networks were assumed during swelling test, in fact pendant chains are not contributed to the total crosslink densities [38]. M_c and corrected M_c^* values are listed in Table 4.

Table 4. Swelling properties of cured epoxy resins in toluene

MHHPA cured Samples	δ $(MPa)^{1/2}$	ρ_{poly} (g/ml)	*Q Swelling ratio*	χ	M_c (g/mol)	M_c^* (g/mol)
Pure DGEBA	19.4	1.18	1.49	0.388	257	257
EGS-DGEBA (10:90)	19.2	1.17	1.50	0.375	253	256
EGS-DGEBA (30:70)	18.9	1.16	1.54	0.356	268	278
EGS-DGEBA (50:50)	18.6	1.16	1.57	0.345	281	299
EGS-DGEBA (70:30)	18.4	1.15	1.61	0.340	304	330
EGS-DGEBA (100:0)	18.0	1.12	1.66	0.344	332	376
ESO-DGEBA (10:90)	19.3	1.17	1.51	0.375	261	267
ESO-DGEBA (30:70)	19.0	1.15	1.55	0.355	273	293
ESO-DGEBA (50:50)	18.6	1.14	1.58	0.343	285	324
ESO-DGEBA (70:30)	18.3	1.12	1.64	0.340	314	382
ESO-DGEBA (100:0)	17.8	1.09	1.84	0.350	464	640

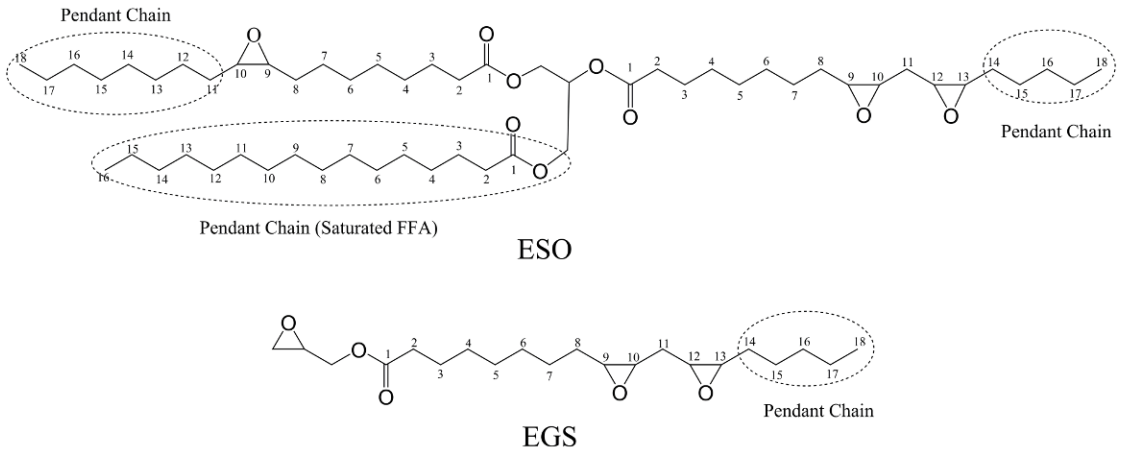

Figure 7. Schematic representation of pendant chain in ESO structure [epoxy moieties in ESO/EGS and methane moiety in glycerol part of ESO are the crosslink sites]

From Table 4, the ρ values of both EGS and ESO systems decrease with the increase of EGS/ESO content that can be attributed to the addition of a large soft/flexible vegetable oil component to decrease the rigid, compact structure of DGEBA polymer. Increase in EGS/ESO content also leads to a higher swelling ratio *Q*, which could indicate not only lower crosslinking density but also a higher solubility of the network in the toluene solvent that is supported by a decreased χ value. M_c and M_c^* values of MHHPA cured neat DGEBA [68] and neat ESO [31] are similar to reported DMA test results. Pure EGS, which has similar oxirane content as ELO, also is close to a reported DMA test result for polymerized ELO [53]. Calculated values based on the van Krevelen model are also comparable to DMA tests.

In general, an increase in ESO or EGS content decreased crosslink density compared to a neat anhydride cured DGEBA. This result is due to the inherently flexible structure of fatty acid chain and thereby prone to form a less compact crosslinked

structure compared to the stiffer aromatic repeat unit of DGEBA. A decrease in crosslink density was also reported by others [20].

Crosslink density is also related to the oxirane value. EGS has higher oxirane value than ESO so all EGS blends had higher crosslink densities compared to ESO blends at the same concentration level. Crosslinking density increasing with oxirane value has also been observed within various EVOs of different oxirane content [69] or for the same vegetable oil with different oxirane content [16]. Surprisingly, 10 wt% EGS concentration had a similar crosslink density as pure DGEBA, which is in part probably due to a higher functionality of EGS compared to pure DGEBA. More anhydride needed to cure the blend would lead to higher crosslink densities. With increases in the EGS content in blends, a lower crosslink density was observed though the crosslink density had minimal change even at 50 wt% concentration. ELO has similar epoxy content as EGS and has been reported to maintain nearly constant crosslink density of the anhydride-cured epoxy at up to 70 wt% concentration [70]. For ESO with much lower oxirane value compared to DGEBA or EGS, the crosslink density of ESO blends decreased with increased ESO concentration that is especially noticeable after Mc correction for pendant chains. The saturated component in ESO thus plays a significant role in reducing the crosslink density. Though crosslink density has been reported to not be changed by the replacement of DGEBA by ESO using mechanical analysis of the rubbery plateau [52], an artificially larger modulus can result for the inherently heterogeneous DGEBA–ESO–anhydride network due to a broadened glass transition temperature range. As heterogeneity will broaden the modulus signal in the rubbery

region, a shear storage modulus value near the glass transition in the rubbery region can be artificially increased resulting in an inflated value for the calculated crosslink density

3.5. THERMAL PROPERTIES

The glass transition temperature (T_g) is considered a fundamental polymer characteristic related to polymer properties and processing. In general, polymers with high crosslink density have higher T_g; however, the composition in the polymer within the crosslinked structure also plays an important role in the T_g behavior. DSC and DMA are widely used to characterize T_g. For most thermosetting plastics, the DMA measurement based on the tan δ peak at a frequency of 1 Hz generally occurs at a temperature as much as 15–20 °C above T_g as measured by dilatometry or DSC [16, 26] but inflection temperature typically correlate better with DMA tan δ than a midpoint value.

The trend of cured epoxy resin blends (polymers) T_g as measured by DSC is shown in Figure 8. The MHHPA cured pure EGS had higher T_g (88°C) which was nearly 40°C higher than ESO-MHHPA. Pure DGEBA-MHHPA polymers which is aromatic and had the highest T_g measured (152 °C). Aliphatic amine [12, 71], or boron trifluoride diethyl etherate [72, 73], cured ESO polymers had low T_g, usually less than 0 °C. While aromatic amine [29], cycloaliphatic amine [74], thermally latent initiator [75], or anhydride [76] cured EVO polymers generally have higher T_g, it is still rare to observe cured ESO polymers [31, 77] with T_g above 60 °C.

Addition of ESO or EGS led to a decrease of T_g. For small EGS/ESO concentration, *e.g.*, below 30 wt%, the T_g values of ESO-DGEBA or EGS-DGEBA systems were quite similar to each other and slightly decreased compared to pure

DGEBA-MHHPA, which indicated the T_g behavior was mainly determined by the crosslink density as measured in the swelling test where only slight increases of M_c or M_c^* were observed. However, the aromatic DGEBA versus aliphatic EGS structure also plays a role because 10 wt% EGS concentration appears to have a slightly higher crosslink density but still a lower T_g. It has been reported that aromatic phthalic anhydride cured EVO had higher T_g but lower crosslink density [31, 53].

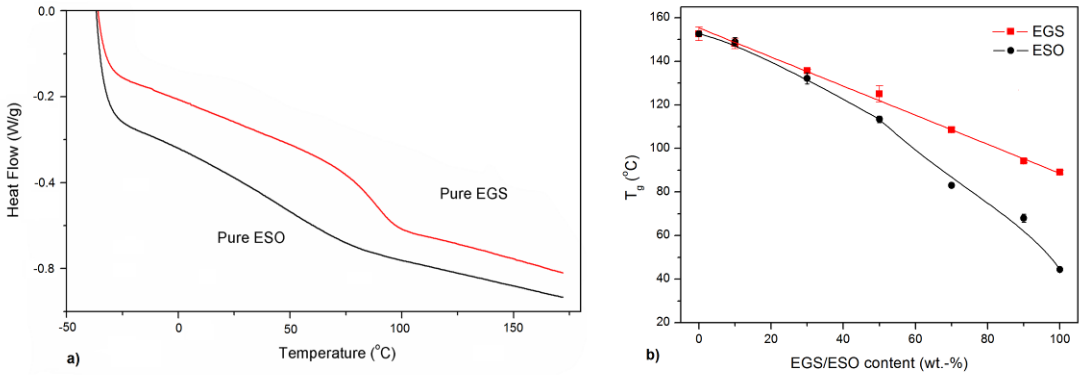

Figure 8. Plots of a) the glass transition region of ESO/EGS-MHHPA neat polymer showing the differences in breadth of the transition; b) the measured inflection point glass transition temperatures of cured epoxy monomer(s) as a function of ESO/EGS-DGEBA blend composition (Lines only to aid visualization of trend)

For further increases in the concentration of EGS/ ESO, the T_g values decreased more rapidly, especially for the ESO system. The inherent, long aliphatic chain structure of ESO, sluggish reactivity of internal oxirane, and lower oxirane content preclude polymer as densely crosslinked as those of EGS or DGEBA. Unreactive saturated components like stearic acid and palmitic acid pendant chains enhance the flexibility and degree of freedom for movements of the molecular chains in the epoxy network. These

factors decrease the polymer T_g. Further depressed T_g was also reported for an epoxidized palm oil system, which had lower oxirane content than ESO [26].

At low ESO concentrations (≤ 50 wt%) a linear, decreasing Tg trend was observed, however, neat ESO or higher ESO concentrations (≥50 wt%) thermosetting polymers showed broad transitions from the glassy to the rubbery state. The blends' T_g seems predominately controlled by the ESO part. Similar behavior was also found in ELO replacement of diglycidyl ether of bisphenol F resin [78]. The plasticizing effect of saturated FAs and/or the different reactivity of ESO and DGEBA leads to a broad distribution of chain segment mobilities [79] and indicate a heterogeneous polymer network [80]. Broad T_g range behavior was not found in the EGSDGEBA systems. Also a nearly linear transition of T_g with increase of EGS was observed, which indicated good synergy and homogeneity of the crosslink structure formation between EGS and DGEBA.

Researchers [16, 69] have noted the influence of EVO monomer oxirane value on polymer T_g. We present trends in relationship between T_g and EVO structure with and without saturated components. Several epoxy resins made from vegetable oils were synthesized and polymerized by MHHPA with EMI as catalyst and/or cationically polymerized with BF_3-MEA initiation. The obtained plot of polymer T_g as a function of oxirane oxygen value is presented in Figure 9.

The glass transition temperatures of anhydride cured copolymers are higher than those of the neat of cationically cured monomers due to the anhydride structural stiffness elevating the copolymer T_g. The T_g are observed to increase fairly linearly with oxirane value. Higher oxirane values are expected to lead to higher crosslink densities upon

curing. A similar T_g for anhydride cured ELO and EGS was observed though ELO has a slightly lower oxirane value. The ELO structure is partially crosslinked, *i.e.*, glycerol crosslinks the three FFAs, and would have a slightly higher oxirane value if converted to the glycidyl structure like EGS. Linseed oil is also richer in linolenic acid content that may facilitate a dense crosslinked structure.

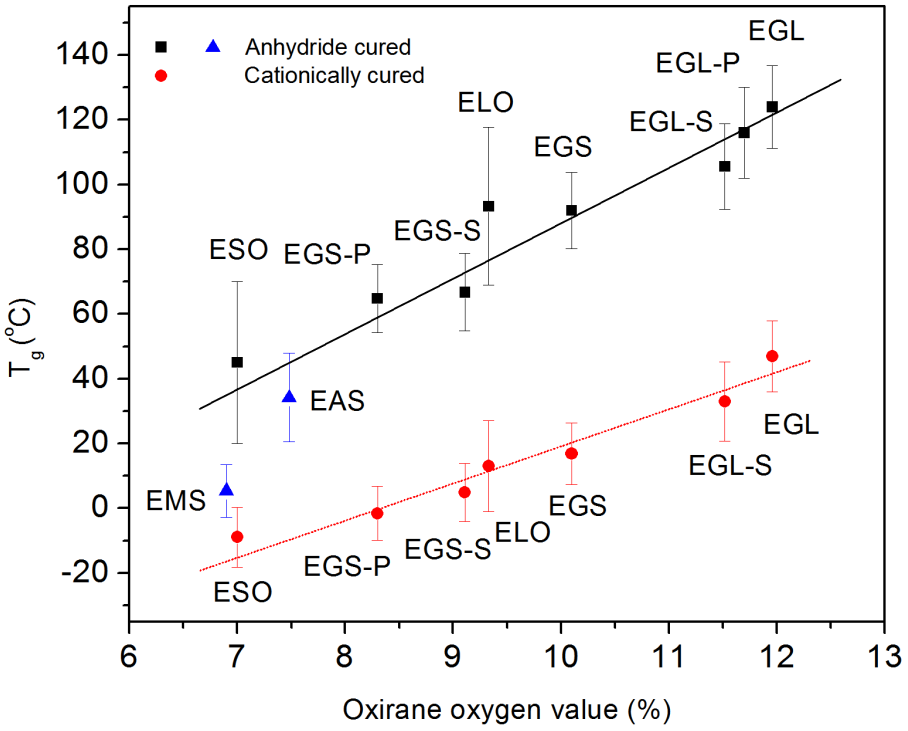

Figure 9. Polymer glass transition temperatures as a function of monomer oxirane contents through cationic homopolymerization and MHHPA copolymerization. [Note: straight lines are to indicate trend; vertical bars indicate the breadth of glass transition region equal to the difference between onset temperature and endset temperature as determined in DSC].

EGS and EGL have much higher T_g compared to their respectively ESO or ELO counterparts. A T_g value of 124°C was measured for EGL, which appears unprecedented for a vegetable oil based thermoset polymer. The T_g increases in EGS-S/ EGS-P and

EGL-S/EGL-P are mainly due to the addition of the reactive glycidyl group compared to ESO and ELO. Removal of the saturated components greatly increases the T_g. A 30 and 20 °C increase in polymer T_g was observed for MHHPA cured EGS and EGL compared to EGS-S and EGL-S, respectively. Such trends are observed in the Mc calculations as a significant increase of crosslink density upon exclusion of the saturated components.

Adding an unreactive function group, *e.g.*, allyl (EAS) or methyl groups (EMS), generates a lower T_g though the oxirane values are similar to that of ESO. Since the allyl group in EAS is partially epoxidized, EAS has even slightly higher oxirane value than ESO. The T_g's are greatly decreased compared to ESO because, unlike ESO that is partially crosslinked through glycerol, transesterification engenders all the fatty acid carbons except carbons in the epoxy groups into pendant chains. In addition, the liberated saturated FFA esters behave as plasticizers in the matrix to increase the chain segment mobility and decrease crosslink density. Monofunctional epoxidized methyl oleate and epoxidized oleic acid have lower oxirane content compared to EMS and were difficult to polymerize by our current curing conditions though polymer T_g of –14 to –50 °C have been reported [36, 81].

Broader T_g regions (onset-endset ranges are provided in Figure 9 using bars; NOTE: the vertical bars are not 'error' bars or deviations but indicate the measured temperature range breadth of the glass transition) indicate a broader distribution of chain environments and heterogeneous structures were observed in anhydride cured ELO and ESO. We ascribe the less homogenous polymer structures to a low reactivity of internal oxirane in ELO or ESO instead of saturated components because even EGS-S and EGL-S with saturated FFAs show relatively sharp glass transition ranges. Indeed, internal epoxy

is more reactive in cationic polymerization where all epoxies show a similar transition breadth when initiated by BF_3-MEA. EMS of all internal oxirane structure and saturated FFA also show a narrow glass transition region, which could be due to greater reactivity of the small molecules during curing compared to large oligomers of ESO or ELO [37].

Figure 10 presents the TGA weigh loss as a function of temperature curves for the polymerized epoxy resin. Since the ESO-DGEBA blend had a similar thermal stability as the EGS-DGEBA blend, only the latter is shown here. TGA results indicated all cured EGS-DGEBA resins appear thermally stable to temperatures at least 300 °C.

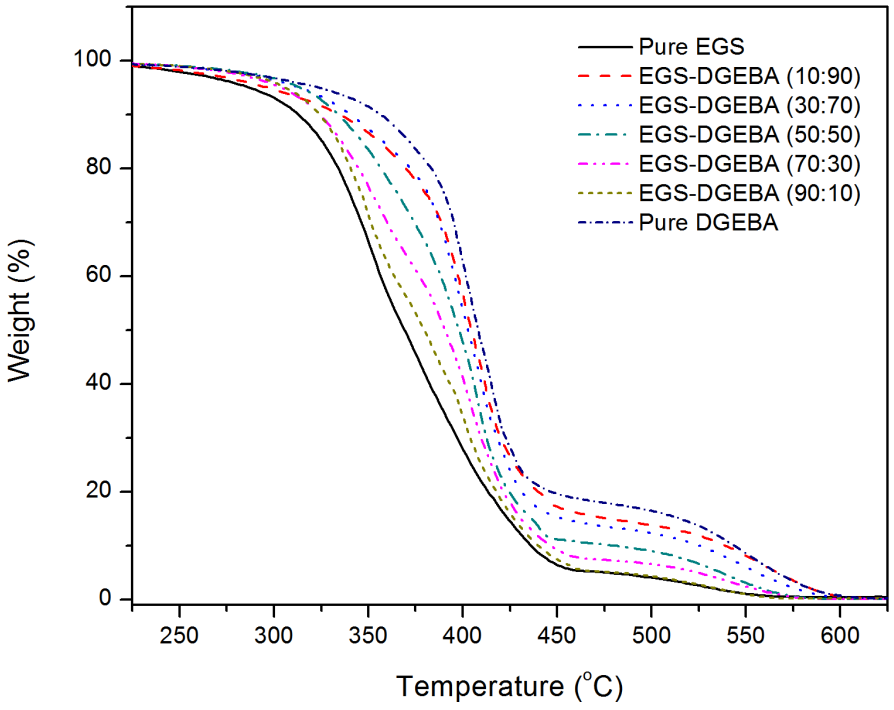

Figure 10. TGA of MHHPA cured EGS-DGEBA blends compared to pure EGS and pure DGEBA

Replacements of DGEBA by EGS led to an earlier onset of degradation. All epoxies presented two stage degradation behavior. The first stage of decomposition from 300 to 450 °C is believed to be due to decomposition of unreacted MHHPA, dehydration of hydroxyl groups, and the pyrolysis of the crosslinked epoxy resin network. The second stage loss from ~ 450 to 600 °C was considered to be the complete decomposition of the smaller fragments like cyclized or aromatic degradation byproducts as indicated by the decrease of char residue when EGS component was increased.

3.6. MECHANICAL PERFORMANCE

Flexural and tensile properties of the polymerized resin systems as a function of ESO/EGS content were determined. The results are shown in Figures 11 and 12. Smaller concentrations of EGS led to only minor changes in strength or modulus compared to neat DGEBA. An improvement in flexural modulus was observed for 10 wt% EGS. Similar results, showing improved modulus at low replacement concentrations, have also been reported for an amine cured, soy-based epoxy resin system [35]. These data correlate with minor changes of M_c calculated at low concentrations of EGS/ESO in DGEBA system blends.

However, the modulus and strength values of the blends systematically decreased with further increases in ESO/EGS concentration. These phenomena are readily explained by a decrease of stiffer, bulky aromatic group content and a decreased crosslinking density of the cured blends. All the EGS-DGEBA blends showed higher strength and modulus than the ESO-DGEBA blends of comparable concentration, which is supported by smaller M_c or M_c^* of EGS compared to ESO. The flexural stress and modulus of EGS-DGEBA exhibited a gradual decrease until 50 wt% followed by a more

abrupt change. For ESO-DGEBA, large materials property losses occurred at ≥30 wt%. The study of ref [35] studied compositions only up to 30 wt% soy epoxy resin. Similarly, the tensile strength of EGS-DGEBA had only minor changes up to 70 wt% concentration whereas a continuous decrease in strength was observed for ESO-DGEBA blends. As observed in Figures 4 and 6, EGS was observed to be more reactive and compatible with DGEBA and a higher content of EGS was achieved with greater homogeneity than comparable ESO blends and greater mechanical strengths.

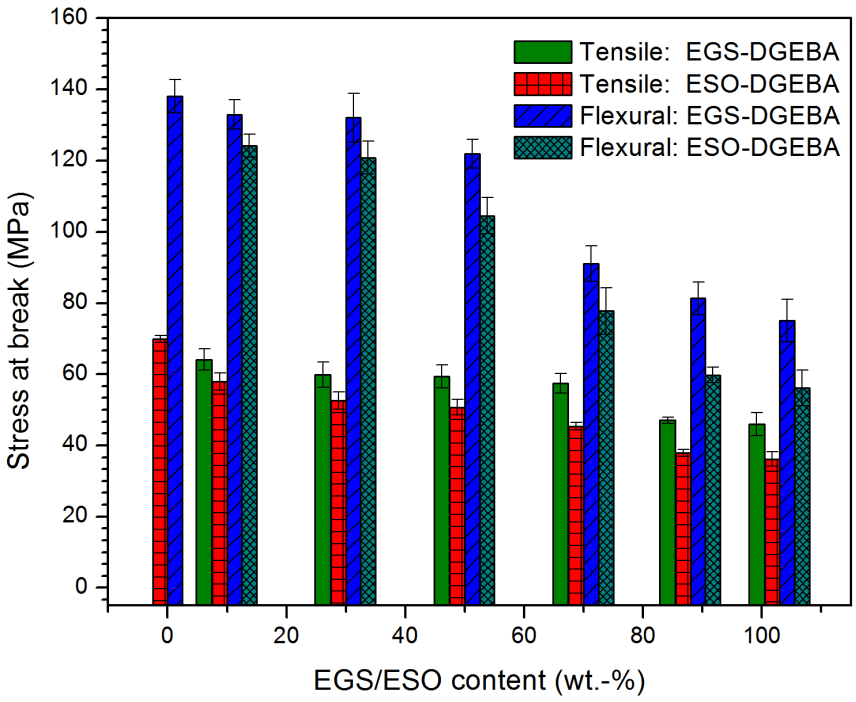

Figure 11. Tensile and flexural strengths of MHHPA and EGS/ESO-DGEBA blend copolymerization products

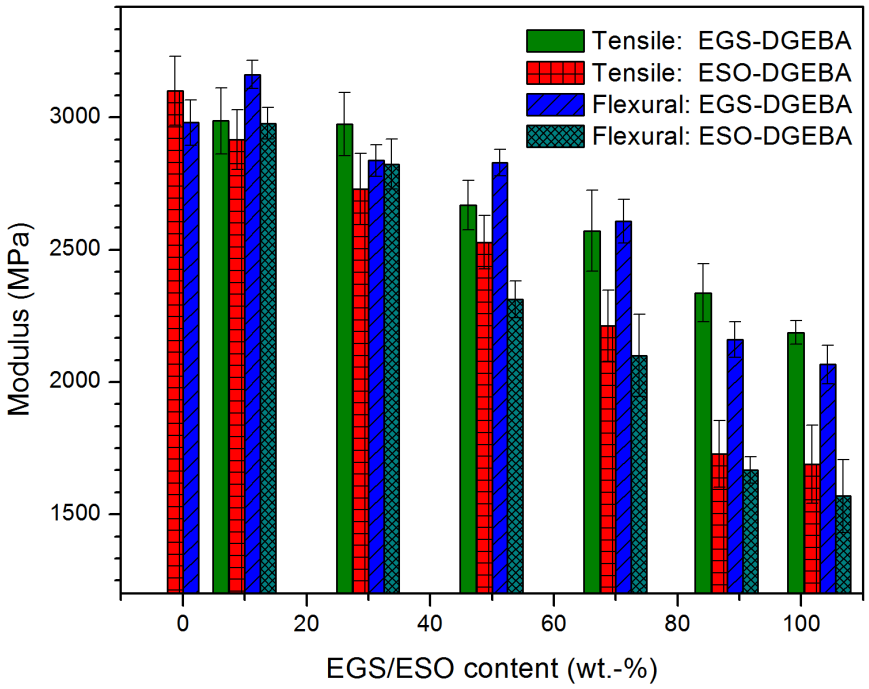

Figure 12. Tensile and flexural moduli of MHHPA and EGS/ ESO-DGEBA blends copolymerization products

3.7. VISCOSITY REDUCING ABILITY

Reactive diluents are used for reducing and controlling the viscosity of epoxy resins to improve wetting and handling characteristics because in the liquid- molding technologies like resin transfer molding or pultrusion, the viscosity and resin flow are critical to achieving a quality laminate [82]. Recent trends toward lower volatile organic compounds (VOC), higher solids epoxy formulations have also resulted in increased utilization of reactive diluents [83]. It was found that EGS had inherently lower viscosity than ESO. EGS has an extra glycidyl group and lower molecular weight compared to ESO, which is a triglyceride and has oligomeric behavior. The viscosity reducing abilities of EGS and ESO were compared at different concentrations of replacement of

the DGEBA resin, which had a relatively high viscosity of 13000 mPa·s (see Figure 13). ESO and EGS have different miscibility with DGEBA resin; however, EGS exhibited a much better viscosity reducing efficiency than ESO. A 30 wt% concentration of EGS reduced the DGEBA resin viscosity to value below 1000 mPa·s, which is indispensable for many applications. At least 50 wt% of ESO was needed to reduce DGEBA resin to 1000 mPa·s viscosity.

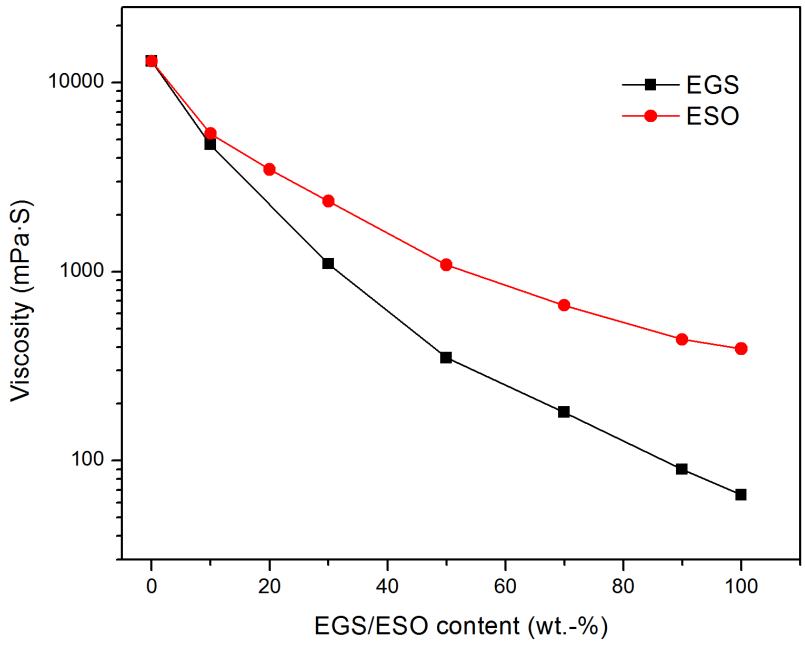

Figure 13. Viscosity of DGEBA blended with various EGS or ESO concentrations

4. CONCLUSIONS

Bio-based epoxy resins, glycidyl ester of epoxidized fatty acids, were produced from soybean or linseed oils with a reduced saturated FFA fraction content. The products were characterized and showed high oxirane contents that were more reactive than ESO

or ELO, which was shown to directly impact polymer homogeneity and glass transition temperature. Epoxy monomers from other vegetable oil sources such as canola, palm, corn, etc., could be fabricated in similar fashion and have similar properties and curing behaviors providing that saturated fatty ester chains are similarly removed.

The vegetable oil based epoxy resins displayed glass transitions that appear to be mostly a function of oxirane content but with additional influences of glycidyl versus internal oxirane reactivity, pendant chain content, and chemical structure and presence of saturated components. Generally, higher oxirane contents (epoxy functionality) lead to higher glass transition temperatures whereas reduced epoxy functionality, non-glycidyl FFA esters, and greater pendant chain contents lead to lower glass transition temperatures. In blends with DGEBA, monomers with only less reactive internal epoxies led to a more heterogeneous polymer structure compared to monomers possessing the more reactive glycidyl group and improved polymer homogeneity, in cure and structure. The inherent, long chain aliphatic structure of these thermoset monomers limits polymer glass transition temperatures compared to commercial, aromatic based epoxy monomers (DGEBA) but our data provide a clear trend and role of oxirane content.

The EGS blends with DGEBA were cured by MHHPA and their thermosetting polymer T_g's measured in comparison to control ESO blends with DGEBA, which were polymerized in similar fashion. The EGS polymers displayed improved T_g's and mechanical properties compared to their ESO counterparts and, in addition to an inherently low viscosity and efficient viscosity reduction, should therefore be more attractive as a reactive diluent. For instance, EGS derived from renewable sources could further enable defect-free fabrication of complex, shaped epoxy composites for structural

composite applications. Our data show ESO produced less homogeneous polymers when blended with DGEBA epoxy that resulted in thermal cure, thermal property, and mechanically inferior materials compared to the more compatible EGS epoxy resin and blends. The compatibility and superior properties arise from the removal of saturated pendant chains, addition of the glycidyl structure, and larger internal oxirane content inherent of EGS.

ACKNOWLEDGEMENTS

Portions of this paper were presented at the 2011 Thermoset Resin Formulators Association annual meeting and at the 2012 American Oil Chemists' Society Annual Meeting & Expo. Authors would like to thank Pranita Nayak and Dr. Rama Vuppalapati for assistance in resin synthesis and mechanical testing and acknowledge facilities and equipment support provided through the Missouri S&T Materials Research Center.

REFERENCES

[1] Raquez J-M., Deléglise M., Lacrampe M-F., Krawczak P.: Thermosetting (bio)materials derived from renewable resources: A critical review. Progress in Polymer Science, 35, 487–509 (2010).

[2] Gandini A.: Polymers from renewable resources: A challenge for the future of macromolecular materials. Macromolecules, 41, 9491–9504 (2008).

[3] Sharma V., Kundu P. P.: Addition polymers from natural oils – A review. Progress in Polymer Science, 31, 983–1008 (2006).

[4] Pfister D. P., Xia Y., Larock R. C.: Recent advances in vegetable oil-based polyurethanes. ChemSusChem, 4, 703–717 (2011).

[5] United Soybean Board: A survey of recent chemical price trends: The potential impact of rising petrochemical prices on soy use for industrial applications. Omni Tech International Ltd. (2010).

[6] Petrovi& Z. S.: Polyurethanes from vegetable oils. Polymer Reviews, 48, 109–155 (2008).

[7] Xia Y., Larock R. C.: Vegetable oil-based polymeric materials: Synthesis, properties, and applications. Green Chemistry, 12, 1893–1909 (2010).

[8] Lu J., Khot S., Wool R. P.: New sheet molding compound resins from soybean oil. I. Synthesis and characterization. Polymer, 46, 71–80 (2005).

[9] Campanella A., La Scala J. J., Wool R. P.: Fatty acidbased comonomers as styrene replacements in soybean and castor oil-based thermosetting polymers. Journal of Applied Polymer Science, 119, 1000–1010 (2011).

[10] Luo Q., Liu M., Xu Y., Ionescu M., Petrovic' Z. S.: Thermosetting allyl resins derived from soybean oil. Macromolecules, 44, 7149–7157 (2011).

[11] Lligadas G., Ronda J. C., Galia(M., Ca'diz V.: Plant oils as platform chemicals for polyurethane synthesis: Current state-of-the-art. Biomacromolecules, 11, 2825– 2835 (2010).

[12] Xu J., Liu Z., Erhan S., Carriere C. J.: Cross-linkers control the viscoelastic properties of soybean oil-based biomaterials. Journal of the American Oil Chemists' Society, 81, 813–816 (2004).

[13] May C. A.: Epoxy resins chemistry and technology. Marcel Dekker, New York (1988).

[14] Raghavachar R., Sarnecki G., Baghdachi J., Massingill J.: Cationic, thermally cured coatings using epoxidized soybean oil. Journal of Coatings Technology, 72, 125–133 (2000).

[15] Chandrashekhara K., Sundararaman S., Flanigan V., Kapila S.: Affordable composites using renewable materials. Materials Science and Engineering: A, 412, 2–6 (2005).

[16] Tanrattanakul V., Saithai P.: Mechanical properties of bioplastics and bioplastic–organoclay nanocomposites prepared from epoxidized soybean oil with different epoxide contents. Journal of Applied Polymer Science, 114, 3057–3067 (2009).

[17] Liu Z., Erhan S. Z., Akin D. E., Barton F. E.: ‘Green’ composites from renewable resources: Preparation of epoxidized soybean oil and flax fiber composites. Journal of Agricultural and Food Chemistry, 54, 2134– 2137 (2006).

[18] Stevens M. P.: Polymer chemistry: An introduction. Oxford University Press, New York (1999).

[19] Adamson M. J.: Thermal expansion and swelling of cured epoxy resin used in graphite/epoxy composite materials. Journal of Materials Science, 15, 1736– 1745 (1980).

[20] Gupta A. P., Ahmad S., Dev A.: Modification of novel bio-based resin-epoxidized soybean oil by conventional epoxy resin. Polymer Engineering and Science, 51, 1087–1091 (2011).

[21] Gelb L., Ault W., Palm W., Witnauer L., Port W.: Epoxy resins from fats. III. Preparation and properties of resins from blends of a commercial diglycidyl ether and epoxidized glycerides cured with phthalic anhydride. Journal of the American Oil Chemists' Society, 37, 81–84 (1960).

[22] Czub P.: Characterization of an epoxy resin modified with natural oil-based reactive diluents. Macromolecular Symposia, 245–246, 533–538 (2006).

[23] Kar S., Banthia A. K.: Epoxy resin modified with epoxidized soybean rubber. Materials and Manufacturing Processes, 19, 459–474 (2004).

[24] Miyagawa H., Misra M., Drzal L. T., Mohanty A. K.: Fracture toughness and impact strength of anhydride cured biobased epoxy. Polymer Engineering and Science, 45, 487–495 (2005).

[25] Jin F-L., Park S-J.: Impact-strength improvement of epoxy resins reinforced with a biodegradable polymer. Materials Science and Engineering: A, 478, 402–405 (2008).

[26] Tan S. G., Chow W. S.: Thermal properties of anhydride- cured bio-based epoxy blends. Journal of Thermal Analysis and Calorimetry, 101, 1051–1058 (2010).

[27] Thulasiraman V., Rakesh S., Sarojadevi M.: Synthesis and characterization of chlorinated soy oil based epoxy resin/glass fiber composites. Polymer Composites, 30, 49–58 (2008).

[28] Lligadas G., Ronda J. C., Galià M., Cádiz V.: Development of novel phosphorus-containing epoxy resins from renewable resources. Journal of Polymer Science Part A: Polymer Chemistry, 44, 6717–6727 (2006).

[29] Earls J. D., White J. E., López L. C., Lysenko Z., Dettloff M. L., Null M. J.: Amine-cured ω-epoxy fatty acid triglycerides: Fundamental structure–property relationships. Polymer, 48, 712–719 (2007).

[30] Pan X., Sengupta P., Webster D. C.: High biobased content epoxy–anhydride thermosets from epoxidized sucrose esters of fatty acids. Biomacromolecules, 12, 2416–2428 (2011).

[31] Gerbase A. E., Petzhold C. L., Costa A. P. O.: Dynamic mechanical and thermal behavior of epoxy resins based on soybean oil. Journal of the American Oil Chemists' Society, 79, 797–802 (2002).

[32] La Scala J., Wool R. P.: Property analysis of triglyceride based thermosets. Polymer, 46, 61–69 (2005).

[33] Meier M. A. R., Metzger J. O., Schubert U. S.: Plant oil renewable resources as green alternatives in polymer science. Chemical Society Reviews, 36, 1788– 1802 (2007).

[34] Nicolau A., Mariath R. M., Martini E. A., dos Santos Martini D., Samios D.: The polymerization products of epoxidized oleic acid and epoxidized methyl oleate with cis-1,2-cyclohexanedicarboxylic anhydride and triethylamine as the initiator: Chemical structures, thermal and electrical properties. Materials Science and Engineering: C, 30, 951–962 (2010).

[35] Zhu J., Chandrashekhara K., Flanigan V., Kapila S.: Curing and mechanical characterization of a soy-based epoxy resin system. Journal of Applied Polymer Science, 91, 3513–3518 (2004).

[36] Reiznautt Q. B., Garcia I. T. S., Samios D.: Oligoesters and polyesters produced by the curing of sunflower oil epoxidized biodiesel with cis-cyclohexane dicarboxylic anhydride: Synthesis and characterization. Materials Science and Engineering: C, 29, 2302–2311 (2009).

[37] dos Santos Martini D., Braga B. A., Samios D.: On the curing of linseed oil epoxidized methyl esters with different cyclic dicarboxylic anhydrides. Polymer, 50, 2919–2925 (2009).

[38] Petrovi& Z. S., Guo A., Zhang W.: Structure and properties of polyurethanes based on halogenated and nonhalogenated soy–polyols. Journal of Polymer Science Part A: Polymer, 38, 4062–4069 (2000).

[39] Pan X., Sengupta P., Webster D. C.: Novel biobased epoxy compounds: Epoxidized sucrose esters of fatty acids. Green Chemistry, 13, 965–975 (2011).

[40] Zong Z., Soucek M. D., Liu Y., Hu J.: Cationic photopolymerization of epoxynorbornane linseed oils: The effect of diluents. Journal of Polymer Science Part A: Polymer Chemistry, 41, 3440–3456 (2003).

[41] Zou K., Soucek M. D.: UV-curable cycloaliphatic epoxide based on modified linseed oil: Synthesis, characterization and kinetics. Macromolecular Chemistry and Physics, 206, 967–975 (2005).

[42] Tan S. G., Chow W. S.: Thermal properties, curing characteristics and water absorption of soybean oil based thermoset. Express Polymer Letters, 5, 480–492 (2011).

[43] Petrovi& Z. S., Zhang W., Javni I.: Structure and properties of polyurethanes prepared from triglyceride polyols by ozonolysis. Biomacromolecules, 6, 713–719 (2005).

[44] Kiatsimkul P-P., Suppes G. J., Sutterlin W. R.: Production of new soy-based polyols by enzyme hydrolysis of bodied soybean oil. Industrial Crops and Products, 25, 202–209 (2007).

[45] Vázquez L., Akoh C. C.: Concentration of stearidonic acid in free fatty acid and fatty acid ethyl ester forms from modified soybean oil by winterization. Journal of the American Oil Chemists' Society, 88, 1775–1785 (2011).

[46] Sharma V., Kundu P. P.: Condensation polymers from natural oils. Progress in Polymer Science, 33, 1199– 1215 (2008).

[47] Chen J-S., Ober C. K., Poliks M. D., Zhang Y., Wiesner U., Cohen C.: Controlled degradation of epoxy networks: Analysis of crosslink density and glass transition temperature changes in thermally reworkable thermosets. Polymer, 45, 1939–1950 (2004).

[48] Brown J. B.: Low-temperature crystallization of the fatty acids and glycerides. Chemical Reviews, 29, 333– 354 (1941).

[49] Brown J. B., Stoner G. G.: Studies on the chemistry of the fatty acids. I. The purification of linoleic acid by crystallization methods. Journal of the American Chemical Society, 59, 3–6 (1937).

[50] Maerker G., Saggese E., Port W.: Glycidyl esters. II. Synthesis of esters of commercial and pure fatty acids. Journal of the American Oil Chemists' Society, 38, 194–197 (1961).

[51] Kester E. B., Gaiser C. J., Lazar M. E.: Glycidyl esters of aliphatic acids. The Journal of Organic Chemistry, 8, 550–556 (1943).

[52] Altuna F. I., Espósito L. H., Ruseckaite R. A., Stefani P. M.: Thermal and mechanical properties of anhydride- cured epoxy resins with different contents of biobased epoxidized soybean oil. Journal of Applied Polymer Science, 120, 789–798 (2011).

[53] Boquillon N., Fringant C.: Polymer networks derived from curing of epoxidised linseed oil: Influence of different catalysts and anhydride hardeners. Polymer, 41, 8603–8613 (2000).

[54] Ratna D.: Handbook of thermoset resins. Rapra, Shropshire (2009).

[55] Brandrup J., Immergut E. H., Grulke E. A., Abe A., Bloch D. R.: Polymer handbook. Wiley, New York (2005).

[56] Barton A. F. M.: Handbook of solubility parameters and other cohesion parameters. CRC Press, Boca Raton (1983).

[57] Van Krevelen D. W.: Properties of polymers. Elsevier, Amsterdam (1990).

[58] Jackson P. L., Huglin M. B., Cervenka A.: Use of inverse gas chromatography to quantify interactions in anhydride cured epoxy resins. Polymer International, 35, 135–143 (1994).

[59] Park S-J., Jin F-L., Lee J-R.: Thermal and mechanical properties of tetrafunctional epoxy resin toughened with epoxidized soybean oil. Materials Science and Engineering: A, 374, 109–114 (2004).

[60] Frischinger I., Dirlikov S.: Two-phase interpenetrating epoxy thermosets that contain epoxidized triglyceride oils. Part I. Phase separation. in ‘Interpenetrating polymer networks’ (Klempner D., Sperling L. H., Utracki L. A.) American Chemical Society, Washington, Vol 239, 517–538 (1994).

[61] Robeson L. M.: Polymer blends: A comprehensive review. Hanser, Cincinnati (2007).

[62] Ratna D., Banthia A. K.: Rubber toughened epoxy. Macromolecular Research, 12, 11–21 (2004).

[63] Harsch M., Karger-Kocsis J., Herzog F., Fejős M.: Effect of cure regime on internal strain and stress development in a filled epoxy resin assessed by fiber Bragggrating optical strain and normal force measurements. Journal of Reinforced Plastics and Composites, 30, 1417–1427 (2011).

[64] Bell J. P.: Structure of a typical amine-cured epoxy resin. Journal of Polymer Science Part A-2: Polymer Physics, 8, 417–436 (1970).

[65] Bellenger V., Morel E., Verdu J.: Solubility parameters of amine-crosslinked aromatic epoxies. Journal of Applied Polymer Science, 37, 2563–2576 (1989).

[66] Kwei T. K.: Swelling of highly crosslinked network structure. Journal of Polymer Science Part A: General Papers, 1, 2977–2988 (1963).

[67] Mahendran A. R., Wuzella G., Kandelbauer A., Aust N.: Thermal cure kinetics of epoxidized linseed oil with anhydride hardener. Journal of Thermal Analysis and Calorimetry, 107, 989–998 (2012).

[68] Gao J., Li J., Benicewicz B. C., Zhao S., Hillborg H., Schadler L. S.: The mechanical properties of epoxy composites filled with rubbery copolymer grafted SiO2. Polymers, 4, 187–210 (2012).

[69] Kim J. R., Sharma S.: The development and comparison of bio-thermoset plastics from epoxidized plant oils. Industrial Crops and Products, 36, 485–499 (2012).

[70] Miyagawa H., Mohanty A. K., Misra M., Drzal L. T.: Thermo-physical and impact properties of epoxy containing epoxidized linseed oil, 2. Macromolecular Materials and Engineering, 289, 636–641 (2004).

[71] Lu P.: Curing chemistry of epoxidized soybean oil and its application for structural composite materials, PhD Thesis, University of Missouri-Rolla, Rolla (2001).

[72] Liu Z., Doll K. M., Holser R. A.: Boron trifluoride catalyzed ring-opening polymerization of epoxidized soybean oil in liquid carbon dioxide. Green Chemistry, 11, 1774–1789 (2009).

[73] Liu Z., Erhan S. Z.: Ring-opening polymerization of epoxidized soybean oil. Journal of the American Oil Chemists' Society, 87, 437–444 (2009).

[74] Czub P.: Application of modified natural oils as reactive diluents for epoxy resins. Macromolecular Symposia, 242, 60–64 (2006).

[75] Park S-J., Jin F-L., Lee J-R.: Synthesis and thermal properties of epoxidized vegetable oil. Macromolecular Rapid Communications, 25, 724–727 (2004).

[76] Gelb L. L., Ault W. C., Palm W. E., Witnauer L. P., Port W. S.: Epoxy resins from fats. I. Epoxidized glycerides cured with phthalic anhydride. Journal of the American Oil Chemists' Society, 36, 283–286 (1959).

[77] Tan S. G., Chow W. S.: Biobased epoxidized vegetable oils and its greener epoxy blends: A review. Polymer- Plastics Technology and Engineering, 49, 1581–1590 (2010).

[78] Miyagawa H., Mohanty A. K., Misra M., Drzal L. T.: Thermo-physical and impact properties of epoxy containing epoxidized linseed oil, 1. Macromolecular Materials and Engineering, 289, 629–635 (2004).

[79] Tan S., Chow W. J.: Curing characteristics and thermal properties of epoxidized soybean oil based thermosetting resin. Journal of the American Oil Chemists' Society, 88, 915–923 (2011).

[80] Miyagawa H., Misra M., Drzal L. T., Mohanty A. K.: Biobased epoxy/layered silicate nanocomposites: Thermophysical properties and fracture behavior evaluation. Journal of Polymers and the Environment, 13, 87– 96 (2005).

[81] Nicolau A., Samios D., Piatnick C. M. S., Reiznautt Q. B., Martini D. D., Chagas A. L.: On the polymerization of the epoxidised biodiesel: The importance of the epoxy rings position, the process and the products. European Polymer Journal, 48, 1266–1278 (2012).

[82] Varley R. J., Tian W.: Toughening of an epoxy anhydride resin system using an epoxidized hyperbranched polymer. Polymer International, 53, 69–77 (2004).

[83] Mark H. F.: Encyclopedia of polymer science and technology. Wiley-Interscience, New York (2004).

III. FABRICATION OF BIO-BASED EPOXY-CLAY NANOCOMPOSITES

Rongpeng Wang[1], Thomas Schuman[1]*, R. R. Vuppalapati[2], K. Chandrashekhara[2]

[1]Department of Chemistry, Missouri University of Science and Technology, Rolla, MO 65409, USA

[2]Department of Mechanical and Aerospace Engineering, Missouri University of Science and Technology, Rolla, MO 65409, USA

* *Correspondence to*: Thomas Schuman (tschuman@mst.edu)

ABSTRACT

Epoxy-clay nanocomposites derived from renewable soybean oils and organo modified montmorillonite clay were efficiently prepared. Better efficiency was achieved through new, low viscosity, glycidyl esters of epoxidized fatty acids (EGS) as epoxy monomer and 4-methyl-1,2-cyclohexanedicarboxylic anhydride as comonomer. Tensile testing showed that 1 wt.-% of clay improved nanocomposite strength and modulus by 22 % and 13 %, respectively. Tensile modulus was increased 34 % by nanocomposite clay without sacrifice of strength. Three types of dispersion technique, mechanical stirring, high speed shearing, and ultrasonication, were carried out to disperse the clay directly into epoxy or anhydride portion of the thermoset system without added solvent. Dispersion of the clay particles into monomer was assessed by means of solubility parameters, optical and scanning electron microscopies and further confirmed by small angle X-ray scattering and transmission electron microscopy. Sonication dispersion of clay into epoxy portion was needed to optimize dispersion and exfoliation of clay and

higher mechanical and thermal strength of the nanocomposites. The nanocomposites' morphologies were a mix of intercalated and exfoliated structures, dependent on the dispersion technique. The optimum tensile strength and glass transition temperatures of the nanocomposites were a function of clay concentration and dispersion morphology.

Keywords: soybean oil; epoxy; clay; nanocomposites; miscibility; morphology; structure property

1. INTRODUCTION

Epoxy nanocomposites have attracted interest over past few years for their ability to generate improved properties with relatively small concentrations (*e.g.*, ≤5 wt.-%) of fillers.[1] Organo modified montmorillonite clay platelets (OMMT), due to unique layered structure, easy processing, availability, *etc.*, are inexpensive reinforcement fillers for epoxies. Once finely dispersed, strong interfacial interactions exist between polymer and nanoclay particles and play a key role in the confinement of polymer chain mobility under stress, and polymer properties like mechanical,[2] thermal,[3] gas barrier resistance,[4] low water absorption properties[5] have been substantially improved.

To obtain well dispersed polymer-clay nanocomposites, three techniques, *i.e.*, in situ polymerization, melt intercalation and solution dispersion are well known. Industrially preferred melt intercalation is not applicable to thermosetting based polymers like epoxies. Due to the high viscosity of common diglycidyl ether of bisphenol A-based epoxy (DGEBA), solution dispersion is an effective way of dispersing clay into epoxy resins with a high degree of exfoliation.[6] Epoxy monomers readily penetrate into the clay galleries, which had been expanded and preoccupied by solvents like acetone. While

large amounts of solvent are required during dispersion and then removed to prevent bubbles trapping in the cured samples, because solvent residue can impact the chemistry and performance of the final nanocomposite.[7] In addition, solution dispersion may also present environmental and health issues.[8] Slurry compounding is another approach to prepare exfoliated epoxy nanocomposites.[2] Pristine clay was first swollen in water and then transformed into an acetone/ethanol slurry, several steps were involved to remove the water and solvent, otherwise the properties of the resultant composites were more likely to be low.[9] The slurry compounding is also a time consuming and non-environmentally benign process. As stated above, developing a highly efficient and environmentally friendly process like solventless is still desirable for the industrial application of epoxy clay nanocomposites.[10]

Polymer nanocomposites have made a significant contribution to the human society due to their extraordinary properties. In recent years, there is continued interest in polymers derived from bio-renewable sources like vegetable oils, which are readily available, renewable, biodegradable and can contribute to a more sustainable polymer industry. While most vegetable oil based polymers are not able to compete with analogous petroleum-based polymers in many structural applications due to inherently low stiffness and strength,[11-13] functionalization, copolymerization with petroleum based monomers, and addition of nano-reinforcement or fiber reinforcement have been applied to improve polymers thermal and/ or mechanical properties.[14-22] Various thermosets ranged from flexible rubbers to hard plastics have been synthesized from vegetable oils by Larock and coworkers,[23-25] in general, modified or unmodified vegetable oils were copolymerized with styrene, dibinylbenzene or dicyclopentadiene by free radical,[26]

cationic,[20] or ring-opening metathesis.[27] Monomers derived from vegetable oil, acrylic acid and/ or maleic anhydride were also prepared and facilitated copolymerized with styrene.[28, 29] The resulting thermosets showed glass transition temperatures (T_g) even higher than 100 °C depend on the monomers ratio and resin compositions.[30] To further improve structural performance, fibers and nano clay reinforcements have been added to above mentioned polymers. The fiber reinforced composites showed improved mechanical properties depend on types of fibers, fiber contents, resin systems and interfacial adhesion.[29, 31-34] The prepared clay nanocomposites generally showed a mix of intercalated and exfoliated structure depend on the clay concentrations[35] and properties of monomers.[36] These nanocomposites generally showed improved thermal stability, mechanical properties especially the modulus and barrier performance, decreased T_g were sometimes observed.[37, 38]

Epoxidized vegetable oil (EVO) such as epoxidized soybean oil (ESO) or epoxidized linseed oil (ELO), is one of the largest industrial utilizations of vegetable oils,[39] directly using EVO as epoxy monomer, however, was hampered from relatively low T_g and the mechanical properties of flexible matter. EVO can be blended with commercial epoxy like DGEBA but generally limited as a minor component (*e.g.* <30 wt.-%),[40] otherwise the resulting polymers or composites performance will mostly be poor due to the plasticizing effect, low reactivity and dangling chains of EVOs at high content replacement.[11, 41-44] Exfoliated clay nanocomposites have been fabricated from anhydride cured ELO/diglycidyl ether of bisphenol F blends, and counterbalanced the reduced storage modulus due to the addition of ELO, but large quantity of solvent was required for clay dispersion.[45] Clay nanocomposites have also been made from pure

vegetable oil based epoxies and showed improved mechanical strengths.[46-48] However, an inherently low T_g, even below room temperature, inevitably limits practical applications. High strength, higher T_g bio-based epoxy resin systems are of interest to improve mechanical and thermal polymer and composite properties.[15, 21, 49]

Bio-based epoxy resins of glycidyl ester of epoxidized fatty acids (EGS) derived from soybean oils have been synthesized and examined.[40] EGS merits include a higher epoxy content and lower viscosity than commercial ESO, ELO or DGEBA. Upon curing cationically, neat polymer displays T_g's above room temperature. Much higher T_g's and improved mechanical properties compared to other bio-based systems were obtained through selection of curing agents.

Low resin viscosity of EGS and similar fatty chain structure to clay modifiers enabled dispersion clay via a solvent free and non-heating process, so fabrication of epoxy clay nanocomposites becomes more efficient and environmentally friendly. The incorporation of bio-based epoxy polymers with relatively low cost clay platelets was also a useful combination toward environmentally friendly and affordable nanocomposites of improved thermal and mechanical properties. In this research, the bio-based epoxy nanocomposites containing different concentrations of clay were prepared. Dispersion methods and clay content effects on the T_g's, thermal stability and mechanical strength are observed.

2. EXPERIMENTAL

2.1. MATERIALS

Refined soybean oil with brand name Great Value™ was purchased from a local grocery store. 2-ethyl-4-methylimidazole (EMI) and 4-methyl-1,2-

cyclohexanedicarboxylic anhydride (MHHPA) were purchased from Aldrich (St. Louis, MO). OMMT with brand name Cloisite® 30B was purchased from Southern Clay Products Inc. (Gonzales, TX). The clay surface modifier is bis-(2-hydroxyethyl) methyl-hydrogenated tallow alkylammonium cation (90 meq/100 g of clay). Mold release agent Chemlease® 41-90 EZ was purchased from Chem-Trend, Inc. (Howell, MI).

2.2. PREPARATION OF BIO-BASED EPOXY-CLAY NANOCOMPOSITES

A detailed synthetic procedure of EGS was previously reported[40] and the chemical structure is shown in Figure 2. The abbreviated general procedure is as follows: Dry sodium soap derived from free fatty acids of soybean oil was reacted with epichlorohydrin under reflux condition with cetyltriethylammonium bromide as a phase transfer catalyst. The prepared glycidyl esters of fatty acids were epoxidized by *meta*-chloroperoxybenzoic acid dissolved in methylene chloride and then washed by sodium sulfite and sodium bicarbonate solution sequentially. Finally, methylene chloride was removed by *in vacuo* rotary evaporation. The prepared EGS have an average oxirane oxygen value of 10.1 % and viscosity of 70 mPa·s at 25 °C.

The process of making nanocomposites is shown in Scheme 1. Two clay dispersion methods, high speed kinetic shear mixing (shearing) and shearing plus sonication (sonication) were compared. A typical nanocomposites fabrication procedure follows: OMMT dried at 60 °C under vacuum for 24 hr were stirred into EGS in proportions of 0, 0.5, 1, 2, 4 or 6 wt.-% concentration. The blend was sheared at 20,000 rpm for 10 min using a kinetic shear homogenizer (Fisher Scientific PowerGen 1000). Ultrasound treatment (Sonics&Materials Inc.) was performed at 900 W for 10 min using. Next, a stoichiometric amount (epoxy/anhydride mole ratio, r = 1.0) of MHHPA and 1

wt.-% (based on EGS) of EMI were added into the blend. After mixing at 300 rpm for 5 min, the blend was degassed in a vacuum oven to remove entrapped air and then poured into a mold, which had been previously sprayed with mold release agent and dried. Curing was performed in a convection oven (Lindberg/Blue MO1440A-1) in three stages: Precured at 80 °C for 30 min, cured at 110 °C for 2 hr, and post cured for 1 hr at 140 °C.

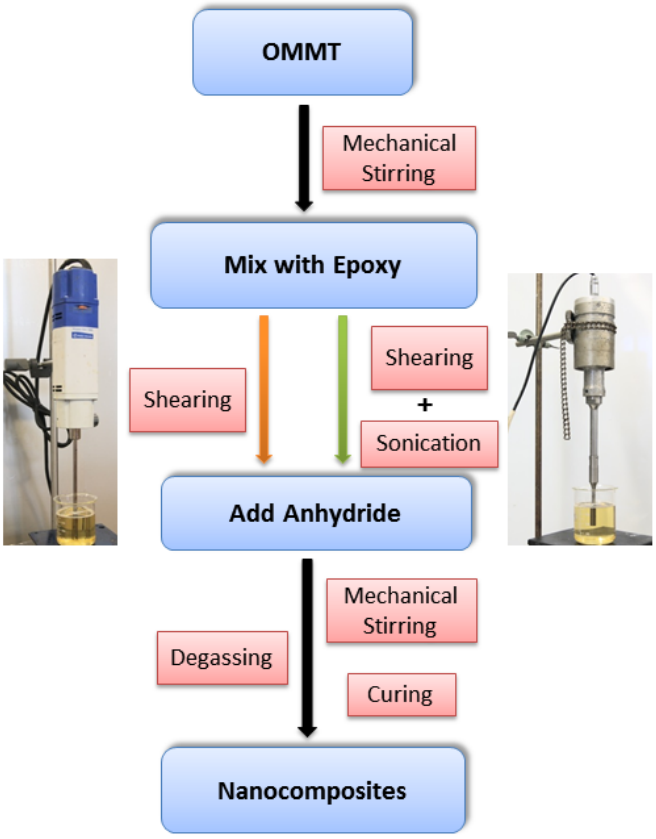

Scheme 1. Procedures for preparation of epoxy clay nanocomposites.

2.3. MECHANICAL CHARACTERIZATION

Tensile tests were performed on an Instron 4469 universal testing machine according to the ASTM D638. Tensile modulus and tensile strength values were

evaluated. All the tensile tests were performed at a crosshead speed of 10 mm/min. At least five specimens were tested for each different resin system.

2.4. DISPERSION CHARACTERIZATION

The dispersion state of clay in EGS or MHHPA monomer was observed using Olympus CX31RBSFA optical microscope with Nikon digital camera DXM1200, a drop of each mixture was spread between the slide and cover slip.

The fracture surfaces of nanocomposites were examined using a Hitachi S-4700 field emission scanning electron microscopy (SEM) with 5 kV accelerating voltage. Sample surfaces were sputtered with a gold coating to improve charge dissipation.

The degree of clay exfoliation in nanocomposites was investigated by small angle X-ray scattering (SAXS). Tests were carried out on a PiXcel detector with Cu-Kα radiation. The scanning range was from 0 to 8°, the step size was 0.01°, and the scan rate was 0.01° every three seconds.

The exfoliated/intercalated structure of nanocomposites was observed with transmission electron microscopy (TEM). Sections of approximately 70 nm were obtained using room temperature ultramicrotomy. The diamond knife angle was set at 4°. A JEOL 1400 TEM with lanthanum hexaboride filament at 120 kV accelerating voltage was used to collect bright-field images of the thin sections of the nanocomposites.

2.5. THERMAL CHARACTERIZATION

Curing behaviors of the neat epoxy and epoxy-clay blends were studied by dynamic scanning calorimetry (DSC) (Q2000, TA Instruments). Mixture weighing 2 to 3 mg was hermetically sealed in an aluminum pan and was scanned at a heating rate of 10 °C/min from 25 to 300 °C.

DSC was also used to determine the T_g of cured resin. Measurement was carried out over a temperature range from -30 to 150 °C at a heating rate of 20 °C/min. Samples were first heated to 170 °C to remove thermal history and then rapidly cooled to -30 °C. Universal Analysis 2000 software by TA Instruments was used to analyze the heat flow as a function of temperature. Inflection temperature (T_i) was reported as the T_g.

Thermal stability and kinetics of thermal degradation of cured neat epoxy and nanocomposites were determined by thermogravimetric analysis (TGA) (Q50, TA Instruments). Measurement was performed from 25 to 800 °C at a heating rate of 5, 10, 15, 20, 25 °C/min under an ambient air flow environment.

3. RESULTS AND DISCUSSION

3.1. MECHANICAL PERFORMANCE

The effect of the clay contents on tensile properties of the EGS-OMMT nanocomposites is presented in Figure 1. Tensile modulus of the nanocomposites was highly dependent upon the OMMT concentrations and was improved with increased clay concentration. This is due to the high modulus of clay platelet. Initially, modulus was improved by 10 % for only 0.5 wt.-% clay incorporation. At higher concentrations, the rate of modulus increase became less, *e.g.*, there is only 13 % increase of modulus for 1 wt.-% OMMT by sonication, this can be attributed to the presence of unexfoliated aggregates in the structure under higher clay concentrations.[50] Modulus was also related to the method of clay dispersion, nanocomposites by sonication had slightly higher moduli than those by shear mixing. Better dispersions by sonication increased interfacial

contact area between the clay particles and epoxy matrix, thus providing a better coupling and a more efficient restriction of epoxy chain mobility under load.

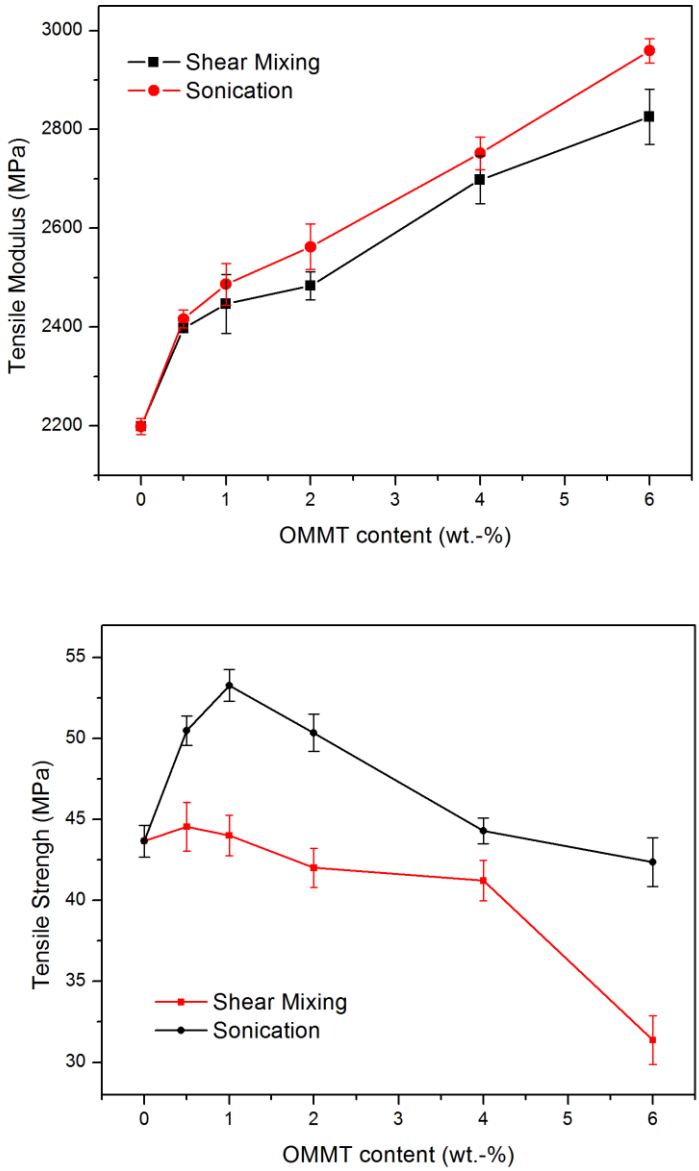

Figure 1. Tensile strength and moduli of polymer and nanocomposites as a function of the clay content.

Tensile strength was also related to the clay dispersion method. For shear mixed composites, no significant change in strength compared to neat polymer was observed at low clay concentrations followed by an abrupt decrease for 6 wt.-% OMMT composites. Sonication dispersed EGS-OMMT nanocomposites lead to improved tensile strength, an increase of 22 % in tensile strength was observed for only 1 wt.-% OMMT content. The nanocomposite strength at 6 wt.-% OMMT concentration, is still closed to that of neat polymer but with 34 % improvement in modulus, such phenomenon is quite unlike the DGEBA based clay nanocomposites, which were often shown reduced tensile strength than their pristine polymers.[1, 51] Very few studies showed an 25 % increase of tensile strength but with much higher 5 wt.-% OMMT content,[52] and similarly a 20.9 % improvement at 3 wt.-% of OMMT.[53] Interestingly, some vegetable oil based epoxy clay nanocomposites have been reported with improved tensile strength,[18, 47, 48] however, all of them were in rubbery states possessed much lower mechanical and thermal strength than those of EGS. So adding trace amount of OMMT not only improved the mechanical strength of EGS, but also potentially render mechanical properties of EGS nanocomposites closing or being comparable to DGEBA based polymers.[40]

Overall, exfoliated structures lead to improved modulus and strength, while the intercalated structures lead to decreased tensile strength. With sonication, exfoliation and intercalation structures probably coexisted at higher clay concentration, thus resulting in reduced mechanical strength. Because the interfacial interaction between OMMT and matrix was reduced at high clay concentration and crack fracture could initiate in clay galleries.[2] Decreased tensile strength has also been attributed to the presence of aggregation of clay particles which is due to the inefficient dispersion or clay

concentrations above the percolation threshold. Aggregation not only reduces the interfacial interactions between clay and polymer but also generate macrocracks.[54] Large aggregates and intercalated structures were co-existed in shear mixed composites, so there is less interfacial interaction between OMMT and matrix compared to the sonication dispersed composites, as will be observed by SEM and TEM tests.

3.2. ESTIMATION OF WETTING AND DISPERSION EFFICIENCY

Clay dispersion is a complex process and influenced by many factors, including process methods, curing agents,[55] and the property of clay or clay modifier.[56] The interaction between clay/modifier, monomers, and solvents is one of key factors to obtain stable suspensions and final intercalated/exfoliated structure.[57] The solubility parameter (δ) approach has been used to interpret intercalation/exfoliation and to predicate nanocomposite morphology.[8, 36, 58] To form homogeneous dispersions, epoxy should have a similar solubility parameter as the clay surface modifier, in accordance with the general rule that structural similarity favors solubility. The group contribution method has been developed to calculate solubility parameters,[59]

$$\delta = \frac{\rho \sum_i F_i}{M}$$

where δ is the solubility parameter, $\sum_i F_i$ are the molar attraction constants summed over the groups present in the compound or repeat unit for polymers, and ρ and M are the density and molecular mass of the compound, respectively. For refinement, solubility parameter components can be further distinguished into dispersive (δ_d), polar (δ_p) and hydrogen bond interactions (δ_h),

$$\delta^2 = \delta_d^2 + \delta_p^2 + \delta_h^2$$

The solubility parameters of monomers, solvent and clay modifier were calculated based on Hoftyzer-Van Krevelen's group contribution method.[59] The chemical structures are listed in Figure 2. For EGS, a total of 2.1 epoxy groups were used for the calculation, which matches on the titrated average oxirane oxygen value. For comparison, the solubility parameters of acetone and styrene are also provided in Table 1.

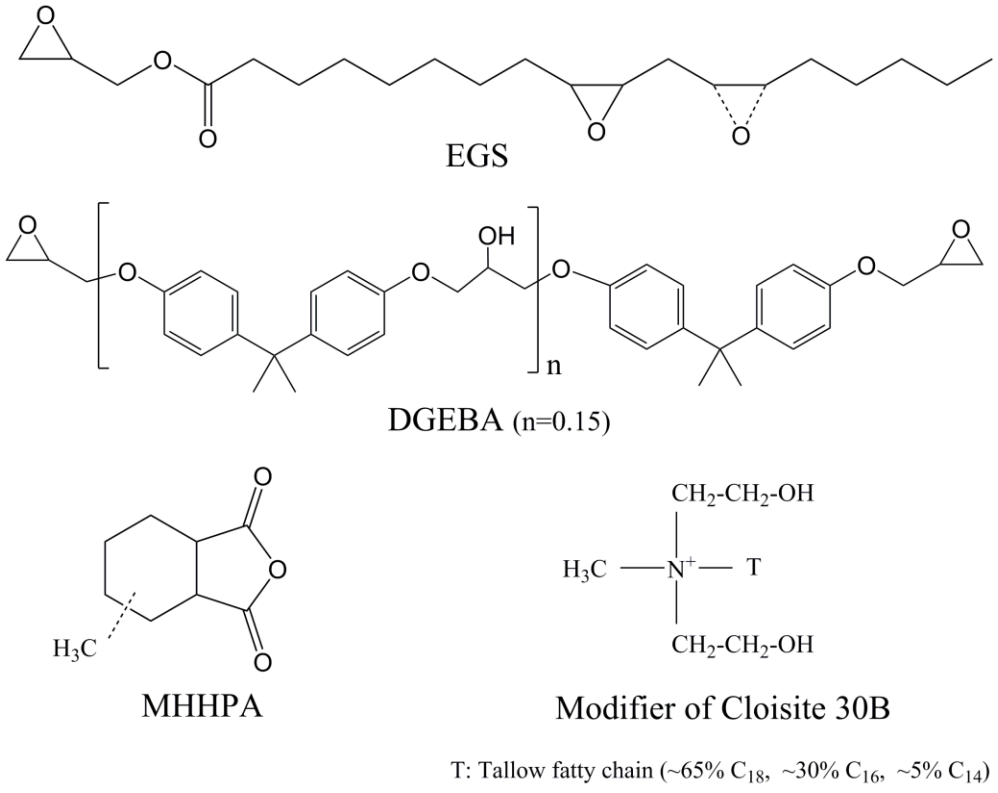

Figure 2. Material chemical structures used for solubility parameters calculation.

From Table 1, DGEBA and acetone have very similar solubility parameters to the OMMT, so the DGEBA based epoxies are compatible with the OMMT,[6] and should readily penetrate into the OMMT galleries with or without the facilitation of acetone. It has also been observed that higher solubility parameter of the polymer raises the basal

spacing of the clay[8] and the δ_p and δ_h (combined as $\delta_a = (\delta_p^2 + \delta_h^2)^{1/2}$) strongly affect the basal space expansion, which facilitates formation of an exfoliated structure.[60] DGEBA has the highest δ value, especially higher δ_a value, are prong to form exfoliated structures,[56] while for styrene both δ and δ_a values are much lower than those of OMMT, so only a smaller *d* spacing of the clay was achieved,[8] and intercalated structures were usually formed.[61, 62]

Table 1. Calculated solubility parameters of monomer, clay modifier and solvent

Solubility Parameter ($MPa^{1/2}$)	OMMT	EGS	MHHPA	DGEBA	Acetone	Styrene
δ	20.0	19.8	21.0	21.6	19.4	18.3
δ_d	16.8	15.7	17.4	16	15.4	18.2
δ_p	2.7	2.8	8.7	11.2	10.5	1.0
δ_h	10.6	11.8	7.9	9.1	5.2	0
$\delta_v=(\delta_d^2 + \delta_p^2)^{1/2}$	17.0	16.0	19.5	19.5	18.6	18.3
$\delta_a=(\delta_p^2 + \delta_h^2)^{1/2}$	10.9	12.1	11.7	14.4	11.7	1.0

Monomer structure, characterized by flexibility or diffusion rate, can also influence the exfoliation.[63] The MHHPA is a low viscosity liquid with a high diffusion rate, can readily penetrate into the clay galleries and expand the basal spacing, and even disrupt the layered structure due to reactions with the organo modifier.[47] Flexible aliphatic amines are prone to form exfoliation compared to rigid cycloaliphatic diamines.[64] Similarly, vegetable oil based anhydrides with flexible fatty chains are also prone to form exfoliated clay nanocomposites.[55]

The EGS have long fatty chains and resemble the modifier structure of Cloisite® 30B and hence the calculated solubility parameter of EGS is quite close to the value of OMMT, as shown in Table 1. EGS as DGEBA was thus expected to be compatible with the OMMT. Plus, EGS also has very low viscosity as MHHPA, so EGS should readily infiltrate into clay galleries even without the facilitation of solvent or sonication, and disrupt the nanoparticle aggregates to form exfoliated/intercalated structures upon shear mixing.

3.3. QUALITATIVE OBSERVATION OF DISPERSION METHODOLOGY RESULTS

Epoxy resins are mostly two part systems of an epoxy monomer and a curing agent. Dispersions can be produced in one of those phases. Since the calculated solubility parameters of MHHPA is also similar to the value of OMMT, the dispersibility of OMMT in epoxy or MHHPA was separately compared under optical microscopy and direct observation as shown in Figure 3. Surprisingly, OMMT did not form a homogeneous dispersion in MHHPA using either sonication or high shear mixing method, and only black precipitates were observed (Figure 3a), which is unlike the original pale yellow color of OMMT or the phase separated blend (Figure 3b). It seems that the modifier structure in OMMT was disrupted and some pristine clay particles were precipitated from the MHHPA.

The δ_h is a critical factor determining whether the OMMT particles remain suspended in a liquid since neither strong nor poor hydrogen-bonding groups suspend clay well.[60] A low δ_h value of MHHPA was observed, similarly, OMMT was also precipitated in acetone with even lower δ_h value. Besides that the hydroxyl group in

OMMT modifier or quaternary ammonium itself will react with MHHPA and form carboxylic acid which is even more polar than anhydride or hydroxyl group alone, *e.g,*. de-exfoliation and aggregation of OMMT in organic solvent has been observed upon the addition of polar amine curing agent.[65] Hence, appropriate mixing sequence should be selected in order to achieve better dispersion of OMMT and higher performance of the nanocomposite,[66] and only low speed shear mixing (magnetic stirring) was utilized to mix MHHPA into EGS-OMMT blends to avoid reaggregation of well dispersed platelets.

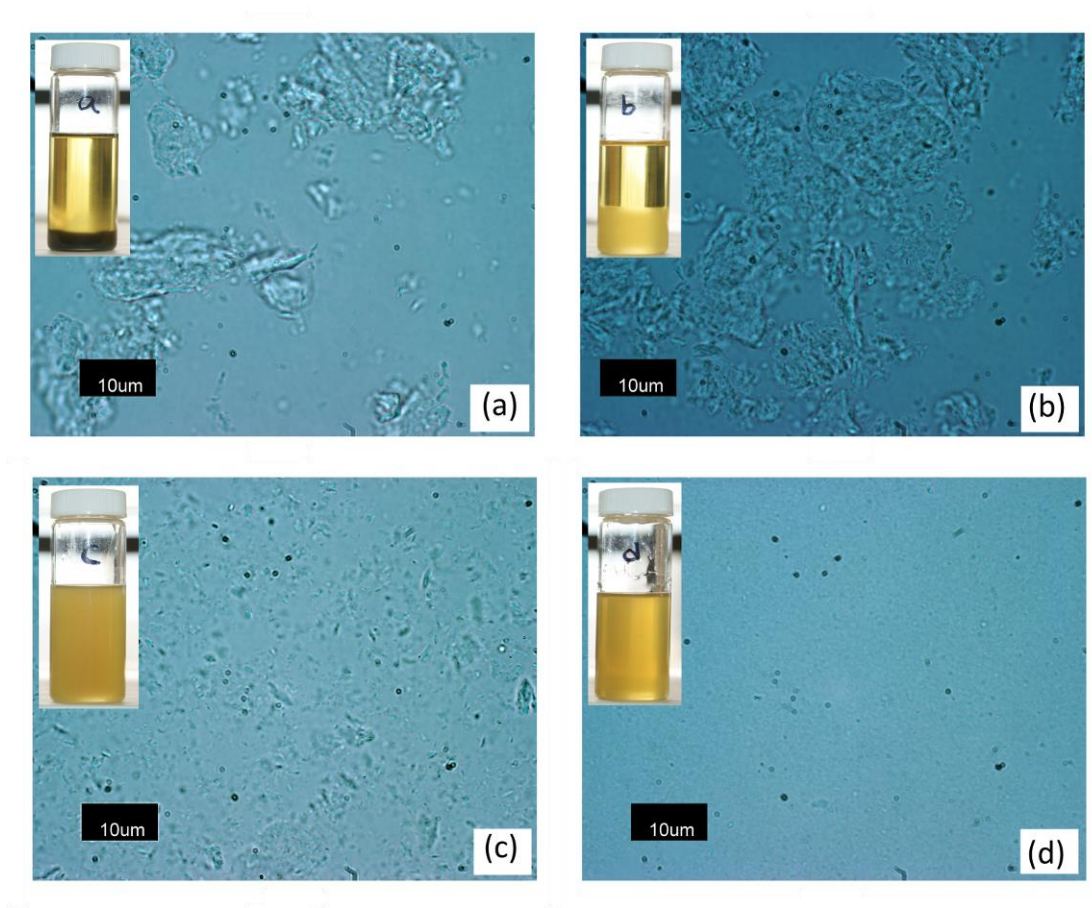

Figure 3. Optical microscopy imaging of the dispersion state of 4 wt% OMMT in monomers upon: (a) sonication in MHHPA, (b) low shear magnetic stirring in EGS, (c) mechanical high shear mixing in EGS, and (d) sonication in EGS.

Low shear mixing in EGS failed to break down the clay particles, large size of clay aggregations and precipitation were observed (Figure 3b). Better dispersion and more stable blend was achieved by high shear mixing method, OMMT agglomerations in size of about 5 μm were observed (Figure 3c), while most particles size were below 2 μm. Blend treated by sonication showed the best dispersion of OMMT and no apparent aggregations were observed (Figure 3d). Good dispersion was also observed by a stable and semi-transparent blend even after 30 days.

The physical appearances of cured blends are shown in Figure 4. Sonication mixing (Figure 4a) produced smaller particles sizes and showed better dispersion of clay in the composite and therefore greater transparency. Shear mixing (Figure 4c) produced slightly more transparency than anhydride mixing, which showed heterogeneous dispersion (Figure 4b). Although intercalation is expected to occur independently of the size of the clay agglomerations as a wetting phenomenon, which is separated from shearing,[65] clay agglomerations that remain during or after crosslinking, are expected to affect properties like transparency, reaction enthalpy, and ultimate mechanical properties.

Figure 4. Physical appearance of cured polymers of 2 wt% concentration OMMT as a function of dispersion methodology: (a) sonication in EGS, (b) sonication in MHHPA, and (c) high speed mechanical shear in EGS.

3.4. FRACTURE SURFACE MORPHOLOGY

Fracture surfaces of the neat EGS and nanocomposites systems were observed by SEM. Figure 5a indicated neat polymer fracture surface is mostly smooth and the crack propagated in a planar manner, while the nanocomposites show considerably rougher surfaces and influence of clay particles (Figure 5b-5f), which imply that the path of the crack tip is distorted by clay platelets and crack propagation may become more difficult or more readily nucleated. The clay nanocomposites also showed different morphologies

depend on the concentrations of clay and the dispersion methods. In Figures 6b and 6e, much better dispersions were observed for composites utilizing the sonication method at same clay concentration compared to shear mixing ones (Figures 5c and 5f).

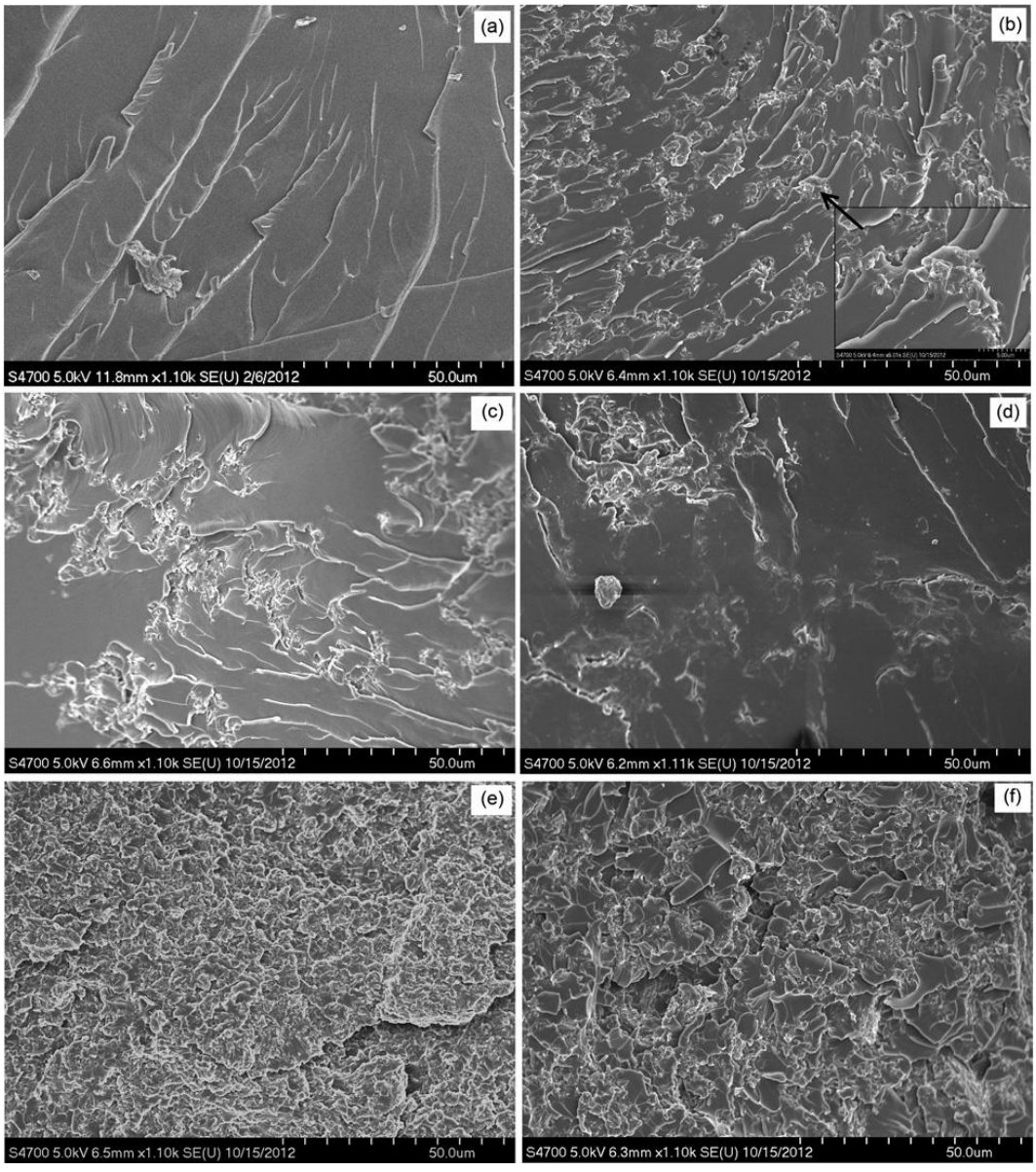

Figure 5. SEM graphs of the fracture surface: (a) neat epoxy, (b) 1 wt% OMMT sonication, (c) 1 wt% OMMT mechanical shear mixing, (d) 1 wt% OMMT sonication in MHHPA, (e) 4 wt% OMMT sonication, and (f) 4 wt% OMMT mechanical shear mixing.

Figure 5e reveals a coarser and flaky fracture surface where clay appears to be in a continuous phase. A weak gel structure accompanied with significantly increased blend viscosity was observed during sonication mixing of 4 wt.-% or higher concentrations of OMMT into EGS, thus the 6 wt.-% OMMT concentration is nearing or above the percolation value and forming percolation-typed structure where existed interactions of clay-clay and clay-monomer.[57]

The nanoclay platelets are intended to interlock with the epoxy networks through the modifiers reaction with monomers. Inspection of the phase morphology supports interfacial adhesion (Figure 5b), while disbonding or macrocracks are clearly observed at the interfacial region of clay aggregates, especially for anhydride dispersed samples (Figure 5d), which further confirmed the poorest dispersion with clearly aggregations. Dispersion heterogeneity, such as clay aggregation, should result in localized stress concentration and crack initiation when the sample is subjected to load.[2] Not surprisingly, thermal and mechanical results from the anhydride mixing samples were mostly lower compared to shear and sonication mixed ones, which showed improved dispersion and provided optimal interaction between the polymer matrix and clay platelets, thus better resistance of crack propagation.

3.5. INTER PARTICLE SPACING

Figure 6 presents the SAXS spectra of OMMT and polymer nanocomposites of different clay concentrations. OMMT showed a characteristic peak at $2\theta = 4.7°$, which corresponds to the basal spacing of 18.5 Å according to Bragg's law. No apparent peaks were detected for 1 and 2 wt.-% clay composites in the range of 2θ from 0.3° to 8°, so the d spacing should be at least larger than 58.9 nm, possibly indicating clay is well

intercalated, being either exfoliated or highly intercalated. Greater background scattering with broadening of shoulder peaks were observed for 4 and 6 wt.-% clay contents for 2θ < 2°, indicating a broader distribution of the d spacing (> 4.4 nm) or a diversity of structures like intercalated and exfoliated coexist.

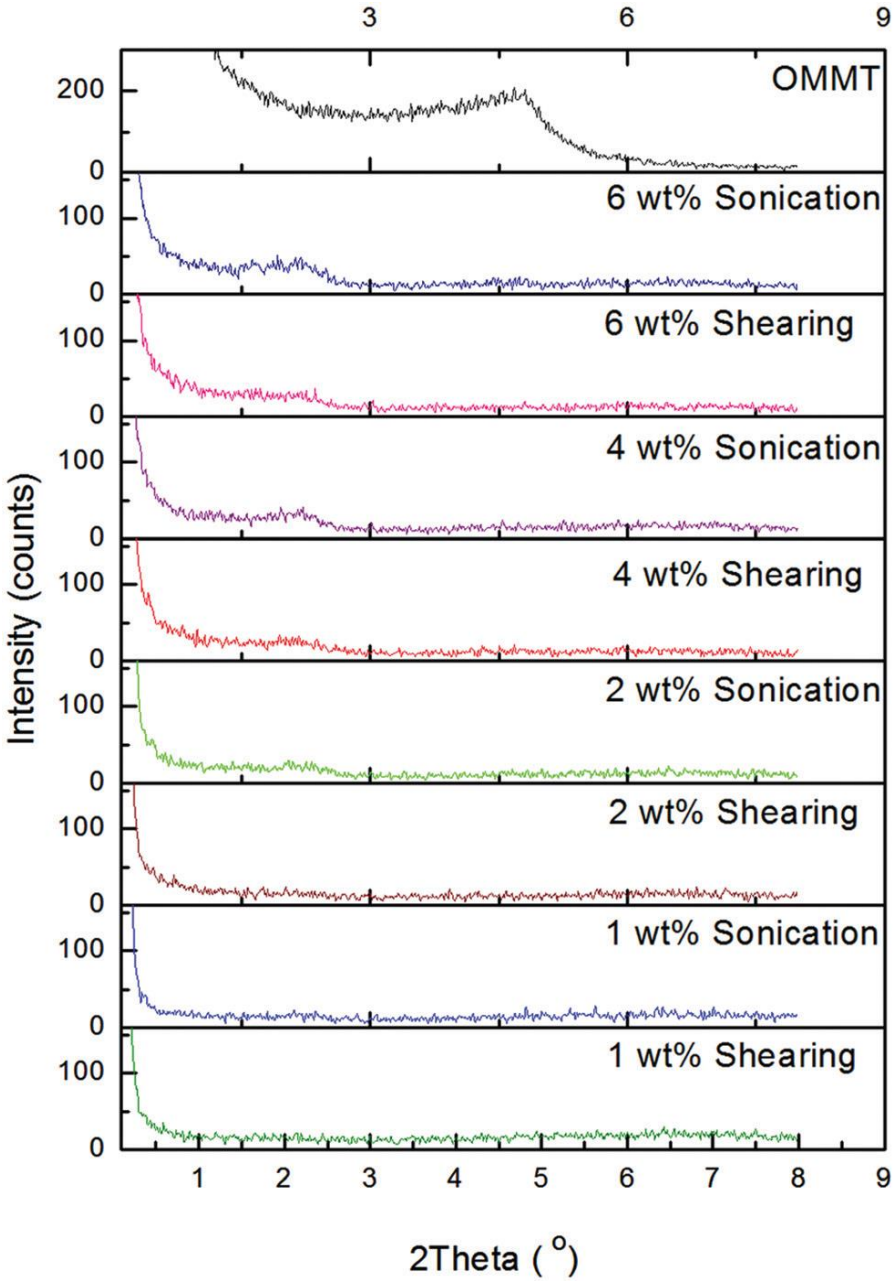

Figure 6. SAXS of nanocomposites with different OMMT contents and dispersion methodology.

Although SAXS can determine wider spacing of the clay interlayer compared to wide-angle X-ray diffraction, less can be inferred about the spatial distribution of the silicate layers or structural non-homogeneity in nanocomposites. To further confirm the structure of nanocomposites, TEM experiments were performed and images are shown in Figure 7.

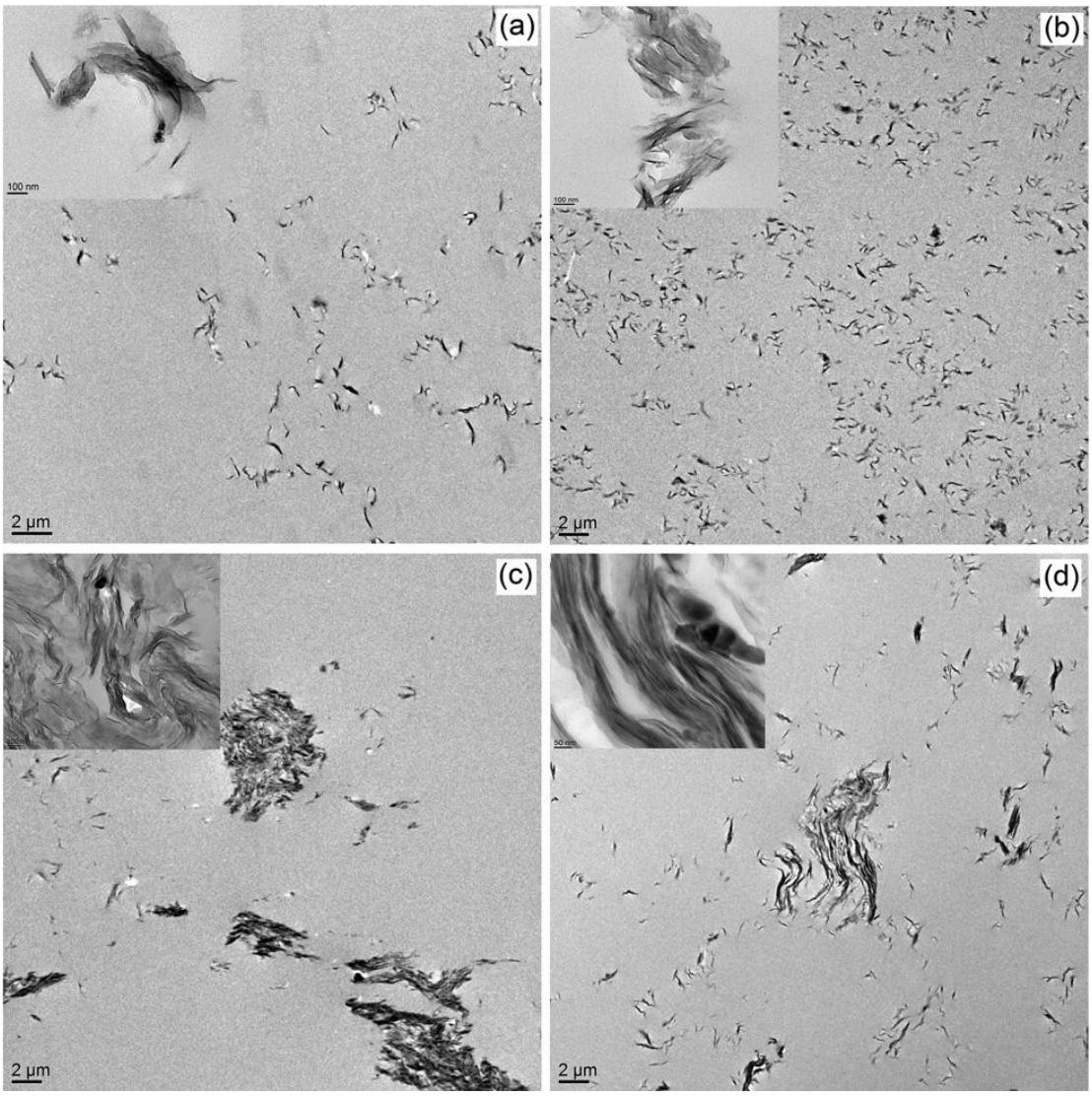

Figure 7. TEM of nanocomposites (a) 1 wt% OMMT sonication, (b) 4 wt% OMMT sonication, (c) 1 wt% OMMT mechanical shear mixing, and (d) 4 wt% OMMT mechanical shear mixing.

Sonication method showed a more homogeneous dispersion of nanoparticles compared to shear mixing. Both 1 wt.-% and 4 wt.-% OMMT nanocomposites by sonication showed exfoliated structures and the presence of tactoid particles (Figure 7a and 7b). At higher magnification, the tactoids were revealed to be either partially exfoliated or highly intercalated with stacked clay platelets.

Shear mixing of 1 wt.-% OMMT lead to an inhomogeneous dispersion, although some dissociated clay layers were present, large and undisrupted clay aggregates were also existed (Figure 7c), such specimen appears as macro clay composite rather than nanocomposite; however, a higher magnification revealed that substantial expansion of the gallery with intercalation occurred, which is also accorded to the SAXS results.

EGS monomer, of flexible molecular structure, low viscosity and similar solubility parameter as OMMT, readily diffused into the galleries even without the facilitation of solvent or sonication. Much better clay dispersion was observed for 4 wt.-% OMMT by shear mixing (Figure 7d). Due to the thixotropic effect of OMMT, increased clay content and viscosity lead to better disruption of clay aggregates presumably to greater shear stress. Where shear mixing retains intercalated tactoids with many stacks of clay layers of average 4 nm basal spacing, is also supported by the SAXS study. Compared to shear mixing, sonication provided much higher shear strength to help monomers diffuse into galleries, and lead to a better expansion of galleries than shear mixing and chemical ability of the monomer alone, thus nanocomposites by sonication generally provided improved thermal and mechanical properties.

3.6. REACTION EXOTHERM STUDIES

DSC was applied to study the curing behavior of the blended epoxy resins. The exothermic peak onsets were characteristic of epoxy curing reactions.[67] Integration of reaction exotherm allowed the determination of the enthalpy of curing reaction (ΔH). Onset curing temperature (T_i) and peak exotherm (T_p) were also determined (Figure 8).

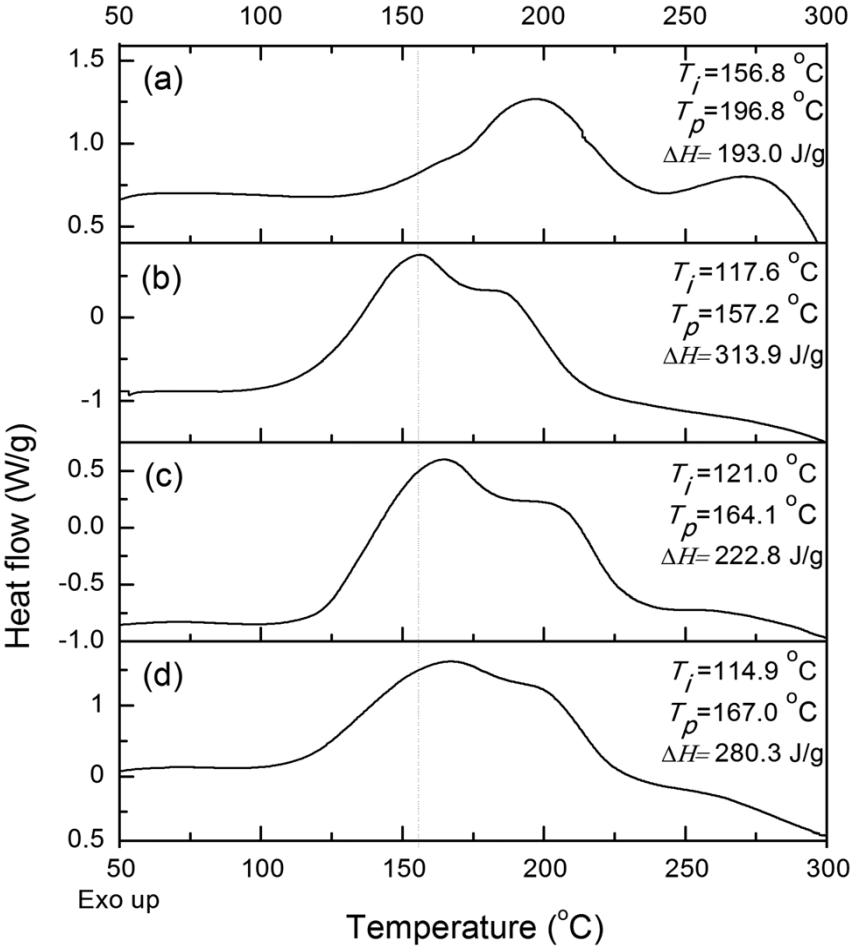

Figure 8. Dynamic thermograms of EGS-MHHPA blends with (a) no catalyst; (b) 1 wt% EMI; (c) 1 wt% OMMT; (d) 1 wt% OMMT and 1 wt% EMI.

The EGS and anhydride reaction without catalyst is sluggish and incomplete, which was indicated by higher T_p value and much lower ΔH value (Figure 8a). The first

exotherm peak is ascribed to a polyaddition between epoxy ring and anhydride. The second exotherm peak at 270 °C is assigned to the side reactions such as etherification and/or homopolymerization. Base accelerators like imidazole greatly reduce T_p and T_i values and enable much higher ΔH values (Figure 8b), and the etherification of epoxy becomes less likely.[67]

The clay surface modifier quaternary amine salt behaving as an accelerator to the epoxy curing reaction is well known.[68] Compared to the EMI catalyzed system (Figure 4b), relatively minor changes in T_i, T_p and shape of DSC curve were observed for an OMMT catalyzed system (Figure 8c) or an EMI-OMMT co-catalyzed system (Figure 8d), which indicated a similar curing energetics for EMI and OMMT catalyzed epoxy-anhydride curing reactions. The surface modifier of Cloisite® 30B has two hydroxyl groups which can also react with anhydride and enable a strongly bonded interface.[47, 53] Lower ΔH values were observed in OMMT only catalyzed curing reactions compared to EMI catalyzed. This may due to the low concentration or inhomogeneous dispersion of OMMT in monomers. In order to enable complete reaction, EMI was added into all EGS-OMMT blends. DSC results are listed in Table 2.

From Table 2, there is slightly decrease in ΔH values varied with OMMT concentrations for both dispersion methods and T_i and T_p values are quite close to the neat resin system. Clay additions leading to lower values of ΔH due to the homopolymerization of epoxy by OMMT have been reported,[69] because the reaction between hydroxyl groups in modifier with monomer can reduce the functionality of monomers and subsequently render a lower ΔH value.[47]

Table 2. DSC results of curing EGS-MHHPA-OMMT systems

wt.-% of OMMT	Dispersion Methods	T_i (°C)	T_p (°C)	ΔH (J/g)	T_g (°C)
0	-	117.6±1.3	157.2±0.9	313.9±2.4	86.0±1.8
0.5	Shearing	118.8±1.8	155.5±1.0	301.3±4.8	83.1±1.5
1	Shearing	118.1±1.8	155.0±0.8	289.8±4.2	82.8±0.9
2	Shearing	119.0±2.0	155.2±0.7	283.2±5.0	84.1±2.8
4	Shearing	115.3±1.5	156.0±0.6	296.0±7.1	83.5±1.3
6	Shearing	114.8±2.7	153.8±1.3	283.2±8.9	83.4±1.3
0.5	Sonication	121.0±0.9	157.5±1.2	308.6±6.9	92.1±0.6
1	Sonication	115.9±1.1	156.7±0.2	306.0±7.0	91.5±1.6
2	Sonication	117.2±1.2	159.4±0.5	303.6±5.3	90.5±0.5
4	Sonication	117.0±1.8	158.4±0.6	306.2±5.9	90.0±0.2
6	Sonication	115.3±3.0	159.1±0.7	305.8±5.8	90.3±0.3

Shear mixing possessed lower ΔH values indicated inhomogeneous clay dispersion will prevent curing reaction. The presence of clay aggregations may impede chain diffusing during gelation process and lead to a lower extent of cure. Sonication dispersion method led to much better dispersions and perhaps a higher concentration of catalyst or improved interactions between monomers and modifiers, thus ΔH values were slightly improved.

3.7. GLASS TRANSITION TEMPERATURE OF THE MATRIX

Effect of clay content on glass transition temperature was evaluated by DSC and results are listed in Table 2. The neat polymer showed a T_g of 86 °C. A decrease in T_g occurred for all composites produced by high shear mixing where the reduction was more significant at low clay concentrations. Poor clay dispersion appeared to reduce polymer reaction enthalpy and cure extent as observed in DSC study. Clay aggregation may act as

a barrier during curing and prevent a highly cross-linked structure, where smaller *d*-spacing may preclude migration of monomers and oligomers within the layers. Decreased T_g has also been found in other intercalated clay composites.[50]

On the other hand, exfoliation of clay into the epoxy matrix by sonication increased T_g. An increase of 6 °C was observed for only 0.5 wt.-% OMMT, then followed a slightly reduced T_g at higher OMMT contents, which implied that OMMT at relatively low content had better dispersion and more restriction to motion of epoxy networks versus the more intercalated structure at relatively higher clay concentrations. Reduced T_g may also be due to the plasticizing effect for a higher fraction of surface modifiers.

3.8. STABILITY AND KINETIC OF THERMAL DEGRADATION

The thermal degradation of the nanocomposites was studied by TGA. From Figure 9, two degradation processes under air atmosphere were observed for all samples of onset temperature at 320 °C and 450 °C. Degradation occurred in the temperature region from 320 to 450 °C was assigned as decomposition of the crosslinked polymer network. Weight loss above 450 °C is mainly a degradation of organic char residue. At temperatures above the second degradation stage, samples residue reflected inorganic content of the nanocomposites. The thermal parameters which characterize the effect of clay concentration and dispersion method on the thermal stability of nanocomposites are shown in Table 3.

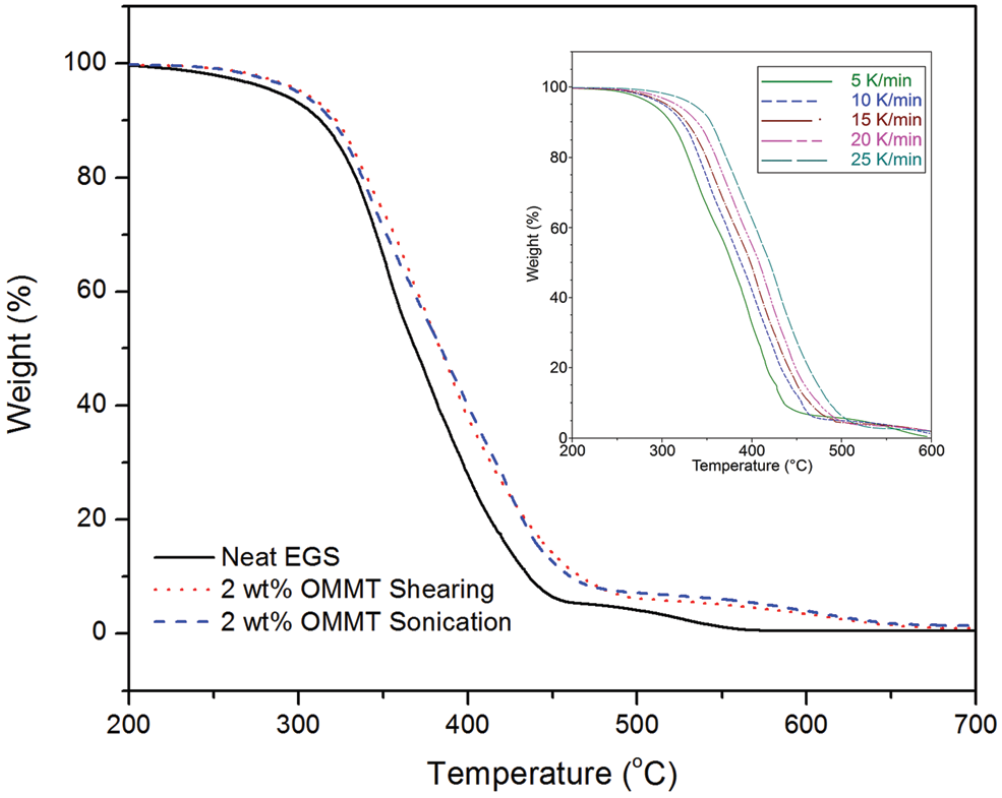

Figure 9. TGA thermograms of nanocomposites with various clay contents and thermograms of neat EGS polymer as a function of heating rate (inset).

From Table 3, the nanocomposites exhibited slightly higher temperatures at onset, 10 % and 50 % weight loss in the first degradation process. Similarly, clay prevented the degradation of the char layer in the second degradation process as the onset degradation temperatures were substantially increased. Thus, clays components have a significant effect on nanocomposites thermal stability. The improved thermal stabilities may be attributed to the formation of low permeable silicates which can reduce the oxygen uptake, the subsequently formed clay char residues layers during combustion may also reduce the heat transfer between the flame and nanocomposite. However, neither increase clay concentration nor the type of dispersion method, had any significant effect upon the current degradation process.

Table 3. Thermal stability of nanocomposites

Sample (wt.% of OMMT)	Dispersion Method	Onset of 1st degradation (°C)	*T* @ 10 % degradation (°C)	*T* @ 50 % degradation (°C)	Onset of 2nd degradation (°C)
0	-	304.1	309.7	376.1	439.6
0.5	Shearing	310.1	321.6	386.1	458.8
1	Shearing	311.3	322.3	382.5	455.9
2	Shearing	311.8	322.3	383.7	456.3
4	Shearing	308.0	319.3	379.4	461.1
6	Shearing	310.6	322.3	377.4	458.6
0.5	Sonication	310.6	317.8	383.2	460.5
1	Sonication	315.6	324.6	384.0	469.8
2	Sonication	312.4	320.0	384.2	452.9
4	Sonication	312.6	317.8	379.4	458.5
6	Sonication	314.7	321.6	379.8	465.0

* Mean values of three measurement

The thermal degradation activation energy (E_a) of many polymers varies with the process conditions.[70] To further characterize the degradation process, a non-isothermal decomposition kinetics analysis based TGA results was performed and the E_a was calculated using the Flynn-Wall-Ozawa's method,

$$\log\beta = \log\left[\frac{AE_a}{Rg(\alpha)}\right] - 2.315 - 0.4567\,\frac{E_a}{RT}$$

α is the degree of conversion defined as the ratio of actual weight loss to total weight loss in TGA; $g(\alpha)$ is the integral function of extent of conversion α; β is the hearing rate; A represents the pre-exponential factor; R is gas constant; T is absolute temperature. Temperature at 5 % weight loss in TGA thermograms was chosen to characterize the thermal stability, which can avoid the high temperature variations at beginning of thermal

decomposition.[71] The E_a could be obtained from the slope of $log\beta$ against $1/T$ at a fixed 5 % conversion but under various heating rates, see Figure 9 and 10.

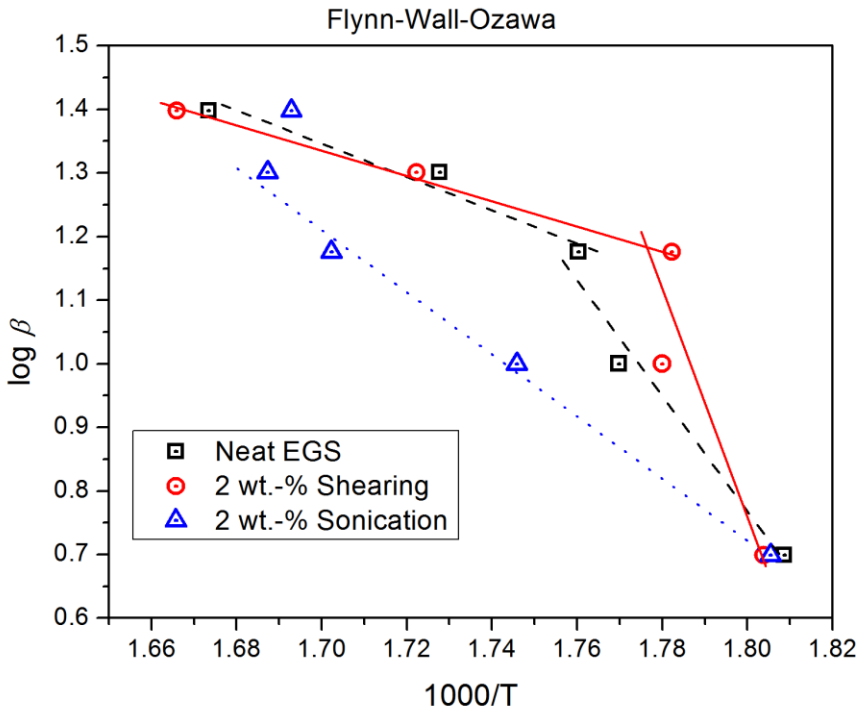

Figure 10. Flynn-Wall-Ozawa plots of logβ vs. 1000/T at 5 % conversion

Figure 10 presents plots of log β versus $1/T$, surprisingly, not all plots displayed excellent linearity, two degradation mechanisms dependent on the rate of degradation was clearly observed for both neat EGS and shearing mixed sample, while sonication method showed a more uniform degradation process this phenomenon may due to the structures variations between two dispersion methods, the sonication provided better clay dispersion, as observed in optical and TEM study, thus formed a more homogeneous clay nanocomposite structure withstand thermal degradation uniformly. On the other hand, the heterogeneous structure due to shear mixing cannot change the thermal degradation

mechanism of EGS, Both activation energies at slow degradation rate (5 to 15 °C/min) and high degradation rate (15 to 25 °C/min) were calculated and indicated as E_{a1} and E_{a2}, respectively, and values are listed in Table 4, for sonication dispersed samples, only E_{a1} were listed, because plots show much better linearity under whole degradation rates.

Table 4. Activation energies and correlation coefficient obtained using Flynn-Wall-Ozawa method

Samples	E_{a1} (kJ mol^{-1})	E_{a2} (kJ mol^{-1})	R_1^2	R_2^2
Neat EGS	76.5	45.1	0.966	0.954
2 wt.-% Shearing	252.6	34.8	0.803	0.997
6 wt.-% Shearing	189.5	45.8	0.985	0.849
2 wt.-% Sonication	84.6	-	0.996	-
6 wt.-% Sonication	90.6	-	0.890	-

From Table 4, it was found sonication method shows higher activation energy than EGS, thus presented better and uniform thermal stability under whole degradation process, also higher OMMT concentration increases the activation energy thus improve the thermal stability, which is also confirmed that higher OMMT concentrations by sonication still proved a good homogeneous structure. Much higher E_{a1} were found for shear mixing method at low degradation rate, while E_{a2} at faster degradation rate showed only a comparable or worse thermal stability than neat EGS, unlike the sonication method, increase the OMMT concentration leads to decrease E_{a1}, again this may be due to the increased heterogeneous. At low degradation rates, the heterogeneous structure like clay aggregation may has more time to form thermal resistance structure, while at

high degradation rate conditions, some weak parts due to the reduced crosslink densities, dangling chains, debonding or macrocracks may degrade more rapidly than the rest of bulk structure. On the contrary, the sonication method lead to more homogeneous structure and less defects or week parts, thus better and uniform resistance under whole degradation rates.

4. CONCLUSION

This work presents a systematic study on the effect of different dispersion methods on the thermal and mechanical properties of bio-based epoxy clay nanocomposites. Exfoliated nanocomposites by sonication showed improved mechanical and thermal properties than those of intercalated nanocomposites by shear mixing. Under optimum condition (1 wt.-% OMMT and sonication), the tensile strength, modulus of nanocomposite improved by 22 %, 13 %, respectively. Further increase clay concentration to 6 wt.-%, the modulus was increased by 34 % and without sacrifice the strength. The T_g was also increased by 4~6 °C for all clay concentrations. The solubility parameters of EGS and organic modifier are quite close and correlated with miscible/compatible composites as supported by optical microscopy, SEM and TEM testing, while the incompatibility was also observed between anhydride and OMMT. The formation of nanostructures was confirmed by SAXS and TEM as a mixture of intercalated and exfoliated structures. Shear mixing led to intercalated structures but with undisrupted tactoids. Sonication provides more energy and caused further clay platelets separation, better dispersion and was more prone to form an exfoliated structure. There were slight increases in thermal degradation stability after adding clay, and thermal degradation mechanisms and thermal stabilities were independent on the dispersion

methods. Dispersion of clay particles to the scale of individual platelets would be improbably using solely a shear mixing method. However, high speed shear mixing combined with sonication can reduce platelets tactoids to much smaller scale, which provided better properties compared to high shear mixing method alone. The clay nanocomposites derived from renewable resources, showed improved properties compared to neat polymer. Clay nano reinforcement may improve the capability of the renewable raw material as an alternative to petrochemical polymers.

REFERENCES

1. A. A. Azeez, K. Y. Rhee, S. J. Park and D. Hui, *Composites Part B: Engineering*, 2013, **45**, 308-320.
2. K. Wang, L. Chen, J. Wu, M. L. Toh, C. He and A. F. Yee, *Macromolecules*, 2005, **38**, 788-800.
3. N. A. Salahuddin, *Polymers for Advanced Technologies*, 2004, **15**, 251-259.
4. T. Ogasawara, Y. Ishida, T. Ishikawa, T. Aoki and T. Ogura, *Composites Part A: Applied Science and Manufacturing*, 2006, **37**, 2236-2240.
5. J.-K. Kim, C. Hu, R. S. C. Woo and M.-L. Sham, *Composites Science and Technology*, 2005, **65**, 805-813.
6. C. Chen and T. B. Tolle, *Journal of Polymer Science Part B: Polymer Physics*, 2004, **42**, 3981-3986.
7. S. Balakrishnan and D. Raghavan, *Journal of Reinforced Plastics and Composites*, 2005, **24**, 785-793.
8. B. N. Jang, D. Wang and C. A. Wilkie, *Macromolecules*, 2005, **38**, 6533-6543.
9. B. Chen, J. Liu, H. Chen and J. Wu, *Chemistry of Materials*, 2004, **16**, 4864-4866.
10. S. Sinha Ray and M. Bousmina, *Progress in Materials Science*, 2005, **50**, 962-1079.
11. K. Chandrashekhara, S. Sundararaman, V. Flanigan and S. Kapila, *Materials Science and Engineering: A*, 2005, **412**, 2-6.
12. J. Zhu, K. Chandrashekhara, V. Flanigan and S. Kapila, *Composites Part A: Applied Science and Manufacturing*, 2004, **35**, 95-101.

13. A. Gandini, T. M. Lacerda and A. J. F. Carvalho, *Green Chemistry*, 2013, **15**, 1514-1519.

14. R. Gu, S. Konar and M. Sain, *Journal of the American Oil Chemists' Society*, 2012, **89**, 2103-2111.

15. K. Huang, P. Zhang, J. Zhang, S. Li, M. Li, J. Xia and Y. Zhou, *Green Chemistry*, 2013, **15**, 2466-2475.

16. G. Mehta, A. K. Mohanty, M. Misra and L. T. Drzal, *Green Chemistry*, 2004, **6**, 254-258.

17. O. Zovi, L. Lecamp, C. Loutelier-Bourhis, C. M. Lange and C. Bunel, *Green Chemistry*, 2011, **13**, 1014-1022.

18. V. Tanrattanakul and P. Saithai, *Journal of Applied Polymer Science*, 2009, **114**, 3057-3067.

19. M. A. Mosiewicki and M. I. Aranguren, *European Polymer Journal*, 2013, **49**, 1243-1256.

20. F. Li, J. Hasjim and R. C. Larock, *Journal of Applied Polymer Science*, 2003, **90**, 1830-1838.

21. X. Pan, P. Sengupta and D. C. Webster, *Green Chemistry*, 2011, **13**, 965-975.

22. R. L. Quirino, Y. Ma and R. C. Larock, *Green Chemistry*, 2012, **14**, 1398-1404.

23. Y. Xia and R. C. Larock, *Green Chemistry*, 2010, **12**, 1893-1909.

24. Y. Xia, R. L. Quirino and R. C. Larock, *Journal of Renewable Materials*, 2012, **1**, 3-27.

25. Y. Lu and R. C. Larock, *ChemSusChem*, 2009, **2**, 136-147.

26. V. Sharma, J. S. Banait, R. C. Larock and P. P. Kundu1, *eXPRESS Polymer Letters*, 2008, **2**, 265-276.

27. T. C. Mauldin, K. Haman, X. Sheng, P. Henna, R. C. Larock and M. R. Kessler, *Journal of Polymer Science Part A: Polymer Chemistry*, 2008, **46**, 6851-6860.

28. M. Mosiewicki, M. I. Aranguren and J. Borrajo, *Journal of Applied Polymer Science*, 2005, **97**, 825-836.

29. S. N. Khot, J. J. Lascala, E. Can, S. S. Morye, G. I. Williams, G. R. Palmese, S. H. Kusefoglu and R. P. Wool, *Journal of Applied Polymer Science*, 2001, **82**, 703-723.

30. J. Lu, S. Khot and R. P. Wool, *Polymer*, 2005, **46**, 71-80.

31. A. O'Donnell, M. A. Dweib and R. P. Wool, *Composites Science and Technology*, 2004, **64**, 1135-1145.

32. P. H. Henna, M. R. Kessler and R. C. Larock, *Macromolecular Materials and Engineering*, 2008, **293**, 979-990.

33. Y. Lu and R. C. Larock, *Macromolecular Materials and Engineering*, 2007, **292**, 1085-1094.

34. H. Cui and M. R. Kessler, *Composites Science and Technology*, 2012, **72**, 1264-1272.

35. L. Zhu and R. P. Wool, *Polymer*, 2006, **47**, 8106-8115.

36. J. Lu, C. K. Hong and R. P. Wool, *Journal of Polymer Science Part B: Polymer Physics*, 2004, **42**, 1441-1450.

37. Y. Lu and R. C. Larock, *Macromolecular Materials and Engineering*, 2007, **292**, 863-872.

38. Y. Lu and R. C. Larock, *Biomacromolecules*, 2006, **7**, 2692-2700.

39. Z. S. Petrović, *Polymer Reviews*, 2008, **48**, 109-155.

40. R. Wang and T. Schuman, *eXPRESS Polymer Letters*, 2013, **7**, 272-292.

41. N. W. Manthey, F. Cardona, G. Francucci and T. Aravinthan, *Journal of Reinforced Plastics and Composites*, 2013, **32**, 1444-1456.

42. J. Zhu, K. Chandrashekhara, V. Flanigan and S. Kapila, *Journal of Applied Polymer Science*, 2004, **91**, 3513-3518.

43. J. D. Espinoza-Perez, B. A. Nerenz, D. M. Haagenson, Z. Chen, C. A. Ulven and D. P. Wiesenborn, *Polymer Composites*, 2011, **32**, 1806-1816.

44. V. Thulasiraman, S. Rakesh and M. Sarojadevi, *Polymer Composites*, 2008, **30**, 49-58.

45. H. Miyagawa, M. Misra, L. T. Drzal and A. K. Mohanty, *Polymer*, 2005, **46**, 445-453.

46. H. Uyama, M. Kuwabara, T. Tsujimoto, M. Nakano, A. Usuki and S. Kobayashi, *Chemistry of Materials*, 2003, **15**, 2492-2494.

47. A. Shabeer, K. Chandrashekhara and T. Schuman, *Journal of Composite Materials*, 2007, **41**, 1825-1849.

48. Z. Liu, S. Z. Erhan and J. Xu, *Polymer*, 2005, **46**, 10119-10127.

49. D. Fourcade, B. S. Ritter, P. Walter, R. Schonfeld and R. Mulhaupt, *Green Chemistry*, 2013, **15**, 910-918.

50. A. Mouloud, R. Cherif, S. Fellahi, Y. Grohens and I. Pillin, *Journal of Applied Polymer Science*, 2012, **124**, 4729-4739.

51. A. Yasmin, J. L. Abot and I. M. Daniel, *Scripta Materialia*, 2003, **49**, 81-86.

52. M.-l. Chan, K.-t. Lau, T.-t. Wong, M.-p. Ho and D. Hui, *Composites Part B: Engineering*, 2011, **42**, 1708-1712.

53. K. Zhang, L. Wang, F. Wang, G. Wang and Z. Li, *Journal of Applied Polymer Science*, 2004, **91**, 2649-2652.

54. B. Qi, Q. X. Zhang, M. Bannister and Y. W. Mai, *Composite Structures*, 2006, **75**, 514-519.

55. W.-B. Xu, S.-P. Bao and P.-S. He, *Journal of Applied Polymer Science*, 2002, **84**, 842-849.

56. X. Kornmann, H. Lindberg and L. A. Berglund, *Polymer*, 2001, **42**, 1303-1310.

57. J. Duchet-Rumeau and H. Sautereau, in *Epoxy Polymers: New Materials and Innovations*, eds. J.-P. Pascault and R. J. J. Williams, Wiley-VCH, Weinheim, 2010, pp. 159-183.

58. D. L. Ho and C. J. Glinka, *Chemistry of Materials*, 2003, **15**, 1309-1312.

59. D. W. van Krevelen, *Properties of polymers*, Elsevier Sciences Publishers, Amsterdam, 1990.

60. Y. S. Choi, H. T. Ham and I. J. Chung, *Chemistry of Materials*, 2004, **16**, 2522-2529.

61. C. Zeng and L. J. Lee, *Macromolecules*, 2001, **34**, 4098-4103.

62. Y. Li and H. Ishida, *Polymer*, 2003, **44**, 6571-6577.

63. J. H. Koo, *Polymer Nanocomposites: Processing, Characterization, and Applications*, McGraw-Hill, New York, 2006.

64. X. Kornmann, H. Lindberg and L. A. Berglund, *Polymer*, 2001, **42**, 4493-4499.

65. P. B. Messersmith and E. P. Giannelis, *Chemistry of Materials*, 1994, **6**, 1719-1725.

66. Y. P. Yap and W. S. Chow, *Journal of Composite Materials*, 2009, **43**, 2269-2284.

67. C. A. May, *Epoxy Resins: Chemistry and Technology, Second Edition,*, M. Dekker, New York, 1988.

68. C. Alzina, A. Mija, L. Vincent and N. Sbirrazzuoli, *The Journal of Physical Chemistry B*, 2012, **116**, 5786-5794.

69. M. S. Wang and T. J. Pinnavaia, *Chemistry of Materials*, 1994, **6**, 468-474.

70. S. Vyazovkin and N. Sbirrazzuoli, *Macromolecular Rapid Communication*, 2006, **27**, 1515-1532.

71. F. Carrasco and P. Pagès, *Polymer Degradation and Stability*, 2008, **93**, 1000-1007.

IV. SOYBEAN OIL DERIVED EPOXY-GLASS FIBERS REINFORCED COMPOSITES FOR STRUCTURAL APPLICATION

Rongpeng Wang,[1] Thomas Schuman,[1]* R. R. Vuppalapati,[2] K. Chandrashekhara[2]

[1]Department of Chemistry, Missouri University of Science and Technology, Rolla, MO 65409, USA

[2]Department of Mechanical and Aerospace Engineering, Missouri University of Science and Technology, Rolla, MO 65409, USA

* *Correspondence to*: Thomas Schuman (tschuman@mst.edu)

ABSTRACT

High performance bio-based composites were manufactured that showed mechanical properties comparable to that of the petroleum based counterparts. Pure glycidyl esters of epoxidized fatty acids derived from soybean oil (EGS), blends of diglycidyl ether of bisphenol A (DGEBA) with EGS, and pure DGEBA were copolymerized with anhydride to yield polymer matrix. Glass fiber reinforced composites were fabricated from the matrices via vacuum assisted resin transfer molding (VARTM). The results indicated that EGS is curing compatible with DGEBA and form single phased structure. EGS significantly reduced viscosity of DGEBA and facilitated fabrication of composites through VARTM at room temperature. Mechanical tests showed that EGS composites possessed comparable properties such as flexure and impact strength compared to DGEBA based counterparts. The glass transition temperature, flexural strength and modulus of EGS composite were as high as 114 °C, 474 MPa and 22.5 GPa, respectively. This high performance bio-based composite has potential to replace petroleum-based epoxy resin as value-added product form vegetable oils.

1. INTRODUCTION

Recently, due to global concern about sustainable development, availability of fossil-organic raw materials and high oil prices, synthesizing polymers from renewable sources such as vegetable oils (VOs), cellulose, starch and lignin, have regained interest for polymer industry[1-3]. Apart from renewability and relatively low prices, VOs such as soybean oils are attractive resources in the synthesis of bio-renewable polymers due to potential to create a diverse set of chemical structures[4-6]. Most VO-based chemical structures are not able to compete with analogous petroleum-based polymers in many structural applications due to inherently low stiffness and strength, *e.g.*, of long chain fatty acid molecules. Functionalization and copolymerization with petroleum based monomers have been applied to improve polymers thermal and/ or mechanical properties[7-9]. Polymers ranging from flexible rubbers to hard plastics have been synthesized using either common VOs or conjugated VOs combined with petroleum based monomers[10-12]. Polymers derived from acrylated and/ or maleated VOs[13-15] and soy polyols of polyurethane[16, 17] have also been widely exploited.

To further improve polymer mechanical properties, high modulus synthetic or natural fibers have been added to above mentioned VO-based polymers, resulting in fiber reinforced composites (FRC) of generally improved mechanical properties compared to the neat polymers[18-21]. Bio-based composites typically require supplementation with petroleum-based materials to optimize performance. While some composites have shown high renewable content, they were more suitable for nonstructural applications[22]. A clear trend toward high performance bio-based materials and "green" composites development for value-added applications exists[23-25].

Epoxy resin, such as diglycidyl ether of bisphenol A (DGEBA), is one of the most widely used matrix materials in FRC. DGEBA is formed from bisphenol A (BPA) and epichlorohydrin (EPCH). EPCH is traditionally produced using propylene as raw material. Recent research and commercialization has produced EPCH from glycerol, which is a byproduct of the biodiesel industry[26]. EPCH can then be obtained as a renewable resource.

Due to concerns for the effect of BPA on health, there have been various attempts toward replacement of BPA with renewable materials derived from wood/lignin [27, 28], rosin [29-32], isosorbide[33, 34], cadanol[35], itaconic acid[36, 37], *etc*. However, these BPA alternatives have inherent problems, such as limited production, low purity, structural complexity, hydrophilicity, and/or unknown toxicity. Efficient and economical synthesis of bio-renewable epoxy is still strongly dependent on the future development in biomass refineries[38].

Epoxidized vegetable oils (EVO), such as epoxidized soybean oil (ESO) or epoxidized linseed oil (ELO), are one of the largest industrial utilizations of VOs with production of about 200,000 tons/year[39]. EVO are mainly used as plasticizers and stabilizers for poly(vinyl chloride). Directly using EVO for synthesis of epoxy thermosetting polymers has been attempted but resulted in limit successes because the internal oxiranes react sluggishly with common anhydrides and polyamine curing agents. The long aliphatic chains also cause incompatibility with other common epoxy components[40]. While Cationic polymerization of EVO using latent initiator[41], UV initiator[42], or strong acid[43, 44] showed improved reactivity, the resulting thermosetting polymers are mostly rubber and of low glass transition temperature (T_g).

To improve thermal and mechanical performance, EVO can be blended with aromatic epoxy, *e.g.*, DGEBA, and the polymer blend can be applied as a matrix material for FRC. Some research has shown that EVO were best when limited as minor component in blends, *i.e.*, < 30 wt% [45-47], because the solely EVO component could not provide the mechanical and thermal properties desired for an FRC. Higher concentrations plasticize the polymer matrix, phase separate, and form weak structures due to the lower reactivity and dangling chains of EVOs[40, 48]. Pure EVO or high EVO content (*e.g.* > 50 wt%) based polymer matrices for high performance composites applications are rare. Novel vegetable oil-based epoxy resins, epoxidized allyl soyate (EAS) have been applied in bio-composite applications but the EAS was also limited as minor component in blends [48-50].

Recently, new bio-based epoxy resins based on glycidyl esters of epoxidized fatty acids (EGS) structures that are obtained directly from VO have been synthesized and evaluated[40]. EGS merits include higher oxirane content, improved compatibility, and much lower viscosity than ESO, ELO or DGEBA. Cured EGS thermosetting monomer and whose blends display improved thermal and mechanical properties than ESO. The tensile/flexural strength and moduli are about 30~40% lower than those of DGEBA based control samples even with the addition of high modulus clay nanoparticles[51].

To further investigate the advantages and limitations of EGS based polymers, FRCs were fabricated using oriented glass fiber reinforcement via a vacuum assisted resin transfer molding (VARTM) process, which is of low cost tooling and well suited for manufacturing complex shaped composites. The thermal and mechanical performance of the bio-based matrix material in FRC was benchmarked against a DEGBA control. We

sought the FRC with high contents of renewable epoxy resins but of high-performance will be a potential value-added application of VOs.

2. EXPERIMENTAL PART

2.1. MATERIALS

Food grade, refined soybean oil was purchased from a local grocery store. Acetone, chloroform, hydrogen peroxide (H_2O_2, 35 wt%), sulfuric acid, sodium hydroxide pellets and glacial acetic acid (AcOH) were purchased from Fisher Scientific (St. Louis, MO, USA). Amberlite® IR120 H ion exchange resin (IER), epichlorohydrin (EPCH), 2-ethyl-4-methylimidazole (EMI) and cetyltrimethylammonium bromide (CTAB) were purchased from Aldrich (St. Louis, MO, USA). 4-methyl-1,2-cyclohexanedicarboxylic anhydride (MHHPA) were purchased from Dixie Chemical (Pasadena, TX, USA). DGEBA was purchased from Momentive (Deer Park, TX, USA) with trade name EPON™ Resin 828. Bi-directional (0°/90°) E-glass woven roving fabric was supplied by Owens Corning (Toledo, OH, USA). Mold release agent Chemlease® 41-90 EZ was purchased from Chem-Trend, Inc. (Howell, MI, USA). Porous peel ply, resin distribution medium, vacuum bag sheet and tack tape were purchased from Airtech International (Huntington Beach, CA, USA).

2.2. PREPARATION OF BIO-BASED EPOXY MATRICES

A detailed synthetic procedure of EGS is previously reported [40]. A slightly modified one more suitable for large-scale production is reported here: Highly unsaturated free fatty acids (FFA) from soybean oil (1000 g, 5.7 mol double bonds), chloroform (1000 g), IER (200 g, 20 wt% of FFA) and AcOH (171 g) were charged to a 5L three-mouth flask equipped with an electric stirrer and a PTFE blade (125 mm in

diameter). The molar ratio of double bonds : H_2O_2 : AcOH was set at 1 : 1.5 : 0.5. After raising the temperature to 65 °C, aqueous H_2O_2 (830.6 g) was added dropwise and completed within 0.5 hr. The reaction was stirred at 1200 rpm for 5 hrs at 70 °C. After filtration of IER, the entire mixture was transferred into a separatory funnel and was washed several times with water to complete remove the AcOH and H_2O_2, chloroform was stripped off using reduced pressure.

The prepared epoxidized FFA (980 g) were mixed with acetone at weight ratio of 1:10, NaOH (357 ml, 10N) was added dropwise. After complete addition of NaOH, stirring was continued for 1 hr and the epoxidized soap was readily filtered by vacuum filtration. The soap powder was dried at 110 °C for 1.5 hrs.

Epoxidized soap powder (950 g) and EPCH (2850 g) at weight ratio of 1:3 was heated to reflux. The CTAB (21.2 g) was then added based on 2 mol% ratio to epoxidized soap (average molecular weight was treated as 326 g/mol). Reflux was continued for 30 min, cooled and centrifuged. The resulting clear solution was decanted to a flask. Excess EPCH was removed by rotary evaporator at reduced pressure. Oxirane concentration of prepared EGS was 9.5% oxygen by mass measured according to ASTM D1652-04. A viscosity of 130 cP at 23°C was measured by Brookfield LVDV-III Rheometer (Middleboro, MA, USA).

The resin formulations were prepared by directly mixing the EGS into base DGEBA resin at the following weight ratios of DGEBA:EGS: 100:0 (pure DGEBA), 50:50 (50% EGS), 0:100 (pure EGS). Curing agent MHHPA was added at a stoichiometric ratio of epoxy to anhydride. Plus 1 phr to epoxy resin of EMI catalyst was also added. The blend was mixed by an electric stirrer and degassed under vacuum (~40

Torr) for 30 min before resin infusion. The EGS reduced viscosity compared to DGEBA. The viscosities of pure DGEBA, 50% EGS and EGS formulations at 23 °C were 1400 cP, 368 cP and 135 cP, respectively.

2.3. COMPOSITE MANUFACTURING

E-glass fiber reinforced composites were manufactured at the Composite Manufacturing Laboratory of Missouri S&T using a VARTM process, where resin blends were infused through the glass reinforcements with the assistance of atmospheric pressure. The schematic of a typical VARTM setup is shown in Fig. 1.

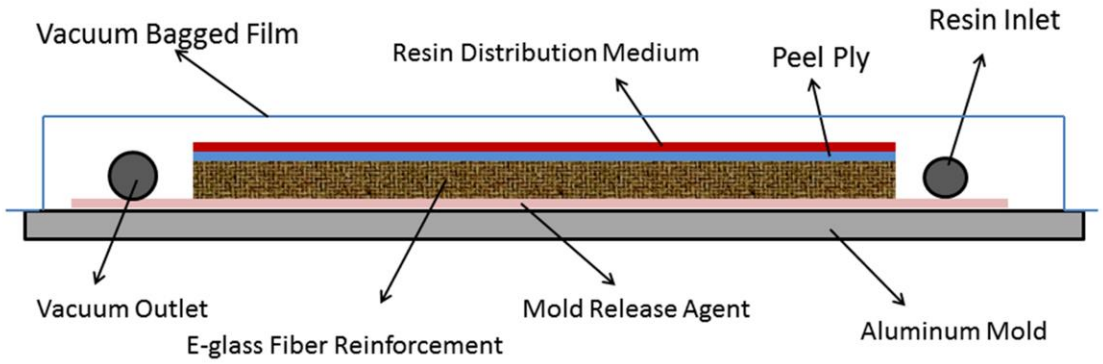

Figure 1. Schematic representation of the single bag VARTM process

The aluminum mold was thoroughly polished (600 grit) to remove scratches, cleaned and sprayed with three coats of mold release agent according to label directions. Six layers of glass fiber woven sheet were cut to the dimensions (20 cm x 20 cm) and laid on the mold with fiber orientation (0°, 90°). A layer of distribution medium was placed between fibers and peel ply cover to speed up the infusion process. The resin inlet and vacuum lines were positioned and then the preform covered with vacuum bag film which was sealed around its perimeter with tack tape.

The packaging was checked for leak under vacuum, then the degassed resin was slowly infused through the inlet till the part was fully infused. The inlet and vacuum lines were closed. Both pure EGS and 50% EGS blends were infused at room temperature, for DGEBA blends, the infusion had to be conducted at 50 °C to reduce the blend viscosity below 1000 cP. The curing cycle in a convection oven was 80 °C for 1 hr, 120 °C 2 hrs and 140 °C for 1 hr. Samples required for flexure and low velocity impact tests were cut from the cured composites using a diamond abrasive blade.

2.4. CHARACTERIZATION OF THE CURING BEHAVIOR

A Q2000 differential scanning calorimeter (DSC) by TA instruments (New Castle, DE, USA) was used to evaluate the resin curing profile by scanning temperature at a heating rate of 10 °C/min from 50 to 280 °C. Samples (2 to 3 mg) were placed in aluminum hermetic cells with an empty cell used as a reference. T_g of cured samples was also determined by DSC: Samples were first preheated to 180 °C and quenched to -30 °C to remove any previous thermal history. Heat flow was recorded over a temperature range scanned from -30 °C to 180 °C at a heating rate 20 °C/min. The onset cure temperature (T_i), peak exothermic (T_p), enthalpy of curing reaction (ΔH), and inflection point T_g were obtained from heat flow data by TA Instruments Universal Analysis 2000 software.

Completion of the reaction was monitored by Thermo Nicolet Nexus 470 E.S.P. (Waltham, MA, USA) Fourier transform infrared (FTIR) spectrometer. Spectra were collected over the range of 3800-550 cm^{-1} at a resolution of 4 cm^{-1} and 32 scans. Peak identities were determined with OMNIC 7.0 software (Thermo Scientific, Madison, WI).

2.5. MECHANICAL TESTING OF COMPOSITES

Flexure strength measurements of composite coupons and neat polymer flexure tests were performed on an Instron 4204 universal testing machine (Norwood, MA, USA) in accordance with ASTM D790. Six specimens of 152 mm × 12.7 mm × 3.0 mm size parallel to a fiber direction were tested for flexural properties at a crosshead speed of 5 mm/min and a support span of 96 mm. Flexural stress and strain were calculated from force versus strain data.

An Instron Model 9250 Impact Testing Machine with impulse control and data system was used to conduct low velocity impact tests on the FRCs. The impactor had mass of 6.48 Kg and diameter of 0.5 in. The composite samples were cut to dimensions of 76 mm × 76 mm × 3.0 mm parallel to a fiber direction. The fixture had an opening of 45 mm × 45 mm. Six specimens were tested for each resin formulation at two energy levels, 2J and 15 J. After specimen was clamped in the fixture, the impactor was raised to the desired drop height corresponding to the energy of impact then dropped onto the clamped specimen. As the impactor made contact with the specimen, the impulse control data acquisition system was triggered to start data acquisition.

Since fiber content affects FRC mechanical response and properties, volume content of fiber reinforcements was measured by polymer matrix pyrolysis using a muffle furnace in accordance with ASTM D3171-11.

2.6. DYNAMIC MECHANICAL ANALYSIS

The dynamic mechanical properties (DMA) of neat polymers and composites were determined using a TA Instruments dynamic mechanical analyzer DMAQ800 (New Castle, DE, USA), operating in 3-point bending mode. Specimen dimensions for both

neat resins and composites were 60 mm × 12.7 mm × 3 mm. Measurements were performed over the temperature range of 25°C to 220°C at a heating rate of 5°C/min, 1 Hz, and amplitude 18 μm. The data were analyzed by the Universal Analysis 2000 software.

2.7. FRACTURE SURFACE ANALYSIS

Scanning electron microscopy (SEM) was performed using a FEI Helios NanoLab^{TM} 600 FIB/FESE instrument (Hillsboro, OR, USA) to investigate the failure interface between fiber and matrix of fracture samples. Samples were fractured flexurally and sputter coated with Au. SEM micrographs were obtained with accelerating voltage of 5.0 kV.

2.8. THERMAL ANALYSIS

Thermal decomposition behavior of composites was examined using a model Q50 thermogravimetric analysis (TGA) instrument by TA Instruments (New Castle, DE, USA). A 20-30 mg mass of sample was heated from 25 °C to 700 °C at a heating rate of 10 °C/min under an ambient air flow environment.

3. RESULTS AND DISCUSSION

3.1. MECHANICAL PROPERTIES

Although mechanical properties of glass fibers reinforced composites are dominated by the fiber portion, which possesses much higher strength and modulus than the matrix polymers, the matrix must be strong enough, *i.e.*, of high crosslink density, and provide good adhesion to fibers to adequately transfer the load to fibers. Inherently flexible matrices require copolymerization or blending with stiffer monomers to increase

crosslink densities and performance of VO-based polymer matrixes.[22, 52] Monomers such as ESO that have low reactivity or have pendant dangling chains, which will become more prominently affect performance. A combination of plasticizing effect, reduced crosslink density of polymer matrixes, and poor fiber-matrix interfacial adhesion result in poor performance of FRCs.[46-48]

Mechanical properties of composites and neat polymers are listed in Table 1. The flexural strength and modulus of neat EGS polymers are 46% and 31% lower than values of neat DGEBA, respectively. All composites, especially the EGS, significantly increased mechanical strength and modulus compared to neat polymers.

Table 1. Mechanical properties of composites and neat polymers

Composites Sample	*Flexural strength* (MPa)	*Flexural Modulus* (MPa)	*Fiber volume fraction (%)*
DGEBA	512.7±20.5 (138.1±4.7)	23276±1213 (2980±85.7)	55.3±0.3
50% EGS	513.5±15.7 (121.9±4.0)	23295±1271 (2829.1±50.7)	55.6±0.5
EGS	474.5±27.9 (75.0±6.0)	22481±1215 (2067±73.0)	52.6±0.2

*Values in bracket are results of neat polymers

Flexural strength and modulus of both DGEBA and 50% EGS are nearly identical as they were of similar fiber volume fractions. Flexural strength and modulus of the EGS composite were 474.5 MPa and 22.5GPa, respectively, slightly reduced due to a reduced fiber volume. Results in Table 1 also indicated that performance of the FRC was maintained even at high concentrations of bio-renewable content. EGS based matrix

materials appear to maintain high crosslink density, which is reflected in its relatively high polymer T_g[40] compared to other bio-based resins provide good adhesion to the reinforcing fibers as we show in following sections.

3.2. IMPACT PROPERTIES

FRCs generally exhibit much higher toughness than that of neat polymers, and the energy absorbing capability is strongly dependent on the tensile strain capacity of the resin and the interfacial strength between fiber and resin. Thus the impact response of FRC is a complex phenomenon involving crack initiation and growth in the resin matrix, matrix fiber delamination, fiber breakage, and fiber pullout.[53] In this study, low velocity impact was used to compare the effect of resin formulations on impact resistance of the FRCs.

Figure 2 shows the measured displacements, loads, and energies as a function of time. The load vs. time curve (Fig. 2a) provides information on threshold and peak forces, contact duration, and delamination and fiber fracture in the sample. The initial, ascending portion of the curve gives the bending stiffness history (modulus) information of the composite under impact loading. The later, descending portion of the curve gives the information about rebound of the impactor and destructive displacement of the composite.

Similar ascending and descending phenomenon are found in the displacement vs. time curve (Fig. 2b). Fig. 2c shows the energy absorbed by the composite specimens. These curves can be divided into three phases, the first phase of the curve indicates the transfer of energy from the impactor to the specimen. The second part of the curve shows the transfer of energy from the specimen to the impactor. The final phase (flat

region) is a measure of the energy absorbed by the specimen. Interestingly, all composites show similar impact behavior, peak load, maximum displacement, and absorbed energy as summarized in Table 2.

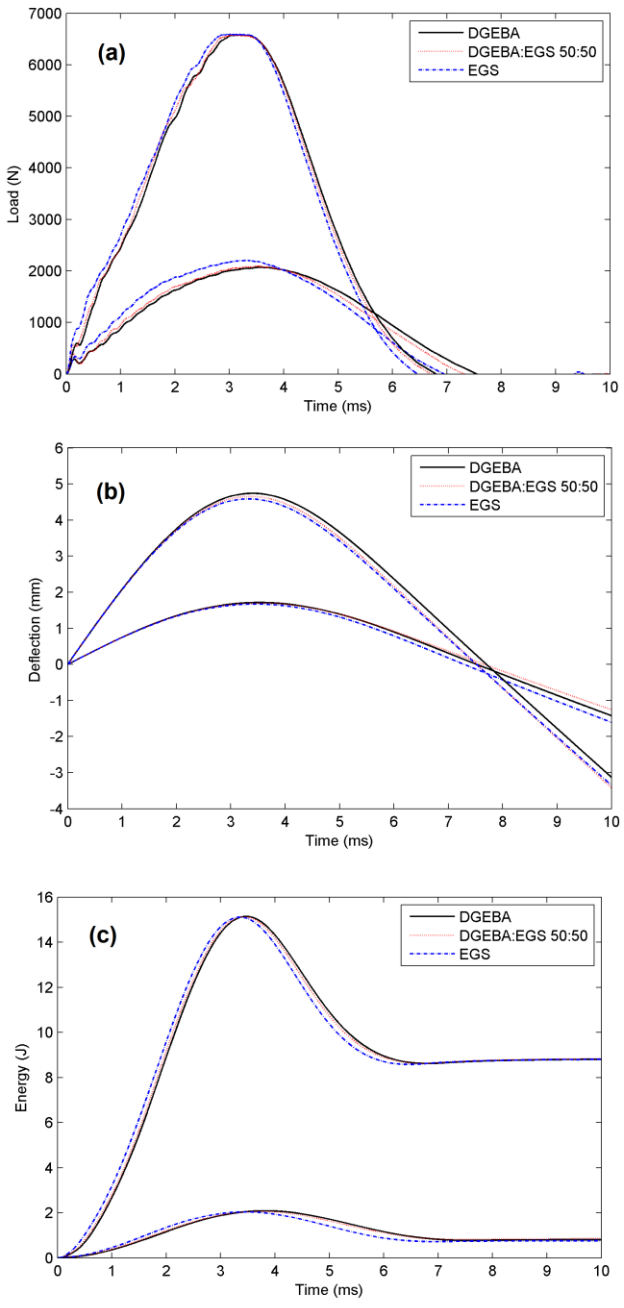

Figure 2. Low velocity impact test results (a) Variation of load vs. time (b) Variation of displacement vs. time (c) Varation of impact energy vs. time

Table 2. Low velocity impact test results

Sample	*Maximum Deflection(2J)*	*Maximum Deflection(15J)*	*Maximum Load(2J)*	*Maximum Load(15J)*	*Energy absorbed (2J)*	*Energy absorbed (15J)*
DGEBA	1.99±0.15	4.80±0.17	2027.7±67.5	6560.8±59.7	0.85±0.05	8.6±0.3
50% EGS	1.82±0.11	4.73±0.06	2047.0±67.2	6574.3±17.2	0.91±0.07	8.8±0.2
EGS	1.70±0.05	4.66±0.19	2187.6±52.7	6580.3±7.2	0.72±0.03	8.6±0.1

DGEBA composites showed slightly higher displacement when compared to the EGS composites at 2 J impact level, which may be due to better energy absorptivity of neat EGS compared to DGEBA. Composites tested at 15 J impact level suggest that the maximum displacements were identical within the manufacturing and testing error. Similarly, maximum loads absorbed by DGEBA composite and EGS composite at both 2 J and 15 J impact levels were comparable within error. Table 2 clearly indicates that the energies absorbed by all composites were similar at higher energy impact (15 J) where the energy absorbed was mainly controlled by the fiber reinforcement.

At low impact levels (2 J), the neat polymers may play a larger role. A more flexible EGS could improve impact resistance of the composites; however, a slightly reduced energy absorption was observed for EGS composite at 2 J that may be explained by lower matrix strength or by a slightly lower fiber volume fraction. For instance, the latter argument is supported by a higher energy absorption observed in 50% EGS sample that is of high fiber volume fraction similar to DGEBA.

3.3. CHARACTERIZATION OF THE CURING BEHAVIOR

The DSC spectra results of the Epoxy-MHHPA-EMI systems are listed in Table 3. Reduced T_g values were measured upon replacement of DGEBA by EGS. Since the

epoxy content of EGS is higher than that of ESO or more saturated FFA epoxies, which behave as dangling chains or plasticizers, the crosslink densities and T_g of EGS polymers are higher than those of ESO.

Table 3. DSC results of curing EGS/DGEBA-MHHPA-EMI matrix systems

Sample	T_i (°C)	T_p (°C)	ΔH (J/g)	T_g (°C)
ESO	182.5	215.8	247.0	44.4
EGS	141.8	167.6	310.1	89.1
50% EGS	137.0	158.9	333.6	125.0
DGEBA	133.7	151.6	352.4	152.6

The polymerization of both DGEBA and ESO show single exothermic peaks, while predominantly higher T_p and T_i values of ESO compared to DGEBA means a much slower reaction rate. Lower reactivity also evidenced by a lower ΔH value. ESO, of lower oxirane content and solely internal oxirane, reacts sluggishly with MHHPA and the polymer matrix is plasticized by saturated, unreactive ESO chains. Unlike either ESO or DGEBA, pure EGS showed two convoluted exotherms, which is believed to be originate from inherently different reactivity of terminal glycidyl versus internal oxirane groups.

Both T_p and T_i values of EGS are near those of DGEBA and much lower than those of ESO. The blending of EGS into DGEBA lead to shifting of T_p to slightly higher values but there were only minor change in T_i and ΔH values. A single exothermic peak was still observed. Thus, EGS was much more reactive than ESO and was cure-compatible with DGEBA.

Evidence of cure-compatibility and improved completion of cure were observed by FTIR by the observation of characteristic peaks at 1862 cm^{-1} (anhydride), 915 cm^{-1} (glycidyl ether), 910 cm^{-1} (glycidyl ester) and 820 cm^{-1} (internal epoxy) after during a cure event (Fig. 3). All peaks disappeared in a 50% EGS sample after 40 min curing at 120 °C (Fig. 3c), replaced by newly formed peaks at 914 cm^{-1} and 901 cm^{-1} that may related to formation of ether groups due to the polyetherification of epoxy. These observations are in agreement with the common epoxy-anhydride curing mechanism as affected by reactivity of the epoxy, molar ratio between epoxy and anhydride, and the presence, type, and concentration of catalyst.[54] EMI is an efficient catalyst for vegetable oil based epoxy-anhydride curing reaction through zwitterion formation with epoxy and subsequent generation of a carboxyl anion with anhydride. Continuation of these alternating steps results in a polyester.[55, 56] The lower reactive internal oxirane and hydroxyl groups in the epoxy may still lead some polyetherification, however, the terminal epoxies (glycidyl ester) in EGS provide a similar reactivity with glycidyl ether of DGEBA, thus, curing EGS and DGEBA will secure an efficient and homogeneous network formation.

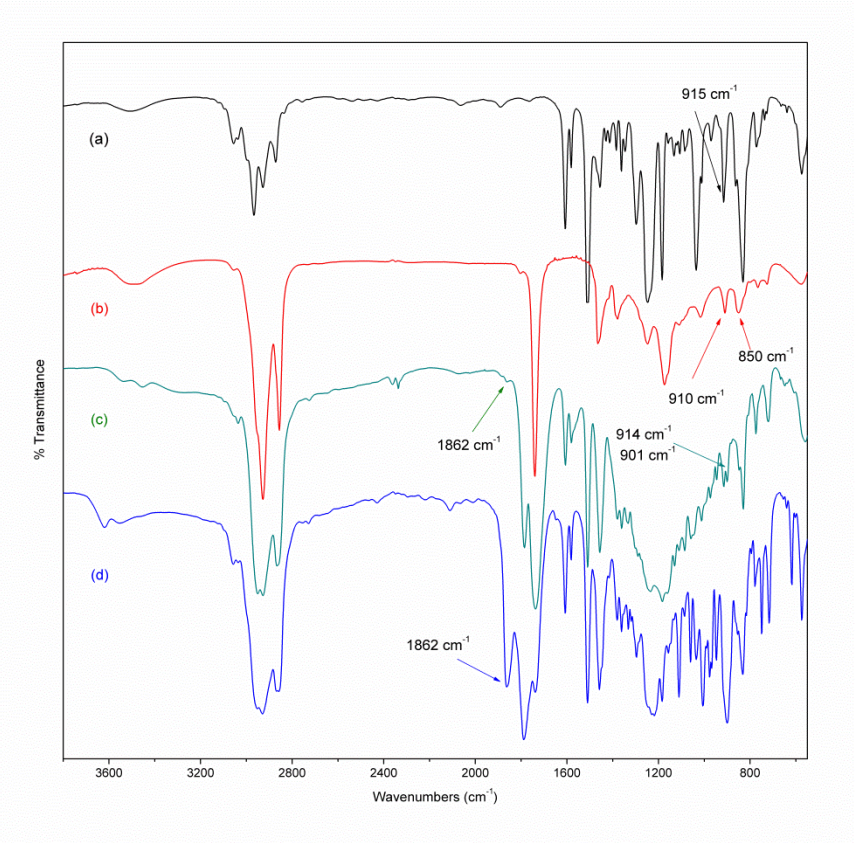

Figure 3. FT-IR spectra of (a) DGEBA; (b) EGS; (c) 50 % EGS cured at 120 °C for 40 min; (d) uncured and liquid 50% EGS blended.

3.4. MORPHOLOGY AND STRUCTURE

The fracture surfaces of neat polymers and composite systems were observed by SEM. The fracture surfaces of both DGEBA (Fig. 4a) and EGS (Fig.4c) are mostly smooth, the crack propagating in a planar manner. The 50% EGS (Fig. 4b) showed a slightly rougher surface with more prominent ridges, which implied that the path of the crack tip was distorted where the crack propagation may be either more difficult or more readily nucleated. The result suggests a more heterogeneous structure exists for 50% EGS than the pure DGEBA or EGS samples. However, no phase separation and sample transparency were observed that confirm that EGS and DGEBA were cure-compatible.

Figure 4. Fracture surface of neat polymer samples (a): DGEBA; (b): 50% EGS; (c): EGS

SEM was also used to exam fracture surfaces of FRCs after flexural strength testing. Fiber pullout is not noticeable for 50% EGS (Fig. 5a) where good adhesion between glass fibers and epoxy matrix is shown. A few noticeable cracks between fiber and the epoxy matrix were observed. Fractures of matrix resins between glass fiber layers (Fig. 5b) were also observed. Interlaminar fracture instead of fiber pullout failure also supported good adhesion between the epoxy and fibers, *i.e.*, adhesion strength greater than matrix strength.

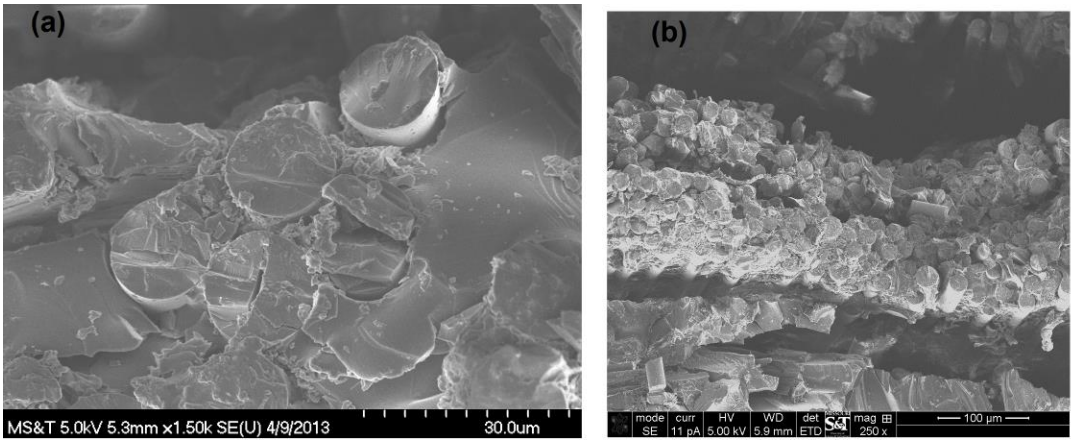

Figure 5. Fracture surface of 50% EGS composite observed under SEM (a): Interface between fibers and matrix; (b): Breakage of matrix resins between fiber layers

3.5. DYNAMIC MECHANICAL ANALYSIS

Figure 6 shows the DMA spectra as a function of temperature for the neat polymers and FRCs. The modulus of the neat polymers depended on polymer crosslink density and stiffness, while the composites exhibited a dramatic increase in storage modulus over the entire temperature range. Due to their high modulus and their strong interaction with the polymer matrices, glass fibers increase the ability to sustain load through local reinforcement of the polymer matrix to increase the modulus of composites.

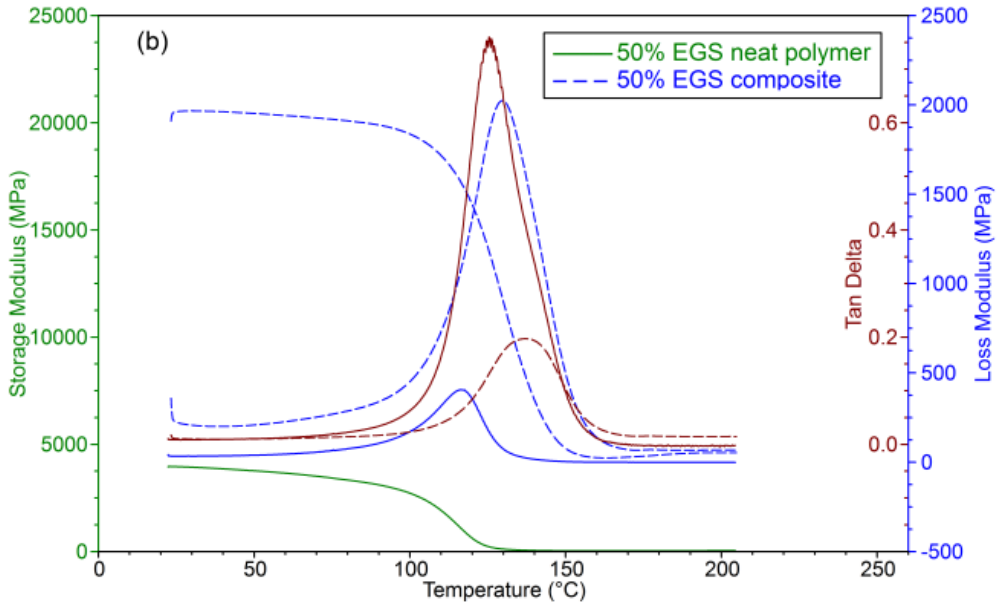

Figure 6. Dynamic mechanical spectra as a function of temperature

A rapid decrease of storage modulus is observed near the matrix glass transition range dependant on the content of neat polymers. Above the T_g, the modulus reaches a rubbery plateau region. The modulus decrease at the T_g corresponds to an energy dissipation shown in the tan δ curve. The temperature at the peak of the tan δ curve is commonly used to define matrix T_g.

Tan δ peaks of composites show reduced height than those of neat polymers (Fig. 7). This is because the incorporated glass fibers restrict the mobility of the polymer and impart elastic stiffness.[57] A broadening of the tan δ peak coincided with increasing EGS content. These changes can be attributed to the heterogeneity of a vegetable oil based structure leading to a wider distribution of molecular weight segments between crosslinks.[58] Upon adding EGS to DGEBA, the matrix tan δ (T_g) in the neat polymers and composites was reduced. The T_g of the EGS composite is 114 °C, which appears unprecedented for a soybean oil based FRC.

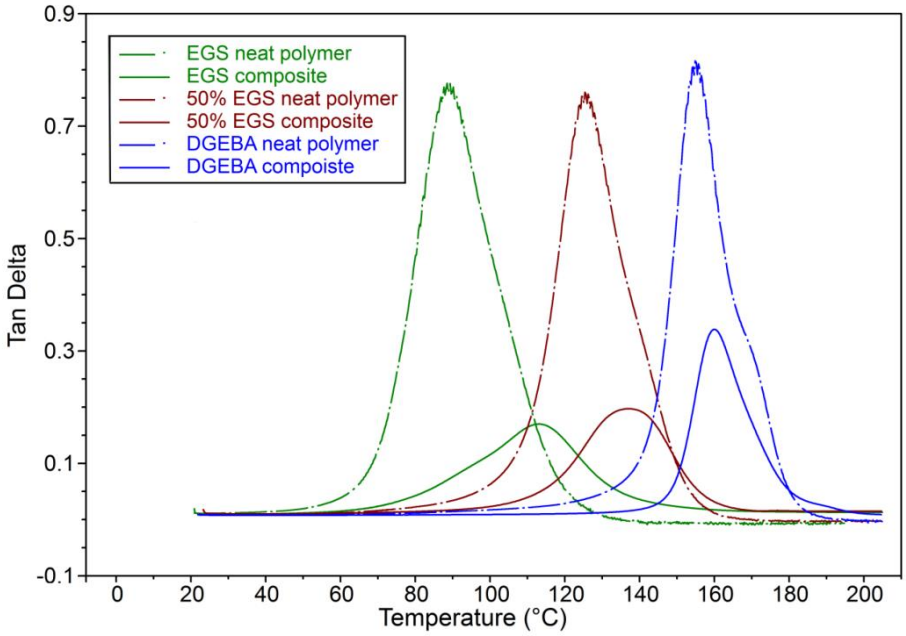

Figure 7. Comparison of tan δ of neat polymers and composites

The glass fibers significantly shift the peaks of loss modulus and tan δ. An increase of 25 °C in the max tan δ was observed for EGS composite compared to the neat polymer while there was less than a 5 °C increase for DGEBA, which implies that the EGS showed better interaction through adhesive coupling with fibers. Improved

interfacial adhesion may come from the much lower viscosity of EGS resins for improved wet-out versus DGEBA during infusion.[49] Some VO-based FRCs with insufficient wetting[19] or loose network structure[20] have shown decreased max tan δ temperatures of than the neat polymers.

3.6. THERMAL STABILITY

The TGA curves of the composites are shown in Figure 8. It can be observed that all composites displayed two, single-step degradation processes with the initial decomposition temperature onset at approximately 300 °C. The first stage of decomposition from 300 to 450°C is believed to be due to pyrolysis of the crosslinked epoxy resin network. The second stage loss from ~ 450 to 600 °C was considered to be the complete decomposition of the smaller fragments, such as cyclized or aromatic degradation byproducts. Replacements of DGEBA by EGS led to a slightly lower temperature onset of degradation due to aliphatic structure of EGS.

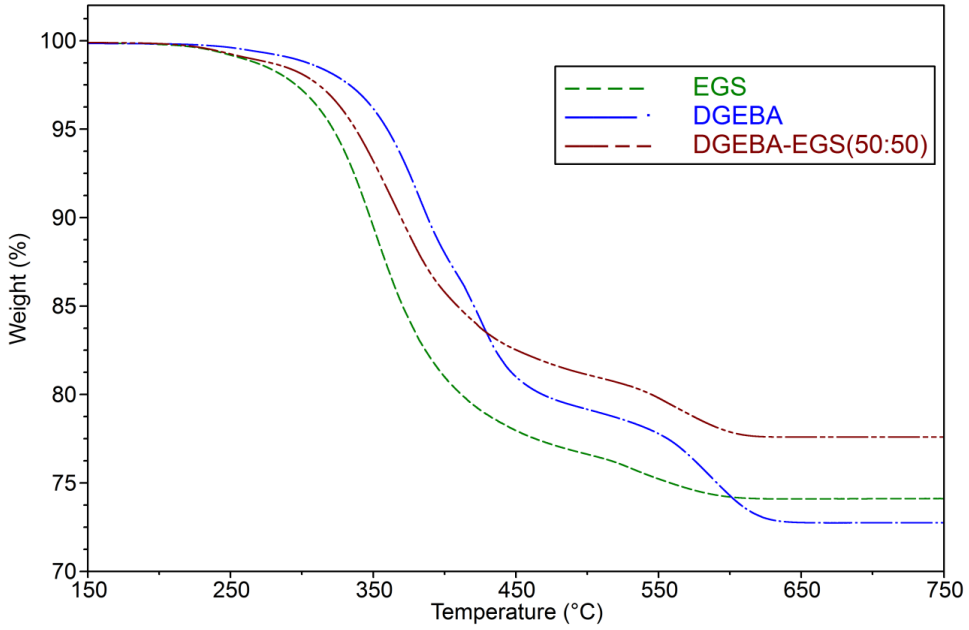

Figure 8. Thermogravimetric analysis of EGS/DGEBA composites

4. CONCLUSION

In this work, the potential of using soybean oil based epoxy resins as polymer matrix of to manufacture FRC is benchmarked against a common, conventional petroleum-based epoxy resin. A new, soybean oil based EGS monomer was characterized by improved reactivity, oxirane content and low viscosity that complements petroleum-based DGEBA. EGS is soluble and cure compatible with DGEBA but has significantly reduced viscosity compared to common DGEBA resins. Pure EGS, DGEBA, and their blends were used as base resins for VARTM processing with glass fibers to obtain FRC. Mechanical characterization of these composites revealed that the flexural strength, modulus, and impact properties of EGS based epoxy are comparable to DGEBA FRC. The EGS performance in FRC of good fiber-matrix interactions and high crosslinking densities are evidenced by interfacial failure surface, and DMA data. Glass transition and thermal stability of EGS are slightly lower than those of DGEBA due to the aliphatic nature of a vegetable oil monomer.

The fabricated bio-based epoxy/glass fiber composites possessed significantly improved mechanical properties compared to neat polymers. Economic and environmental advantages of EGS resins only become attractive alternatives to petroleum based material given high mechanical performance that can lead to a value–added product from vegetable oils. The resulting composites display excellent room temperature infusibility, high strength, high Tg, and compatibility with other resin materials. The bio-based FRC appear to have applicability to a wide variety of structural application areas, such as agricultural equipment, civil engineering, and the automotive and construction industries.

REFERENCES

1. A. Gandini, *Macromolecules*, 2008, **41**, 9491-9504.
2. M. N. Belgacem and A. Gandini, Elsevier.
3. G. Lligadas, J. C. Ronda, M. Galià and V. Cádiz, *Materials Today*, 2013, **16**, 337-343.
4. M. A. R. Meier, J. O. Metzger and U. S. Schubert, *Chemical Society Reviews*, 2007, **36**, 1788-1802.
5. F. Seniha Güner, Y. YagcI and A. Tuncer Erciyes, *Progress in Polymer Science*, 2006, **31**, 633-670.
6. J. M. Raquez, M. Deléglise, M. F. Lacrampe and P. Krawczak, *Progress in Polymer Science*, 2010, **35**, 487-509.
7. R. Gu, S. Konar and M. Sain, *Journal of the American Oil Chemists' Society*, 2012, **89**, 2103-2111.
8. K. Huang, P. Zhang, J. Zhang, S. Li, M. Li, J. xia and Y. Zhou, *Green Chemistry*, 2013, **15**, 2466-2475.
9. F. Li, J. Hasjim and R. C. Larock, *Journal of Applied Polymer Science*, 2003, **90**, 1830-1838.
10. Y. Xia and R. C. Larock, *Green Chemistry*, 2010, **12**, 1893-1909.
11. Y. Lu and R. C. Larock, *ChemSusChem*, 2009, **2**, 136-147.
12. C. Liu, W. Lei, Z. Cai, J. Chen, L. Hu, Y. Dai and Y. Zhou, *Industrial Crops and Products*, 2013, **49**, 412-418.
13. S. N. Khot, J. J. Lascala, E. Can, S. S. Morye, G. I. Williams, G. R. Palmese, S. H. Kusefoglu and R. P. Wool, *Journal of Applied Polymer Science*, 2001, **82**, 703-723.
14. J. La Scala and R. P. Wool, *Polymer*, 2005, **46**, 61-69.
15. C. Liu, J. Li, W. Lei and Y. Zhou, *Industrial Crops and Products*, 2014, **52**, 329-337.
16. D. P. Pfister, Y. Xia and R. C. Larock, *ChemSusChem*, 2011, **4**, 703-717.
17. M. Desroches, M. Escouvois, R. Auvergne, S. Caillol and B. Boutevin, *Polymer Reviews*, 2012, **52**, 38-79.
18. A. O'Donnell, M. A. Dweib and R. P. Wool, *Composites Science and Technology*, 2004, **64**, 1135-1145.
19. P. H. Henna, M. R. Kessler and R. C. Larock, *Macromolecular Materials and Engineering*, 2008, **293**, 979-990.

20. Y. Lu and R. C. Larock, *Macromolecular Materials and Engineering*, 2007, **292**, 1085-1094.

21. R. L. Quirino, Y. Ma and R. C. Larock, *Green Chemistry*, 2012, **14**, 1398-1404.

22. D. P. Pfister and R. C. Larock, *Composites Part A: Applied Science and Manufacturing*, 2010, **41**, 1279-1288.

23. M. A. Mosiewicki and M. I. Aranguren, *European Polymer Journal*, 2013, **49**, 1243-1256.

24. E. Zini and M. Scandola, *Polymer Composites*, 2011, **32**, 1905-1915.

25. A. K. Mohanty, M. Misra and G. Hinrichsen, *Macromolecular Materials and Engineering*, 2000, **276-277**, 1-24.

26. E. Santacesaria, R. Tesser, M. Di Serio, L. Casale and D. Verde, *Industrial & Engineering Chemistry Research*, 2009, **49**, 964-970.

27. H. Kishi, Y. Akamatsu, M. Noguchi, A. Fujita, S. Matsuda and H. Nishida, *Journal of Applied Polymer Science*, 2011, **120**, 745-751.

28. T. Koike, *Polymer Engineering & Science*, 2012, **52**, 701-717.

29. A. M. Atta, R. Mansour, M. I. Abdou and A. M. Sayed, *Polymers for Advanced Technologies*, 2004, **15**, 514-522.

30. X. Q. L. Liu, W. Huang, Y. H. Jiang, J. Zhu and Z. C. Z., *eXPRESS Polymer Letters*, 2011, **6**, 293-298.

31. X. Liu and J. Zhang, *Polymer International*, 2010, **59**, 607-609.

32. S. Carlotti, S. Caillol, C. Mantzaridis, A.-L. Brocas, G. Cendejas, A. Llevot, A. Remi and H. Cramail, *Green Chemistry*, 2013, **15**, 3091-3098.

33. J. Łukaszczyk, B. Janicki and M. Kaczmarek, *European Polymer Journal*, 2011, **47**, 1601-1606.

34. M. Chrysanthos, J. Galy and J.-P. Pascault, *Polymer*, 2011, **52**, 3611-3620.

35. F. Jaillet, E. Darroman, A. Ratsimihety, R. Auvergne, B. Boutevin and S. Caillol, *European Journal of Lipid Science and Technology*, 2013, **116**, 63-73.

36. S. Ma, X. Liu, Y. Jiang, Z. Tang, C. Zhang and J. Zhu, *Green Chemistry*, 2013, **15**, 245-254.

37. S. Ma, X. Liu, L. Fan, Y. Jiang, L. Cao, Z. Tang and J. Zhu, *ChemSusChem*, 2014, **7**, 555-562.

38. R. Auvergne, S. Caillol, G. David, B. Boutevin and J.-P. Pascault, *Chemical Reviews*, 2013, **114**, 1082-1115.

39. Z. S. Petrović, *Polymer Reviews*, 2008, **48**, 109-155.

40. R. Wang and T. Schuman, *eXPRESS Polymer Letters*, 2013, **7**, 272-292.

41. S.-J. Park, F.-L. Jin, J.-R. Lee and J.-S. Shin, *European Polymer Journal*, 2005, **41**, 231-237.

42. M. Shibata, N. Teramoto, Y. Someya and S. Suzuki, *Journal of Polymer Science Part B: Polymer Physics*, 2009, **47**, 669-673.

43. Z. Liu and S. Z. Erhan, *Journal of the American Oil Chemists' Society*, 2009, **87**, 437-444.

44. Z. Liu, K. M. Doll and R. A. Holser, *Green Chemistry*, 2009, **11**, 1774-1780.

45. S. G. Tan, Z. Ahmad and W. S. Chow, *Polymer International*, 2013, n/a-n/a.

46. N. W. Manthey, F. Cardona, G. Francucci and T. Aravinthan, *Journal of Reinforced Plastics and Composites*, 2013, **32**, 1444-1456.

47. J. D. Espinoza-Perez, B. A. Nerenz, D. M. Haagenson, Z. Chen, C. A. Ulven and D. P. Wiesenborn, *Polymer Composites*, 2011, **32**, 1806-1816.

48. K. Chandrashekhara, S. Sundararaman, V. Flanigan and S. Kapila, *Materials Science and Engineering: A*, 2005, **412**, 2-6.

49. J. Zhu, K. Chandrashekhara, V. Flanigan and S. Kapila, *Composites Part A: Applied Science and Manufacturing*, 2004, **35**, 95-101.

50. S. Sundararaman, A. Shabeer, K. Chandrashekhara and T. Schuman, *Journal of Biobased Materials and Bioenergy*, 2008, **2**, 71-77.

51. R. Wang, T. Schuman, R. R. Vuppalapati and K. Chandrashekhara, *Green Chemistry*, 2014, **16**, 1871-1882.

52. S. Husić, I. Javni and Z. S. Petrović, *Composites Science and Technology*, 2005, **65**, 19-25.

53. D. Ratna, Smithers Rapra Technology.

54. C. A. May, *Epoxy Resins: Chemistry and Technology, Second Edition,*, M. Dekker, New York, 1988.

55. S. G. Tan, Z. Ahmad and W. S. Chow, *Industrial Crops and Products*, 2013, **43**, 378-385.

56. A. Mahendran, G. Wuzella, A. Kandelbauer and N. Aust, *Journal of Thermal Analysis and Calorimetry*, 2012, **107**, 989-998.

57. N. H. Mohd Zulfli, A. Abu Bakar and W. S. Chow, *High Performance Polymers*, 2013.

58. J. V. Crivello, R. Narayan and S. S. Sternstein, *Journal of Applied Polymer Science*, 1997, **64**, 2073-2087.

SECTION

4. CONCLUSION

This dissertation has discussed the synthesis, characterization and application of a new VO-based epoxy monomer structure, the glycidyl esters of epoxidized fatty acids. The thermosets prepared by cationic and co-reactive polymerization were observed to display a wide range of thermal and mechanical properties from soft and flexible rubbers to hard and rigid plastics. Increasing the epoxy functionality and reducing the amount of saturated components were keys to achieving high thermal and mechanical strengths. As added benefits to addition of the telechelic glycidyl functionality to the ester were a facilitated removal of saturated fatty acids, better resin-glass fiber/clay platelet interactions, and improved thermal and mechanical performance compared to materials made from traditional EVO. Nanoclay and glass fiber reinforced EGS composites showed significantly improved performances, even comparable to an industrial standard, commercial DGEBA epoxy composite control sample.

In PAPER I., recent advances in epoxy thermoset polymers prepared from EVO and analogous, fatty acid derived epoxy monomers resins were reviewed. The scope, performance, and limitations with respect to the utilization of such materials in various applications are highlighted. The EVO has found various commercial applications. However, inherently less reactive internal epoxy groups and flexible carbon chain structures in EVO has prevented their applications as high performance thermoset

polymers for structural applications. A remaining opportunity for EVO application is as a supplement for petroleum-based commercial epoxy monomers in matrix materials for coatings, composites or as nanocomposites. The development of a new, VO-derived epoxy monomers with higher reactivity, higher oxirane functionality, and higher polymer performance would provide new opportunities to apply and expand EVO application as 'green,' environmentally friendly and sustainably produced, materials.

In PAPER II., EGS, EGL and analogous epoxy monomers were synthesized to control oxirane content, reactivity, and viscosity as a structure-property study in comparison to ESO and ELO benchmark materials. The EGS and ESO, for comparison, were used as neat monomer and in comonomer blends with DGEBA. Thermosetting polymers were fabricated from the epoxy monomer/monomer blends using either BF_3 catalyzed cationic polymerization or by anhydride reagent condensation. The curing behaviors and resulting glass transition temperatures, crosslink densities and mechanical properties were measured.

The results indicated T_g was a function of oxirane content with some added influence of glycidyl versus internal oxirane reactivity, pendant chain, chemical structure and presence of saturated components. The measured T_g of EGL polymer was as high as 124 °C, which is unprecedented for a VO-based epoxy. Although the T_g and mechanical strength of EGS polymers were still lower than the DGEBA control samples, EGS provided better compatibility with DGEBA as a comonomer compared to ESO/ELO, providing improved intermolecular crosslinking and polymer glass transition temperatures, and yielded mechanically superior polymer materials than obtained using ESO/ELO.

In PAPER III., epoxy-clay nanocomposites derived from EGS and OMMT were more efficiently dispersed in EGS monomer due to a lower viscosity of EGS and improved solvent interaction with OMMT compared to ESO. Three types of dispersion technique, mechanical stirring, high speed shearing, and ultrasonication, were carried out to disperse the clay directly into epoxy or anhydride portion of the thermoset system without added solvent. Sonication dispersion of clay into epoxy portion was needed to optimize dispersion quality and achieve exfoliation of clay and optimal mechanical and thermal strength of the resulting nanocomposites. The nanocomposites' morphologies were a mix of intercalated and exfoliated structures, dependent on the dispersion technique.

Tensile testing showed that 1 wt.-% of clay improved nanocomposite strength and modulus by 22 % and 13 %, respectively. Importantly, the EGS polymer tensile modulus could be increased 34 % upon a well-dispersed addition of nanocomposite clay without sacrifice of strength. The EGS clay nanocomposite properties were more comparable to the values of a neat DGEBA polymer benchmark control than the neat EGS polymer and were superior to those of an ESO composite control.

In PAPER IV., high performance bio-based matrix composites were manufactured that showed mechanical properties comparable to those obtained with petroleum based benchmark matrix composites. Pure EGS, blends of DGEBA with EGS, and pure DGEBA were copolymerized with anhydride to yield polymer matrices. Continuous, long glass fiber (0, 90) reinforced composites were fabricated utilizing liquid monomer matrices via VARTM processing and subsequent polymerization. The results indicated that EGS was chemically compatible with DGEBA and formed single phased

polymer structures. As a reactive diluent, the chemically compatible EGS significantly reduced the viscosity of DGEBA and thus facilitated fabrication of composites through VARTM at room temperature. Mechanical testing showed that EGS composites possessed comparable mechanical properties, such as flexural and impact strengths, compared to DGEBA based counterparts. The T_g, flexural strength and modulus of the EGS composites were as high as 114 °C, 474 MPa and 22.5 GPa, respectively.

The advantages of vegetable oil raw materials provide for continued interest as renewable feedstock materials. Epoxidized vegetable oils are currently commercial materials whose wider application is performance limited. Higher performance monomers based on the EGS or similar monomer structures derived from other types of VOs, especially those with fatty acids of greater initial degree of unsaturation, have an improved potential to replace petroleum-based epoxy resin as value-added products from VOs.

This research work applied the EGS monomer structures in nanocomposite and long fiber composite applications as anhydride polymerized materials to produce a now-demonstrated capability for structural application. Future research could expand to include other polymerization mechanisms, monomers, and crosslinking reagents with applications in surface coatings, as reactive diluents, and composites' polymer matrices. The continuing challenge is to develop a cost-effective manufacturing process at pilot scale, and potentially full scale, commercial production.

VITA

Rongpeng Wang was born in Ju'nan, Shandong Province, China. He received his Bachelor's degree in Chemistry from Weifang University, Shandong, China in 2005. In 2008, he obtained his Master degree in Physical Chemistry from Taiyuan University of Technology, Shanxi, China. He joined Missouri University of Science and Technology in August 2008, and began his doctoral study under the guidance of Dr. Thomas Schuman. During the course of his study, Rongpeng has published several peer-reviewed papers, and won the 2011 Annual Excellence in Thermoset Polymer Research, Thermoset Resin Formulators Association (TRFA) and the 2012 Industrial Oil Products Division (IOP) Student Excellence Award, American Oil Chemists' Society (AOCS). He has served as the Vice Chairman of IOP Division of AOCS and the Poster session chair of 105^{th} AOCS Annual Meeting & Expo. Rongpeng Wang completed his PhD requirements in chemistry in May 2014.